

**A COMPARISON OF THE NFRC AND CEN THERMAL
TRANSMITTANCE CALCULATION METHODS IN NORTH AMERICA'S
EIGHT CLIMATE ZONES**

by

Peta-Gaye Ebanks, BA, Trent University, 1998

A thesis

presented to Ryerson University

in partial fulfillment of the

requirements for the degree of

Master of Applied Science

in the Program of

Building Science

Toronto, Ontario, Canada, 2014

©(Peta-Gaye Ebanks) 2014

Author's Declaration Page

I hereby declare that I am the sole author of this thesis or dissertation.

I authorize Ryerson University to lend this thesis or dissertation to other institutions or individuals for the purpose of scholarly research.

I further authorize Ryerson University to reproduce this thesis or dissertation by photocopying or by other means, in total or in part, at the request of other institutions or individuals for the purpose of scholarly research.

Abstract

A COMPARISON OF THE NFRC AND CEN THERMAL TRANSMITTANCE CALCULATION METHODS USING DIFFERENT ASSUMPTIONS AND BOUNDARY CONDITIONS IN NORTH AMERICA'S EIGHT CLIMATE ZONES

Master of Applied Science, 2014

Peta-Gaye M. Ebanks

Building Science

Ryerson University

Studies have found that the CEN and NFRC methods produce different U-values for the same window. A comparative evaluation of the NFRC and CEN U-value calculation methods was conducted for North American residential high performance window products, as well as several parameters that are most influential in determining the whole window U-value for high performance windows, when utilizing different assumptions and boundary conditions, in North America's eight climate zones. Using 2-D simulation software, THERM and WINDOW, four North American high performance frame types with double, triple and quad glazing combinations, were simulated and calculated according to the NFRC and CEN standard methods. Overall, the trend showed that for the specific window combinations of this study, the higher the performance of the IGU, the lesser the differences in the whole window U-value of both methods. Several strategies were proposed to support the possibility of the harmonization of both calculation methods.

Acknowledgements

I would like to thank the Academy, my agent and my fellow cast members...

I've always dreamed of giving an acceptance speech at the Oscars.

I give such gratitude to my dear friends that were there through the highs and lows and who always gave heartfelt support, inspiration, guidance, laughter and wisdom. They were all instrumental in helping me complete my thesis: Felicity Fernandes, Francie Corry, Corinne Henry, Sheryl Henry, Catherine Longboat, Byron and Trissy Matwewinin, Carly Graner, Urpi Pine, Fran and Todd Buchanan.

I would like to thank all of the building science buddies that I have met at Ryerson for their support and for sharing the same angst and passion for building science. They have taught me in their work and in lively debates. They all helped me in critical moments of my thesis.

I would like to give thanks to my supervisor Dr. Russell Richman for being supportive, encouraging and for challenging me to go beyond my own expectations in my thesis.

I would also like to thank Dr. Joanne Dallaire and Dr. Ramani Ramakrishnan for their guidance and support as well as many others who were part of my journey.

I would like to thank my parents, Myrna and Jerry Ebanks, for their loving support with my son, especially during the last stretch towards the completion of my thesis.

Foremost, I thank my son, Amari Ebanks, to whom all this is for. Without him I would not be the woman I am today. It was because of him why I decided to pursue a Master of Applied Science.

Table of Contents

1	Introduction	1
1.1	Research Focus and Objectives.....	2
1.2	Background	3
1.3	Research Contribution	6
2	Literature Review	7
2.1	Thermal Transmittance Challenges	7
2.2	The NFRC Thermal Transmittance Calculation Method	9
2.2.1	U_{frame} Calculation in the NFRC Method	10
2.2.2	U_{edge} Calculation in the NFRC method	11
2.2.3	Phi Variable	12
2.2.4	NFRC Boundary Conditions	13
2.3	The European (CEN) Thermal Transmittance Calculation Method.....	14
2.3.1	CEN U_{window} Calculation Method	15
2.3.2	U_{frame} calculation in the CEN method.....	16
2.3.3	Thermal Conductance of the Frame with the Calibration Panel	17
2.3.4	Thermal conductance of the Frame with Glazing Unit	18
2.3.5	Ψ -Value Calculation Method	18
2.4	Primary Differences between the NFRC and CEN U_{window} Calculation Methods.....	19
2.4.1	U_{frame} and Edge Effects	21
2.4.2	Frame Cavity Methods.....	22
2.4.3	Radiation Models for Frame Cavities.....	23
2.4.4	Unventilated and Ventilated Frame Cavity Models.....	25
2.4.5	Impacts of these Differences on Whole Window U-values	26
3	Methodology.....	30
3.1	Summary	30
3.2	Window Type and Size	31
3.3	Frame Materials.....	31
3.4	Spacer Materials	34
3.5	Glazing Configurations	34

3.5.1	Double IGU	35
3.5.2	Triple IGU	35
3.5.3	Quadruple IGU	36
3.5.4	Triple IGU (with Heat Mirror™).....	36
3.5.5	Quadruple IGU (with Heat Mirror™).....	37
3.6	Gas Infill Mixtures	37
3.7	Interior Temperature Boundary Conditions	40
3.8	Exterior Temperature Boundary Conditions of North America’s Climate Zones	40
3.9	Winter and Summer Design Conditions.....	40
3.10	North America’s Climate Zones: Inland and Coastal locations	42
3.11	Climate Specific U-values	42
3.12	Solar Heat Gain Coefficient	43
3.13	Gap Sizes	45
3.14	Location Specific Wind Velocities in North America’s Climate Zones	45
3.15	Material Thermal Conductivities.....	46
3.16	Surface Film Coefficients (Boundary Conductances)	47
3.16.1	NFRC Exterior Convective Film Coefficient	49
3.16.2	CEN Exterior Surface Film Coefficient	50
3.17	NFRC and CEN Interior Surface Convective and Surface Film Coefficients.....	54
3.18	Frame Cavity Methods	54
3.19	Ψ-Values.....	54
4	Summary and Justification of Simulations	56
5	Results and Discussion	58
5.1	Solar Heat Gain Coefficient Simulations	58
5.2	U _{cog} Simulations.....	63
5.2.1	U _{cog-NFRC} and U _{cog-CEN} Comparison in the 8 Climate Zones	63
5.2.2	U _{cog-NFRC} in Reference to -18°C	65
5.2.3	U _{cog-CEN} in Reference to 0°C.....	65
5.2.4	U _{cog} Values with Different Gap Spacing Sizes in the 8 Climate Zones.....	66
5.3	U _{frame} Simulations	67
5.3.1	U _{frame-NFRC} , U _{frame-CEN} and U _{frameIGU-CEN} Calculation Methods.....	67
5.3.2	U _{frame-CEN} with CEN and NFRC Frame Cavity Methods	70

5.3.3	$U_{\text{frame-CEN}}$ Comparison with CEN and NFRC Surface Film Coefficients.....	73
5.3.4	$U_{\text{frame-CEN}}$ of Four Frame Types with a Calibration Panel	73
5.3.5	$U_{\text{frame-CEN}}$ Comparisons with Various Material Thermal Conductivities	74
5.4	U_{window} Simulations	75
5.4.1	$U_{\text{window-NFRC}}$ and $U_{\text{window-CEN}}$ Standard Comparison	75
5.4.2	$U_{\text{window-NFRC}}$ and $U_{\text{window-CEN}}$ with Various Material Thermal Conductivities	79
5.4.3	$U_{\text{window-NFRC}}$ and $U_{\text{window-CEN}}$ with NFRC and CEN Surface Film Coefficient Sets	82
5.4.4	$U_{\text{window-NFRC}}$ and $U_{\text{window-CEN}}$ using NFRC and CEN Frame Cavity Methods	84
5.4.5	$U_{\text{window-NFRC}}$ and $U_{\text{window-CEN}}$ Comparison with 4 Frame Types.....	86
5.5	Ψ -Value Comparison with Various Frame and Spacer Types	88
5.6	U_{window} Simulations in the 8 Climate Zones	96
5.6.1	$U_{\text{window-NFRC}}$ and $U_{\text{window-CEN}}$ Comparison in the 8 Climate Zones	96
5.6.2	$U_{\text{window-NFRC}}$ Comparison in Reference to -18°C	102
5.6.3	$U_{\text{window-CEN}}$ Values Comparison in Reference to 0°C	103
5.6.4	$U_{\text{window-NFRC}}$ and $U_{\text{window-CEN}}$ Comparison with 3 Spacer Types	105
5.6.5	$U_{\text{window-NFRC}}$ and $U_{\text{window-CEN}}$ Comparison of Inland and Coastal Locations	111
5.7	Harmonization of the CEN and NFRC U_{window} Calculation Methods.....	115
6	Further Research and Conclusions.....	121
6.1	Conclusion.....	121
6.2	Areas of Further Research	122
7	Appendix A.....	123
8	Appendix B	126
9	Appendix C	128
10	Appendix D.....	130
	U_{window} : Spacer Comparison.....	130
11	Appendix E	132
	Problems with Computer Simulations and Error Possibilities	132
12	References	134

List of Tables

Table 1 Boundary Conditions used for NFRC U- value calculations.....	13
Table 2 NFRC 100-2010 Interior and Exterior Convective Film Coefficient Boundary Conditions for Total Fenestration Products.....	14
Table 3 Differences between the NFRC and CEN calculation methods for determining the U-value (McGowan, 2013)	19
Table 4 Differences between the NFRC and CEN calculation methods for determining the Solar Heat Gain Coefficient or "g-value" (McGowan, 2013).....	20
Table 5 Surface Resistances (horizontal heat flow) of the CEN and NFRC Calculation Methods (National Fenestration Rating Council, 1997) (ISO, 2012)	20
Table 6 Simulation Matrix.....	31
Table 7 Product Type and Model Sizes (NFRC, 2010)	31
Table 8 Double IGU High SHGC	35
Table 9 Double IGU Low SHGC.....	35
Table 10 Triple IGU High SHGC	35
Table 11 Triple IGU Low SHGC	36
Table 12 Quadruple IGU High SHGC	36
Table 13 Triple IGU (with Heat Mirror™) High SHGC.....	36
Table 14 Triple IGU (with Heat Mirror™) Low SHGC.....	37
Table 15 Quadruple IGU (with Heat Mirror™) High SHGC.....	37
Table 16 Quadruple IGU (with Heat Mirror™) Low SHGC.....	37
Table 17 Thermal Conductivity of Pure Gases- EN 673	38
Table 18 NFRC and CEN Infill Gas Thermal Conductivities - THERM.....	38
Table 19 Gas property calculator (WINDOW), air 5%/krypton 95%, NFRC and CEN Thermal Conductivities	39
Table 20 Gas property calculator (WINDOW), air 10%/krypton 90%, NFRC and CEN Thermal Conductivities	39
Table 21 NFRC and CEN Winter Boundary Conditions.....	41
Table 22 Summer Boundary Conditions according to the NFRC and ISO 15099, Section 8.2	41
Table 23 North American Climate Zones: Inland Locations	44
Table 24 North American Climate Zones: Coastal Locations	44
Table 25 Different NFRC and CEN Material Thermal Conductivities	47
Table 26 Surface Film Coefficients used by the NFRC and CEN methods.....	48
Table 27 Equivalent Total Surface Film Conductances (ASHRAE, 1981).....	48
Table 28 NFRC Exterior Convective Film Coefficients for Inland and Coast Locations in NA Climate Zones	50
Table 29 CEN/ISO 6946 Exterior Surface Film Coefficients Calculation Table – Inland Locations.....	52
Table 30 CEN/ISO 6946 Exterior Surface Film Coefficients Calculation Table – Coastal Locations	53
Table 31 Summary of Simulations	56

Table 32 NFRC and CEN SHGC: IGU only	58
Table 33 Fiberglass SHGC according to the NFRC and CEN Methods	59
Table 34 Thermally Broken Solid Wood SHGC according to the NFRC and CEN Methods	59
Table 35 Solid Wood SHGC according to the NFRC and CEN Methods	60
Table 36 U-PVC SHGC according to the NFRC and CEN Methods	60
Table 37 NFRC and CEN U _{cog} Values	79
Table 38	81
Table 39 Frame Measurements from the Sightline	96
Table 40 U _{window-NFRC} Comparison in Reference to -18°C	102
Table 41 U _{window-CEN} Values Comparison in Reference to 0°C	103
Table B-42 U _{window} : Percentage Change between NFRC and CEN Methods	126
Table B-43 Exterior Temperature Symmetry of the NFRC and CEN Methods: U _{window}	127
Table C-44 Double High SHGC: U _{cog} Values with Various Gap Spacing Sizes	128
Table C-45 Double Low SHGC: U _{cog} Values with Various Gap Spacing Sizes	128
Table D-46 Triple High SHGC: U _{cog} Values with Various Gap Spacing Sizes	129
Table C-47 Triple Low SHGC: U _{cog} Values with Various Gap Spacing Sizes	129

List of Figures

Figure 1 First Insulated Glazing Unit by Thomas Stetson (Lingnell, 2011).....	7
Figure 2 Window Product Diagram (NFRC, 2010).....	8
Figure 3 Frame Section with Calibration Panel Insert (ISO, 2012).....	17
Figure 4 Frame section with glazing installed (ISO, 2012).....	19
Figure 5 Solid Wood Frame with Double and Triple IGUs.....	32
Figure 6 U-PVC Frame with Double and Triple IGUs.....	32
Figure 7 Fiberglass Frame with Double and Triple IGUs.....	33
Figure 8 TBSW Frame with Double, Triple and Quad IGUs.....	33
Figure 9 Spacers: A, B and C.....	34
Figure 10 Annual Average Temperatures of North America's 8 Climate Zones.....	43
Figure 11 High and Low SHGC Double IGUs: NFRC vs CEN U_{cog} values (Percentage Change).....	63
Figure 12 High and Low SHGC Triple and Quad IGUs: NFRC vs CEN U_{cog} Values (Percentage Change)....	64
Figure 13 $U_{cog-NFRC}$ and $U_{cog-CEN}$ with Double IGUs: Various Gap Spacing Widths.....	66
Figure 14 $U_{cog-NFRC}$ and $U_{cog-CEN}$ with Triple IGUs: Various Gap Spacing Widths.....	66
Figure 15 TBSW U_{frame} : NFRC and CEN Frame Methods.....	68
Figure 16 U-PVC U_{frame} : NFRC and CEN Frame Methods.....	68
Figure 17 Fiberglass Frame: $U_{frame-NFRC}$ vs $U_{frame-CEN}$ and $U_{frameIGU-CEN}$	69
Figure 18 Solid Wood Frame: $U_{frame-NFRC}$ vs $U_{frame-CEN}$ and $U_{frameIGU-CEN}$	69
Figure 19 CEN U_{frame} : CEN vs NFRC Frame Cavity Methods (FCM).....	71
Figure 20 U-PVC and TBSW Frames with a Calibration Panel.....	72
Figure 21 Fiberglass and Solid Wood Frames with a Calibration Panel.....	73
Figure 22 $U_{frame-CEN}$ with Four Frame Types.....	74
Figure 23 $U_{frame-CEN}$: CEN and NFRC Thermal Conductivities.....	75
Figure 24 TBSW Frame: NFRC and CEN U_{window} Values (Percentage Change).....	75
Figure 25 Solid Wood Frame: NFRC and CEN U_{window} Values (Percentage Change).....	76
Figure 26 Fiberglass Frame: NFRC and CEN U_{window} Values (Percentage Change).....	76
Figure 27 U-PVC Frame: NFRC and CEN U_{window} Values (Percentage Change).....	77
Figure 28 Fiberglass Frame: NFRC U_{window} : NFRC and CEN Thermal Conductivities (TC) (Percentage Change).....	80
Figure 29 $U_{window-NFRC}$ TBSW Frame: NFRC and CEN Thermal Conductivities (TC) (Percentage Change)....	80
Figure 30 $U_{window-NFRC}$ Solid Wood Frame: NFRC and CEN Thermal Conductivities (TC) (Percentage Change).....	81
Figure 31 $U_{window-NFRC}$ and $U_{window-CEN}$ TBSW Frame: NFRC Material Thermal Conductivities (Percentage Change).....	82
Figure 32 $U_{window-NFRC}$ and $U_{window-CEN}$ TBSW Frame: NFRC Material Thermal Conductivities (Percentage Change).....	82
Figure 33 Fiberglass Frame: NFRC vs CEN Surface Film Coefficients using the NFRC Method.....	83
Figure 34 Fiberglass Frame: NFRC vs CEN Surface Film Coefficients using the CEN Method (Percentage Change).....	83

Figure 35 TBSW Frame: NFRC vs CEN Surface Film Coefficients using the NFRC Method (Percentage Change)	83
Figure 36 TBSW Frame: NFRC vs CEN Surface Film Coefficients using the CEN Method (Percentage Change)	84
Figure 37 U-PVC Frame: NFRC vs CEN Frame Cavity Methods using the NFRC Method (Percentage Change)	85
Figure 38 U-PVC Frame: $U_{\text{window-CEN}}$ using NFRC and CEN Frame Cavity Methods (Percentage Change) ..	86
Figure 39 Frame Types with Double IGUs: $U_{\text{window-NFRC}}$ (Percentage Change).....	86
Figure 40 Frame Types with Triple IGUs: $U_{\text{window-NFRC}}$ (Percentage Change)	87
Figure 41 Frame Types with Double IGUs: $U_{\text{window-CEN}}$	87
Figure 42 Frame Types with Triple IGUs: $U_{\text{window-CEN}}$	88
Figure 43 Fiberglass Frame with Double IGU (High SHGC) Ψ -Values: Spacer Comparison	88
Figure 44 Fiberglass Frame with Triple IGU (High SHGC) Ψ -Values: Spacer Comparison.....	89
Figure 45 Ψ -Values of Solid Wood with Double IGUs: Spacer Comparison.....	89
Figure 46 Ψ -Values of Solid Wood with Triple IGUs: Spacer Comparison	89
Figure 47 Ψ -Values of TBSW Frame with Double IGUs: Spacer Comparison	90
Figure 48 Ψ -Values of TBSW Frame with Triple IGUs: Spacer Comparison	90
Figure 49 TBSW Frame with Quad IGU (High SHGC) Ψ -Values: Spacer Comparison.....	90
Figure 50 Ψ -Values of U-PVC Frame with Double IGUs: Spacer Comparison.....	91
Figure 51 Ψ -Values of U-PVC Frame with Triple IGUs: Spacer Comparison	91
Figure 52 Solid Wood Frame with Double IGU and Spacer C: High vs Low SHGC (Percentage Change)...	92
Figure 53 Solid Wood Frame with Triple IGU and Spacer C: High vs Low SHGC (Percentage Change)	92
Figure 54 U-PVC Frame with Double IGU and Spacer C: High vs Low SHGC (Percentage Change)	92
Figure 55 U-PVC Frame with Triple IGU and Spacer C: High vs Low SHGC (Percentage Change).....	93
Figure 56 Ψ -Values of Fiberglass Frame with Double IGUs (Percentage Change)	93
Figure 57 Ψ -Values of Fiberglass Frame with Triple IGUs (Percentage Change).....	93
Figure 58 Ψ -Values of TBSW Frame with Double IGUs (Percentage Change)	94
Figure 59 Ψ -Values of TBSW Frame with Triple IGUs (Percentage Change)	94
Figure 60 Double IGU Fiberglass Frame: U_{window} Values in 8 Climate Zones (Percentage Change)	97
Figure 61 Triple IGU Fiberglass Frame: U_{window} Values in 8 Climate Zones (Percentage Change).....	97
Figure 62 TBSW Frame with a Double IGU: Spacer Comparison	98
Figure 63 Triple and Quad IGU TBSW Frame: U_{window} Values in 8 Climate Zones (Percentage Change)....	98
Figure 64 U-PVC Frame with a Double IGU: Climate Zones (Percentage Change)	99
Figure 65 Triple IGU U-PVC Frame: U_{window} Values in 8 Climate Zones (Percentage Change)	99
Figure 66 Solid Wood Frame with a Double IGU: Climate Zones (Percentage Change)	100
Figure 67 Triple IGU Solid Wood Frame: U_{window} Values in 8 Climate Zones (Percentage Change)	100
Figure 68 Double IGU Fiberglass Frame: Different Spacers in 8 Climate Zones	110
Figure 69 Triple IGU Fiberglass Frame: Different Spacers in 8 Climate Zones.....	110
Figure 70 Triple IGU TBSW Frame: Different Spacers in 8 Climate Zones	111
Figure 71 Quad IGU TBSW Frame: Different Spacers in 8 Climate Zones.....	111
Figure 72 TBSW Frame: U_{window} NFRC and CEN Values of Inland and Coastal Location in 8 Climate Zones	112

Figure 73 Solid Wood Frame: U_{window} NFRC and CEN Values of Inland and Coastal Location in 8 Climate Zones.....	112
Figure 74 Fiberglass Frame: U_{window} NFRC and CEN Values of Inland and Coastal Location in 8 Climate Zones.....	113
Figure 75 U-PVC Frame: U_{window} NFRC and CEN Values of Inland and Coastal Location in 8 Climate Zones	113
Figure 76 Fiberglass Frame: $U_{\text{window-NFRC}}$ Values of Inland and Coastal Locations in 8 Climate Zones	114
Figure 77 U-PVC Frame: $U_{\text{window-NFRC}}$ Values of Inland and Coastal Locations in 8 Climate Zones	114
Figure 78 NFRC and CEN U-window Values with NFRC Exterior Temperature Boundary Condition	116
Figure 79 NFRC and CEN U-window Values Percentage Changes at NFRC Exterior Temperature Boundary Condition.....	118
Figure 80 NFRC and CEN U-window Values Percentage Changes at CEN Exterior Temperature Boundary Condition.....	118
Figure D-81 Solid Wood Frame with a Double IGU: Spacer Comparison	130
Figure D-82 Solid Wood Frame with a Triple IGU: Spacer Comparison	130
Figure D-83 U-PVC Frames with Double and Triple IGUs: Spacer Comparison	131

List of Abbreviations

NFRC	National Fenestration Rating Council
CEN	European Committee for Standardization
IGU	Insulated Glazing Unit
Low-E	Low emissivity coating
SHGC	Solar Heat Gain Coefficient
TBSW	Thermally Broken Solid Wood Frame
U_{cog}	Center-of-Glazing U-value
$U_{cog-NFRC}$	Center-of-Glazing U-value in the NFRC method
$U_{cog-CEN}$	Center-of-Glazing U-value in the CEN method
$U_{edge-NFRC}$	Edge-of-Glazing U-value in the NFRC method
U_{frame}	Frame U-value
$U_{frame-NFRC}$	Frame U-value in the NFRC method
$U_{frame-CEN}$	Frame U-value in the CEN method
$U_{frameIGU-CEN}$	Frame U-value in the CEN method with the IGU inserted in the frame
U'_{frame}	Frame U-value in the CEN method with the Calibration panel in the frame
U'_p	Calibration panel U-value
U_{window}	Whole window U-value
$U_{window-NFRC}$	Whole window U-value in the NFRC method
$U_{window-CEN}$	Whole window U-value in the CEN method

1 Introduction

The figurative and historical significance of windows presents a striking opportunity for architects, engineers, builders, manufacturers and homeowners, to challenge themselves in the design process by considering the potential impact of their design decisions on people. A window's thermal performance, size, orientation, visible light transmittance and solar gain, are factors that all need to be considered in creating a home because they influence people's health, well-being, and energy consumption.

The residential building sector has opportunities to minimize its cumulative impact on energy consumption in Canada. In 2009, the residential sector was the third largest consumer of energy in Canada, consuming 17% of the total energy used and producing 15% of total greenhouse gas emission production (Natural Resources Canada, 2012). In the U.S., residential and commercial buildings consume 40% of primary energy consumption; residential buildings comprise 21% of that total (U.S. Department of Energy, 2011). In Canada, space heating comprised the largest portion of residential energy use, consuming 63% (Natural Resources Canada, 2012). In a typical home, 30-50% of the energy used is transmitted through the windows; thus, 30-50% of the energy that is derived from fossil fuels and nuclear power is transmitted through windows and not conserved (Gustavsen, Grynning, Arasteh, Petter Jelle, & Goudey, 2011). Windows thus account for the majority of heat loss within a building (Gustavsen, Arasteh, Petter Jelle, & Curcija, 2008) and affects the energy used for heating, cooling, lighting and ventilation (U.S. Department of Energy, 2011). Window frames account for 20 to 30% of the whole window area yet can be responsible for more than 30% of the rate of heat transfer (Gustavsen, Arasteh, Petter Jelle, & Curcija, 2008). The rate of heat transfer through the frames can be much greater for high performance (low conductance) windows. Considering that Canada is the third largest energy consumer per capita in the world (The World Bank, 2013), followed by the U.S., a reduction in energy consumption through the use of high performance windows would have a significant effect on reducing our cumulative environmental impact, particularly pollutants that exacerbate climate change, for the benefit of present and future generations.

The essential part of this research focuses on how the rate of heat transfer, or thermal transmittance, is calculated and measured for windows. The way in which the technicalities are dealt with, in the thermal transmittance calculations and measurements, are integral to determining and defining what actually makes a window high-performing. Seeing that these technicalities are dealt with differently internationally, a number of complexities have emerged over the years and continue to be addressed by

the International Standard Organization (ISO). Presently, it is difficult to compare different window products between Europe and North America because the overall U- values are calculated differently and not all of the parameters used are the same. The majority of North American window manufacturers use the National Fenestration Rating Council (NFRC) [Ducker Research Company, 2012] calculation method for determining the overall U-value of their window products and Europe manufacturers use the European Committee for Standardization (CEN) [Sack, 2013] method. Throughout the literature, it is evident that there is a significant discrepancy between the NFRC and the CEN methods in determining the overall window U-value as to which is more accurate. As stated by the Passive House Institute U.S. (PHIUS), “there is a longstanding disagreement between the CEN and NFRC methods” (Wright, 2012). In fact, for the same window, studies have found that the CEN and NFRC methods produce different U-values. This has created confusion amongst window manufacturers, builders, building scientists, energy modellers, architects and home owners (Wright, 2012). In terms of the type of energy performance metrics used and how these metrics are calculated, these aspects are integral in giving equal metrics to contribute to adequately informed decision making decisions in the design phase of any building process and to compare window products on the same level of energy performance metrics and methods.

1.1 Research Focus and Objectives

The focus of this study is to conduct a comparative evaluation of the NFRC and CEN U-value calculation methods for North American residential high performance window products and to evaluate the parameters that are most influential in determining the whole window U-value for high performance windows when utilizing different assumptions and boundary conditions in North America’s climate zones.

The objectives of this research are to:

- 1.** What are the differences between the NFRC and CEN calculation methods for determining the U-value for window products?
- 2.** What parameters can be harmonized between the two methods?
 - 2.1.** Where there are no differences, what parameters can be omitted?
- 3.** How are these parameters affected by the different boundary conditions in North America’s eight climate zones?

1.2 Background

According to CANMET Energy (2010), windows alone were deemed as the largest thermal loss attributed to space heating in a typical new house, representing 27% of annual space heating needs (Parekh, 2010). In the United States, Apte and Arasteh (2006) estimate that windows alone contribute to 29% of the energy used for overall residential space conditioning; more specifically, windows comprise 24% of residential heating energy use (only 3% less than in Canada) and 42% of cooling energy use. A Norwegian study compared the thermal transmittance values (U-values) of windows with those of the wall, roof and floor constructions. This study found that windows typically account for about 30–50% of the total transmission heat loss through the building envelope (Gustavsen et al., 2011). Following the laws of thermodynamics and in particular, Fourier's law of conduction, heat follows the path of least resistance and seeing that windows have a higher thermal transmittance than the wall, roof and floor, 0.7-1.0 W/m²K compared to 0.1 and 0.2 W/m²K, heat is readily transmitted through the window (Gustavsen et al., 2011). Taking into account the thermal transmittance of the windows, they can significantly lower the overall thermal transmittance of an elevation. Since windows are the largest source of heat loss within a building, the use of high insulating windows is thus integral to conserving heating and cooling energy. There is thus a great need for the incorporation of higher insulating windows as part of a high performing building envelope in the residential sector.

High performance windows are generally defined as windows that resist condensation, provide thermal comfort, and impede the flow of heat between the indoor and outdoor environments more efficiently than the majority of the windows available in the market; such as single-pane or double-pane (3.12 and 2.73 W/m²K), air-filled windows with non-insulated frames (ASHRAE, 2009). In Ontario, the building code requires that residential windows have a maximum U-value of 2 W/ m²K as detailed by the energy efficiency compliance packages (Ministry of Municipal Affairs and Housing, 2006). Energy Star windows in Canada require a maximum value of 1.6, 1.4 and 1.2 W/ m²K in climate zones 1, 2 and 3 respectively (Rogers, 2014). In Denmark, an 'energy efficient sealed unit' is defined as a double glazed unit with one low emissivity glass with a U-value of less than 1.8 W/m²K; which is considered to be a high U-value for a Nordic country (Avasoo, 2007). In Sweden, energy efficient windows are rated from 1.5 to 0.9 W/m²K or less (Avasoo, 2007).

Currently the highest performing glazing (including translucent aerogel products) have approximate U-values of 0.3–0.5 W/m²·K (Gustavsen et al., 2011). The highest performing window frames currently have approximate U-values of 0.6–0.8 W/m²K (Gustavsen et al., 2011). To achieve a U-value of approximately 0.5 W/m²K, there typically needs to be three panes with krypton or xenon gas fill, two or

more layers of low-E coating and insulated spacers (Gustavsen et al., 2011). For this research, based on ASHRAE's typical North American residential window U-values, the Efficient Windows Collaborative and PHI's recommended glazing for various climatic regions, the definition of a high performance window for a cold climate contains double panes, argon gas infill, low-E coating(s), insulated spacers and an insulated non-metal frame with a maximum U-value of $1.25 \text{ W/m}^2\text{K}$ (Passivhaus Institut, 2012) (ASHRAE, 2009) (Efficient Windows Collaborative, 2012). For the warmer climatic regions of North America, a high performance window contains at least two panes, argon gas infill, a low-E coating, solar control coatings, insulated spacers and an insulated non-metal frame with a maximum U-value of 1.70 (Passivhaus Institut, 2012; ASHRAE, 2009; Efficient Windows Collaborative, 2012).

Currently, however, in North America, high performance windows are minimally used. Rather, the most common residential window being used is the double-glazed vinyl framed window (Hopwood, 2013). In Canada, 54% of window frames were made of vinyl, 39% wood and wood-clad, 6% aluminum and 1% was made of other materials (Parekh, 2010). In the U.S., vinyl accounts for 67.9% or two thirds of the residential market, wood-framed windows follow comprising approximately 20%; aluminum and other materials such as fiberglass and composites (including insulated PVC) cover the least portion of the market with roughly 5-6% each (Ducker Research Company, 2012).

Seeing that the metrics for thermal performance are integral in determining what defines a high performance window, the calculation methods that these metrics are derived from are very significant. Since the U-values of North American and European window products are being calculated differently, there are numerous impacts on the building industry. North American window manufacturers are particularly interested in this debate for they are adversely affected by the difference in stated U-values for window products, depending on the calculation method used, considering that builders of high performance homes tend to choose windows with the lowest U-value (Hanam, 2013). For a typical window, because the NFRC method tends to give a higher U-value, builders tend to choose European windows rather than North American windows (Hanam, 2013). How can products be compared appropriately if the performance values are not calculated in the same way? Energy modellers may be inputting numbers without the understanding of where they come from and not understanding or realizing that the numbers are not necessarily correct or appropriate for a specific climate zone. Generally speaking, NFRC testing methods generally give a specific window an approximation of 10% more heat flow than the value derived from tests according to European standards (Straube J. , 2009) (Rosenbaum & White, 2009). Arestah et al. (2001) found that for a typical vinyl window frame, the

frame U-value differs by $\pm 10\%$ between the interpretations of the NFRC and CEN method. However, according to the literature, the differences between the calculations depend upon various assumptions and boundary conditions and when looking at high performance windows, the results do not align with the generalized assumption of 10% (Hanam, 2013).

In addition to the U-value, there is more thermal transmittance, or thermal bridges, that occur at the junctions of materials. Since windows are “held structurally in the building [envelope], windows almost always involve thermal bridges” (Hutcheon & Handegord, 1995). A performance metric that measures potential thermal bridges is the Linear Thermal Bridge Coefficient or Ψ -value. The Ψ -value is described as the additional linear thermal transmittance, which is the additional heat loss that is transmitted through the junctions between different materials; it is the additional transfer of heat that occurs between and through the different materials that are conjoined in an area. Ψ values are used by European window manufacturers who abide by standards set by the International Standard Organization (ISO) and the European Committee for Standardization (CEN). European Passive House window manufacturers use the CEN /ISO linear method (EN 673/ISO 10077) for calculating various detailed thermal values for a window that includes: total solar energy transmittance, Ψ -value, U-value of the frame, Ψ - value of the spacer, and center-of-glazing U-value.

Generally in the building industry in North America, there is a lack of information about the Ψ -values of different window types and the ways in which to use this parameter in measuring potential thermal bridging that is already widely used in Europe. Manufacturers are not required to calculate Ψ -values; the main energy performance ratings that are voluntarily reported on the NFRC label are U- values and SHGC values (Ducker Research Company, 2012) (NFRC, 2012). Ψ -values are voluntarily given only by a few individual window manufacturers that choose to include them in their technical specifications. Maximum Ψ values are not required by any building codes, thus, unless a builder is determined to calculate the potential thermal bridge losses for an individual project, there is otherwise a lack of incentive to do so since this parameter is not required by code.

Currently, energy performance testing of windows is not mandatory in all of Canada; it is only required in some provinces such as Ontario, British Columbia, Yukon and Nova Scotia (NRC, 2012) and for windows exported to the United States. The NAFS (North American Fenestration Standard), in conjunction with the Canadian Standards Association’s standard A440S1-09, are currently replacing older Canadian standards in order to harmonize the Canadian and American performance standards (NRC, 2012) (Rogers, 2014). These standards specify minimum performance ratings for the U-value,

wind load resistance, air tightness and water tightness (Canadian Standards Association, 2009). The U-values that are used in the energy performance ratings, specified by these standards, are calculated according to the NFRC U-value calculation method (Canadian Standards Association, 2009). Thus, the U-value calculation method is integral to establishing the energy performance ratings for national window standards and for setting energy efficiency targets as outlined, for example, in Ontario's supplementary standard SB-12 (Ministry of Municipal Affairs and Housing, 2006).

There is a lack of information in the literature as to the nature of the thermal transmittance of a window, the overall U-value and Ψ value, and changes according to different boundary conditions within the climate zones in North America. According to the IECC and ASHRAE, there are eight climate zones for North America; four of these are in Canada. A comparative evaluation of the differences between the NFRC and CEN methods of calculating the overall U-values and Ψ -values and how these values change for high performance windows when applying different assumptions and boundary conditions, were explored in the research using the IECC's eight climate zone specifications. Furthermore, the possible harmonization of both methods will be postulated.

1.3 Research Contribution

By highlighting the parameters and assumptions that affect the overall U-value in the eight climate zones in North America, window design can be tailored to achieve high thermal performance in climate specific areas. Drawing comparisons of the NFRC and CEN U-value calculation methods using different boundary conditions can enhance the current research specific to North America. Evaluating the Ψ -value can help measure the magnitude of the potential for thermal bridging in various window frames in the eight climate zones. This research is relevant for the North American window manufacturers, building scientists, architects, engineers, energy modellers, and builders of high performance homes.

2 Literature Review

North American contributions to the window industry have been extremely significant, seeing that it was a North American inventor that profoundly changed the window industry with the beginnings of a high performance design. An American patent solicitor and expert, Thomas Stetson patented the first insulating glass unit in 1865 (see Figure 1) (Stetson, 1865). It consisted of two panes of glass tightly joined at their edges, nailed or tacked to the sash; the panes were kept separated by a strip of wood or string (Stetson, 1865). The first spacer was made of wood or string. Putty, made of whiting (finely ground chalk) and oil (linseed), or other material, was placed along the edges in between the panes in order to provide a seal and bind them together (Stetson, 1865). Today, innovation in window design continues to be a very lucrative area for window manufacturers to focus upon as the demand for high performance glazing grows with the demand for high performance buildings.

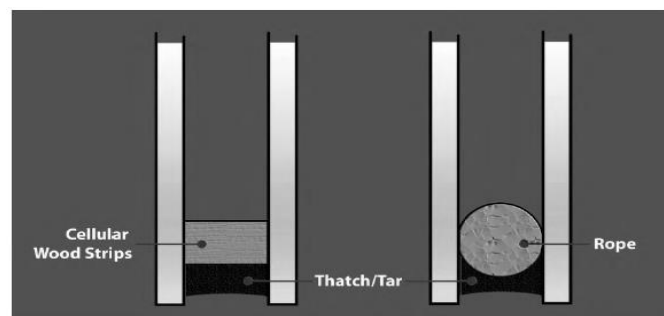


Figure 1 First Insulated Glazing Unit by Thomas Stetson (Lingnell, 2011)

2.1 Thermal Transmittance Challenges

The U- value or thermal transmittance through the frame and glazing depends upon the configuration and properties of the glazing system materials; i.e. thermal conductivity, thermal expansion, vapour pressure etc.

The thermal transmittance is typically lower in the glazing than the frame due to the material and gas properties. In the past, the thermal transmittance of the center-of-glass area (see Figure 2), was used by window manufacturers to describe the energy performance of the whole window product (Canadian Standards Association, 2009). The U_{cog} area does not take into account for the area where the thermal bridging effects of the interaction of the frame and sash materials and thus gave energy performance values that were overstated in the past when single or double glazing was used (Canadian Standards Association, 2009). These values were thus also misleading for builders that installed these windows who were lead to believe that they were using a certain U- value when in fact the overall U- value was

much less after installation when factoring in the different thermal transmittance values of the window components and their effect on the whole window thermal transmittance.

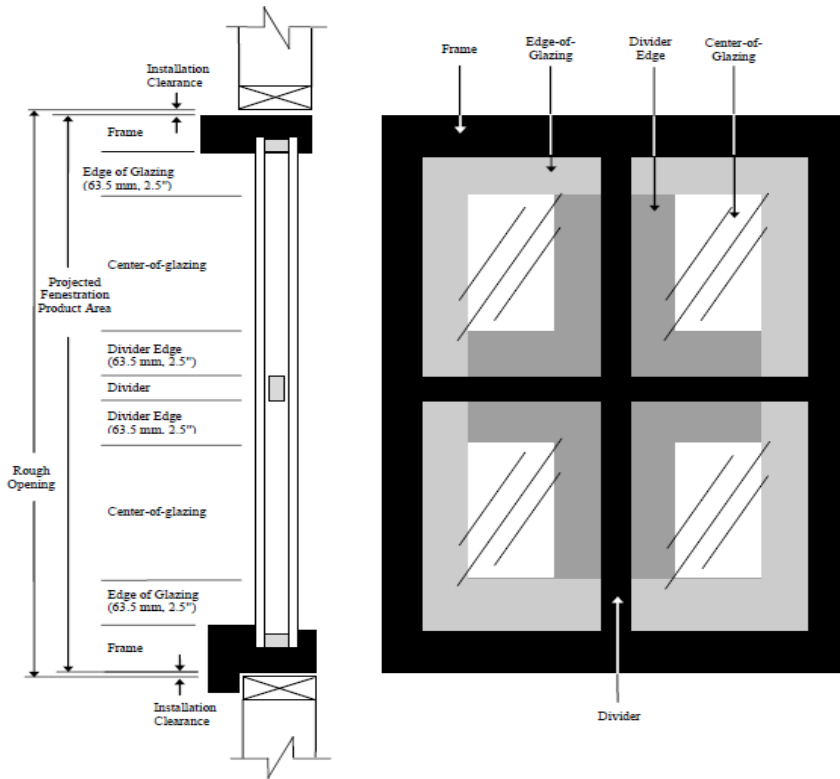


Figure 2 Window Product Diagram (NFRC, 2010)

What compounds the complexity of this situation is that not only do various component details possess different U-values, the calculation methods used to determine whole window product U-values, (U_{window}), in North America and Europe have significant differences. Straube identifies that for a specific window, NFRC testing methods generally give an approximation of 10% more heat flow than the value derived from tests according to European standards (Straube J. , 2009) (Rosenbaum & White, 2009) (Varshneya, Rosaa, & Shapiroa, 2012). However, according to the literature, when specific windows are evaluated, the results do not congrue with the generalized assumption of 10%. In a comparative study of three double-glazed windows, (vinyl, fiberglass and certified PH), $U_{\text{window-NFRC}}$ was typically 5-7% higher than $U_{\text{window-CEN}}$ (Hanam, 2013). For triple-glazed windows, the differences were smaller (Hanam, 2013). When high and low solar heat gain glazing were compared, there was a 12% difference between the NFRC and CEN solar heat gain coefficients for the low solar heat gain glazing and only a 1% difference for the high solar heat gain glazing (Hanam, 2013). This difference was attributed to the different values for the instant solar radiation in both methods (Hanam, 2013).

These numerous differences have spurred a long standing debate leaving more questions as to which thermal transmittance calculation is more accurate and what parameters in the boundary conditions are the most influential and how do these parameters affect the overall thermal transmittance of a window.

2.2 The NFRC Thermal Transmittance Calculation Method

The NFRC created a windows ratings system that is currently used by the majority of window manufacturers in Canada and the US. These ratings give performance metrics whereby window products can be compared with each other on the same level with specific metrics. The NFRC product labels primarily give whole product energy performance ratings, specifically the U- value, solar heat gain coefficient, and visible transmittance. Additionally the labels may include air leakage and condensation resistance. The U- value of a window is derived from the material properties of the different component materials that constitute the glazing, the frame and spacer (Section 5.2, NFRC 100). According to section 4.3 of NFRC 100-2010[E0A7] Procedure for Determining Fenestration Product U-values, the overall U- value is calculated *only* according to the area –weighted method outlined in ISO 15099 Section 4.1.3; a specific model size is used [see Table 7]. From the initial draft of an ASHRAE standard in the 1990s (by ASHRAE Special Project Committee 142), then further developed by the ISO with contributions from the CEN member nations, thermal transmittance calculation methods were established in the standard ISO 15099 (ASHRAE, 1998) (Blanusa, et al., 2007). “This standard includes both the one-dimensional thermal calculation methodologies used in the WINDOW (LBNL, 1994) and VISION (Wright J. , 1995) programs and in ISO 10077-1 (ISO, 2000) and the two-dimensional frame/spacer heat transfer calculation methodologies used in the FRAME (EEL, 1995) and THERM (LBNL, 1998) programs and in ISO 10077-2 (ISO, 2012) (Blanusa, et al., 2007).” In this method, the frame, divider, edge-of-divider, edge-of-glazing and center-of-glazing U- values are multiplied by their associated areas and summed altogether. This summed value is then divided by the projected fenestration project area to give the total fenestration product U-value, as seen in Equation 1:

$$U_{W-NFRC} = \frac{[\sum(U_{frame}A_{frame}) + \sum(U_dA_d) + \sum(U_{edge}A_{edge}) + \sum(U_{de}A_{de}) + \sum(U_{cog}A_{cog})]}{A_{pf}} \quad (1)$$

Where:

U_{W-NFRC} = Whole Window U- value

A_{pf} = Projected Fenestration Product Area

U_{frame} = Frame U- value

U_{edge} = Edge-of-Glazing U- value

A_{edge} = Edge-of-Glazing Area

U_{de} = Edge-of-Divider U- value

A_{frame} = Frame Area
 U_d = Divider U- value
 A_d = Divider Area

A_{de} = Edge-of-Divider Area
 U_{cog} = Center-of-Glazing U- value
 A_c = Center-of-Glazing Area (ISO, 2003)

The projected area (i.e. surfaces facing the plane), is placed on a plane parallel to the glass and does not comprise the total surface area of the frame and edge-of-glazing (LBNL, 2013) (see Figure 2). The frame, divider, edge-of-divider, edge-of-glazing and center-of-glazing U- values are calculated using a 2-D heat transfer simulation program approved by the NFRC.

The U_{cog} values for the NFRC and CEN methods and the whole window U-values (U_{w-NFRC}) for the NFRC method (U_{w-NFRC}), are determined using the WINDOW 6.3 program. The THERM program applies a finite element method to a 2-D energy equation in order to calculate the frame and edge-of-glazing U-values; these values are utilized in WINDOW to determine the overall U-value (LBNL, 2013).

THERM and Window (6.3 and 7.2) are part of the NFRC approved software list for conducting heat transfer modelling for fenestration products (NFRC, 2012). The NFRC procedure for determine whole window U-values (NFRC 100-2010) also states that all thermal transmittance calculations are to be based on computer simulations. Simulations in this research utilize THERM and WINDOW 6.3 to determine fenestration U-values since this version is specified for NFRC certification purposes; version 7.2 is primarily for fenestration products with shading devices.

2.2.1 U_{frame} Calculation in the NFRC Method

In calculating U_{frame} , the rate of heat flow through the frame with the glazing unit inserted is accounted for along the projected length of the frame along the inside edge (see Figure 2). The rate of heat flow, Φ , is largely influenced by the temperature difference between the interior and exterior environments. The definition and calculation of the heat flow through the frame, Φ_{fr} , will be discussed further. The NFRC method and THERM use the following equation to calculate the frame U-value:

$$U_{frame-NFRC} = \frac{\Phi_{frame}}{l_{frame}(T_{ni}-T_{ne})} \quad (2)$$

Where:

$U_{frame-NFRC}$ = frame U-value (W/m^2K)

Φ_{frame} = Phi of the frame; rate of heat flow through the frame (W/m)

l_{frame} = projected length of the frame area on the inside edge (m)

T_{ni} = temperature of the interior environment (K)

T_{ne} = temperature of the exterior environment (K) (ISO, 2003)

Since the frame U-value is determined by the NFRC method with the insulated glazing unit insert, $U_{\text{frame-NFRC}}$ not only accounts for the thermal transmittance through the frame, it also accounts for a portion of the thermal transmittance effects of the glazing and spacer materials and configurations upon the frame. The majority of these thermal transmittance effects are comprised in the $U_{\text{edge-NFRC}}$ variable.

2.2.2 U_{edge} Calculation in the NFRC method

According to the NFRC method, by calculating an area-weighted edge-of-glazing region, (see Equation 3) the edge effects that occur at the junction of the frame, spacer and edge of glass area are taken into account (ISO, 2003). The edge effects describes the additional thermal transmittance that occurs between the glazing, frame, spacer and seals and helps to account for the interactions that occur and how they are influenced by differences in material thermal conductivities and configurations. The edge-of-glazing area is situated 63.5mm (2.5") from the inside frame edge. $U_{\text{edge-NFRC}}$ accounts for the rate of heat flow through the edge-of-glazing area along the projected length of the inside edge of the frame with the glazing unit insert. Similar to $U_{\text{frame-NFRC}}$, the $U_{\text{edge-NFRC}}$ calculation is largely influenced by the temperature difference between the interior and exterior environments. The NFRC method uses the following equation to calculate the edge-of-glazing U-value:

$$U_{\text{edge-NFRC}} = \frac{\Phi_{\text{edge}}}{l_{\text{edge}}(T_{\text{ni}} - T_{\text{ne}})} \quad (3)$$

Where:

$U_{\text{edge-NFRC}}$ = edge-of-glazing U-value ($\text{W}/\text{m}^2\text{K}$)

Φ_{edge} = rate of heat flow through the edge-of-glazing area (W/m)

l_{edge} = projected length of the frame on the inside edge (m)

T_{ni} = temperature of the interior environment (K)

T_{ne} = temperature of the exterior environment (K) (ISO, 2003)

The length of the edge-of-glazing area of 63.5 mm is used to lessen the difference between the two different thermal transmittance methods (ISO, 2003). The value of 63.5 mm that denotes the edge-of-glazing area was determined using 2-D computer modeling based on only conduction heat transfer effects. However, ASHRAE states that “in reality, because of convective and radiative effects, this area may extend beyond 63.5 mm (Beck et al., 1995; Curcija and Goss, 1994) and depends on the type of insulating glazing unit and its thickness” (ASHRAE, 2009). The variability of the area affected by the edge effects is discussed further in the section “Differences between the NFRC and CEN U-value Calculation Methods”.

2.2.3 Phi Variable

Phi in the $U_{\text{frame-NFRC}}$ and $U_{\text{edge-NFRC}}$ calculations is defined as the “heat flow in the direction of normal of the frame boundary segments for the frame section, and all of the edge boundary segments for the edge” (Curcija C. , Windows and Envelope Materials Group, LBNL, 2014). THERM calculates Phi, on the indoor side of the frame boundary (from the end of the adiabatic surface to the sightline) (Curcija C. , Windows and Envelope Materials Group, Lawrence Berkeley National Laboratory, 2013). Phi-frame and Phi-edge account for the heat transfer effects of the glazing and the spacer “through the indoor surfaces of the frame and edge-of-glass areas (ISO, 2003)”. Although Phi is a three dimensional variable, the NFRC method calculates U-values in a 2-D fashion using 2-D software (Curcija C. , Windows and Envelope Materials Group, Lawrence Berkeley National Laboratory, 2013). Therefore, the 3-D effects are not taken into account. 3-D modeling of the window components only achieves less than 1% of an improvement in accuracy; the amount of time and complexity of this modeling, in the point of view of various experts, does not seem suitable in order to attain this minute improvement (Curcija C. , Windows and Envelope Materials Group, Lawrence Berkeley National Laboratory, 2013).

Some of the nomenclature used by the NFRC method is not the same nomenclature as what is found in ISO 15099 (Curcija C. , Windows and Envelope Materials Group, LBNL, 2014). Heat flow, or Phi, is instead labeled as Q, which is considered standard notation for heat flow (Curcija C. , Windows and Envelope Materials Group, LBNL, 2014). The governing equation that THERM uses for 2D conductive heat transfer or Q is sourced from the Conrad 5 & Viewer 5 Technical and Programming Documentation (LBNL, 2006) and is noted as follows:

$$-\left[\frac{\partial}{\partial x} \left(k_{11} \frac{\partial T}{\partial x}\right) + \frac{\partial}{\partial y} \left(k_{22} \frac{\partial T}{\partial y}\right)\right] = Q \quad (4)$$

Where:

K_{11} = conductivity in the x direction

k_{22} = conductivity in the y direction

T = temperature on surface (constant temperature on boundary surface) (LBNL, 2006)

This calculation assumes that all materials have constant physical properties and that there is a constant temperature on each boundary surface.

2.2.4 NFRC Boundary Conditions

According to Section 8.2 of ISO 15099, “Unless a specific set of boundary conditions is of interest (e.g., to match test conditions, actual conditions or to satisfy a national standard), the following standard boundary conditions shall be used.” In order to adjust the international standard to be more fitting with the US (North American) climate as opposed to the European climate, the NFRC uses different boundary conditions than those outlined in the ISO 15099, for determining the overall U- value. For example, the ISO 15099 uses different exterior temperature, incident solar radiation, wind speed and surface film coefficients (see Table 1 & 2).

The NFRC winter boundary conditions are outlined in the following table:

Table 1 Boundary Conditions used for NFRC U- value calculations

Boundary Condition		NFRC	ISO 15099
Interior Ambient Temperature	T_{in}	21°C	20°C
Exterior Ambient Temperature	T_{out}	-18°C	0°C
Wind Speed	V	5.5 m/s	4 m/s (EN ISO 6946)
Outdoor Mean Radiant Temperature	$T_{rm,out}$	T_{out}	T_{out}
Indoor Mean Radiant Temperature	$T_{rm,in}$	T_{in}	T_{in}
Total flux of incident solar radiation	I_s	0 W/m ²	300 W/m ²

Thermophysical properties of materials are referenced only from NFRC 101. The indoor and outdoor convective film coefficients are determined according to Section 8.3 in ISO 15099. The outdoor convective heat transfer coefficient is calculated based on the wind speed and then used on the outdoor surface of the glass and frame. Table 2 gives standard values that can be used for the outdoor convective film coefficient. The indoor convective heat transfer coefficient of the indoor surfaces of the glass and edge of glass area is based on the center-of-glazing temperature and the whole window height. The indoor convective film coefficients of the indoor surface of the frame are constants and vary according to the type of frame material; these are listed in Table 2.

Table 2 NFRC 100-2010 Interior and Exterior Convective Film Coefficient Boundary Conditions for Total Fenestration Products

Boundary Condition	NFRC (Tilt = 90°) (W/m ² K)	ISO 15099 (W/m ² K)
NFRC 100-2001 Exterior	26.00	20
Interior Aluminum Frame (convection only)	3.29	3.6
Interior Thermally Broken Frame (convection only)	3.00	
Interior Thermally Improved Frame (convection only)	3.12	
Interior Wood/Vinyl Frame (convection only)	2.44	

2.3 The European (CEN) Thermal Transmittance Calculation Method

According to a convenor of one of the ISO responding CEN working group, European manufacturers currently use the U_{window} calculation as outlined in ISO 10077-1:2006 to determine the thermal transmittance of their window products (Norbert Sack, Convenor CEN TC89/WG7, and Dick van Dijk, August 12, 2013). “The thermal losses caused by the installation of the window in the wall are not taken into account in the U-value of the window.” (Norbert Sack, Convenor CEN TC89/WG7, August 12, 2013) It is important to note that U_{window} only refers to the actual window product, the thermal characteristics of the window after installation differs and another calculation can be used to determine the thermal performance of the installed window. The Passive House Institute currently uses the installed window thermal transmittance, or Ψ_{install} for their calculations (Feist, 2006). Ψ_{install} measures “the linear thermal bridge at the junction of the wall and the window frame, and accounts for all additional losses or unexpected gains” (Speier, 2012). Techniques such as over-insulating the window frame on the exterior side can increase the thermal performance of the whole window (Speier, 2012).

Although the NFRC and CEN thermal transmittance calculations differ, both procedures abide by the ISO standards.

As noted by one of these experts, the reason why there are different methods to calculate the U-value and solar heat gain coefficient is because of the “autonomy of each Technical Committee combined with historic reasons” (van Dijk, 2013). The industry sector is reluctant to certain changes because changing a standard would lead to a change in the product values and thus create conditions that are not always amicable on the point of view of the industry sector (van Dijk, 2013). Extrapolating from this, there is sometimes a large learning curve to learn the new method of calculating a window product value. It takes time and money to transition to the new changes and these changes would further involve retesting and recalculating the multitude of window products of every manufacturer. This is part of the reason why the window industry may be reluctant and why it takes time for changes to occur.

Despite this reluctance, if required by codes and standards, manufacturers in effect, step up to the plate and meet the requirements in order to have their products on the market. Sweden, as mentioned earlier, mandated the use of triple-glazed windows as early as 1976 (Wilson, 2009). New methods may change the product values which may raise or lower the performance of individual window products. In the case of window products that receive a lower performance level with the new method, this situation can present itself as a challenge to manufacturers to improve the performance of their products. In this way the quality of window products on the market are raised.

As of this writing, as assigned by ISO/TC 163/SC 2, experts are working to further the international standardization by removing the differences in the U-value and solar transmittance CEN and ISO calculation methods as well as removing the differences between the glazing product standards and window standards (Dick van Dijk, Sept 2, 2013). In this way, bridges are being forged between the standards and manufacturers in order to aid in the transition towards the use of amalgamated calculation methods.

2.3.1 CEN U_{window} Calculation Method

Since the 1980s, the ISO worked on the development of thermal transmittance calculation methods for windows; the result of this work is the ISO 10077-1:2006 standard. The European Committee for Standardization (CEN) formulated the ISO 10077-2 to address the heat transfer specificities in the frame, particularly along the spacer and edge-of-glazing areas. In the CEN U-value calculation method of a single window, the thermal transmittance of the glazing and frame are calculated separately and the linear thermal transmittance (Ψ value) is added to the summation (see Equation 5). The edge effects are taken into account in the Ψ value (see Equation 8). European window manufacturers refer to the

following calculation to determine the whole window U-value, as outlined in ISO 10077-1; the U-value of the frame is calculated according to the procedures outlined in ISO 10077-2.

$$U_{w-CEN} = \frac{\sum A_g U_{cog} + \sum A_{frame} U_{frame} + \sum l_g \Psi_g}{\sum A_g + \sum A_f} \quad (5)$$

Where:

U_{w-CEN} = Whole window U-value

A_g = Glazing Area

$U_{cog-CEN}$ = Center-of-Glazing U-value

A_{frame} = Frame Area

U_{frame} = Frame U-value

l_g = length of the glazing area on the inside edge

Ψ_g = Ψ value or linear thermal transmittance due to the combined thermal effects of the glazing, spacer and frame (ISO, 2012)

This method is sometimes referred to as the ‘linear method’ because it assumes that “the additional heat transfer due to the existence of the spacer is proportional to the glazing/frame sightline distance that is also proportional to the total glazing spacer length”, thus giving a linear basis to the spacer heat transfer effects (Blanusa, et al., 2007).

2.3.2 U_{frame} calculation in the CEN method

In calculating $U_{frame-CEN}$, a calibration panel with a thermal conductivity of 0.035 W/mK replaces the glazing, (see Figure 3) in order to measure the thermal transmittance of the frame **without** the effect of the glazing (ISO, 2012). The center-of-panel U-value (U_p) is located 190 mm from the sightline in order to obtain the U-value of the panel without potential thermal transmittance effects of the frame upon its U-value. The CEN method uses the following equation to calculate the frame U-value.

$$U_{frame-CEN} = \frac{L_{frame}^{2D} - U_p b_p}{b_{frame}} \quad (7)$$

Where:

$U_{frame-CEN}$ = thermal transmittance of the frame (W/m²K)

L_{frame}^{2D} = thermal conductance of the section shown in Figure 2

U_p = center of panel U-value (W/m²K)

b_p = visible width of the panel (larger width) (m)

b_f = projected width of the frame section (m) (ISO, 2012)

This constant approach in using the calibration panel to measure the thermal transmittance of the frame component allows for different frame products to be compared fairly (Richman, 2013).

2.3.3 Thermal Conductance of the Frame with the Calibration Panel

The thermal conductance of the frame with the calibration panel (L_{frame}^{2D} ; see Figure 3) is calculated by taking $U_{frame-CEN}$ and multiplying it by the projected width of the frame section and adding it to the U-value of the calibration panel multiplied by its length. The U-value of the calibration panel (U'_p) differs from the U-value of the center of the panel (U_p), whereby U'_p is calculated 190 mm from the sightline and the length of the calibration panel is set at 190 mm by ISO 10077-2. The calculation for the frame's thermal conductance with the calibration panel is as follows:

$$L_{frame}^{2D} = U'_{frame} b_{frame} + U'_p b_p \quad (6)$$

Where:

L_{frame}^{2D} = thermal conductance of the section shown in Figure 2 (W/mK)

U'_{frame} = frame U-value with the calibration panel inserted (W/m²K)

b_{frame} = projected width of the frame section (m)

U'_p = calibration panel U-value (190 mm from sightline) (W/m²K)

b_p = length of the calibration panel for 2-D heat transfer effects (fixed at 190 mm by ISO/CEN 10077) (mm) (LBNL, 2009)

Since the U-value of the panel (U'_p) is obtained along the entire 190 mm panel length (b_p), the U'_p accounts for a portion of the thermal transmittance effects that the frame materials and configuration has upon the panel's overall U-value.

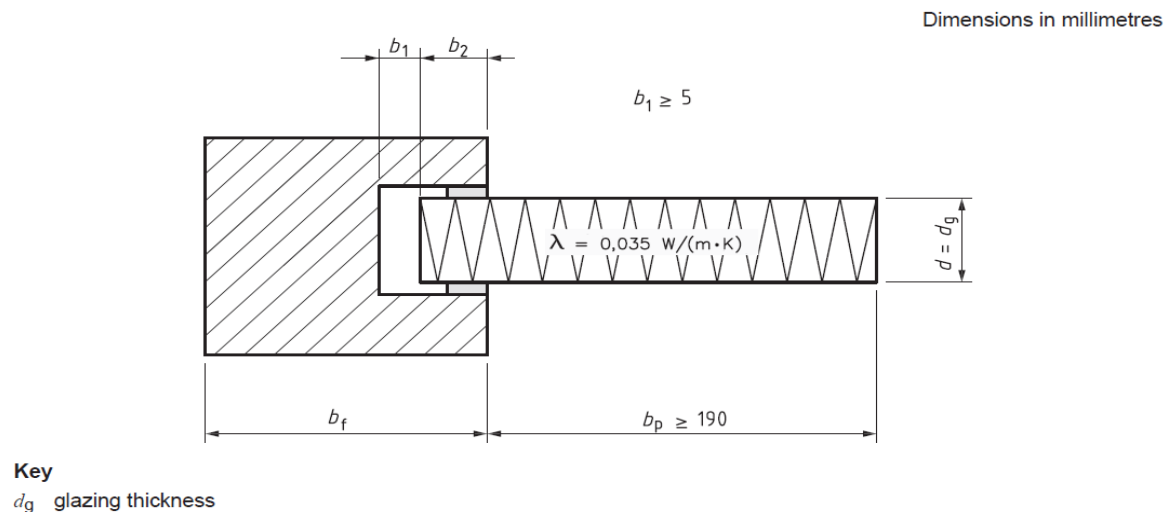


Figure 3 Frame Section with Calibration Panel Insert (ISO, 2012)

2.3.4 Thermal conductance of the Frame with Glazing Unit

The thermal conductance of the frame with the glazing unit (L_{Ψ}^{2D}), is calculated linearly using the projected width of the frame section and the height of the edge-of-glazing is 190 mm from the sightline. The thermal conductance affected by the interactions of the glazing, spacer and frame are accounted for by this calculation and the 190 mm edge-of-glazing area gives a sufficient length to account for any potential edge effects on the glazing. The thermal conductance calculation of the section shown in Figure 3 is as follows:

$$L_{\Psi}^{2D} = U_{frameIGU-CEN} b_{frame} + U_{edge-CEN} b_g \quad (8)$$

Where:

L_{Ψ}^{2D} = thermal conductance of the section shown in Figure 2 (W/m·K)

$U_{frameIGU-CEN}$ = frame U-value with glazing unit (W/m·K)

b_{frame} = projected width of the frame section (m)

$U_{edge-CEN}$ = edge of glazing U-value (W/m·K)

b_g = height of the edge-of-glazing (m) (190 mm from the sightline) (LBNL, 2009)

2.3.5 Ψ -Value Calculation Method

The Ψ value calculation below describes the additional linear thermal transmittance, or Ψ -value (Ψ), that is derived by subtracting the thermal transmittance of the frame (see Equation 6) and the glazing by itself (U_g), from the two dimensional thermal conductance of the frame with the glazing installed (see Figure 4). In this way, the additional thermal transmittance that occurs from the interactions of the spacer, glazing and frame are taken into account in the Ψ value.

$$\Psi = L_{\Psi}^{2D} - U_{frame-CEN} b_{frame} - U_{cog-CEN} b_g \quad (9)$$

Where:

Ψ = Ψ -value (linear thermal transmittance) (W/m·K)

L_{Ψ}^{2D} = thermal conductance of the section shown in Figure 3 (W/m·K)

$U_{frame-CEN}$ = frame U-value (with calibration panel)

b_{frame} = projected width of the frame section (m)

$U_{cog-CEN}$ = glazing U-value

b_g = visible width of the glazing (m) (ISO, 2012)

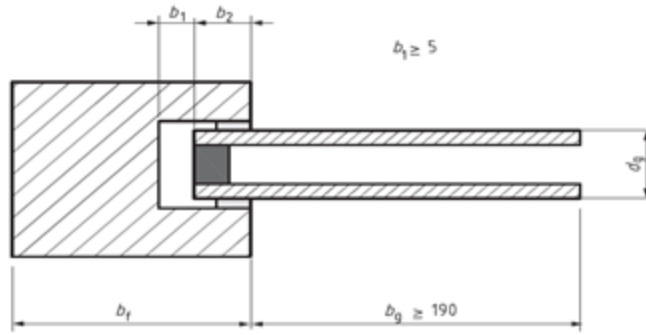


Figure 4 Frame section with glazing installed (ISO, 2012)

In a study of the heat distribution of various components of a variety of residential buildings, the determination and evaluation of the Ψ value showed that the thermal bridging through windows junctions entailed the largest thermal transmittance, 40% of the total specific heat loss of all the junctions (including the roof, walls and floor junctions) (Janssens, Van Londersele, Vandermarcke, Roels, Standaert, & Wouters, 2007). A Ψ value of 0.10 W/mK was determined to be the maximum value for a window in order to prevent significant heat loss through the building envelope (Janssens et al., 2007). In determining the Ψ values and isothermal lines of various window constructions, Ben-Nakhi (2002) found that the magnitude of thermal bridges could be assessed as well as the effectiveness of different window designs used to minimize thermal bridges. In this way design decisions can be compared and evaluated.

2.4 Primary Differences between the NFRC and CEN U_{window} Calculation Methods

The primary differences in the boundary conditions and other parameters between the NFRC and CEN methods for calculating U_{window} and the Solar Heat Gain Coefficient are outlined in Tables 3 and 4. The key boundary conditions highlighted are the interior and exterior temperatures, wind velocities, incident solar flux, and surface film coefficients.

Table 3 Differences between the NFRC and CEN calculation methods for determining the U-value (McGowan, 2013)

	North America (NFRC)	Europe (CEN)
ISO Standard Used	ISO 15099	ISO 10077
Interior Temperature	21.1°C	20°C

Exterior Temperature	-18°C	0°C
Exterior Wind Velocity	5.5 m/s	4 m/s

Table 4 Differences between the NFRC and CEN calculation methods for determining the Solar Heat Gain Coefficient or "g-value" (McGowan, 2013)

	North America (NFRC)	Europe (CEN)
ISO Standard Used	ISO 15099	ISO 10077
Interior Temperature	24°C	25°C
Exterior Temperature	32°C	30°C
Exterior Wind Velocity	2.8 m/s	1m/s
Incident Solar Flux	783 W/m ²	500 W/m ²
Solar Spectrum	NFRC 300, ASTM E891	EN 410

Table 5 shows the way in which the surface resistances are given different values by both methods. The difference in the surface resistance values are significant because the surface resistance can be very influential in the overall insulative properties of a window (Hutcheon & Handegord, 1995). Griffith et al. (1996) found that the surface resistances or surface film coefficients differ according to local conditions.

Table 5 Surface Resistances (horizontal heat flow) of the CEN and NFRC Calculation Methods (National Fenestration Rating Council, 1997) (ISO, 2012)

Calculation Method	Position	External, R _{se} (W/m ² K)	Internal, R _{si} (W/m ² K)
ISO 10077-2 (CEN)	Normal (plane surface)	25	7.69
ISO 10077-2 (CEN)	Reduced radiation/convection [in edges between two surfaces]	25	5
NFRC	Aluminum	26	3.29
	Thermally Broken Frame	26	3.00
	Thermally Improved Frame	26	3.12
	Wood/Vinyl Frame	26	2.44

The NFRC and CEN methods translate 2-D into 3-D thermal transmittance effects differently in their calculations (see Equations 1 and 5). In the NFRC method, the “2-D results for U_{frame} and U_{edge} (defined as 63.5 mm of glazing measured from sightline) and 1-D results for U_{cog} (glazing area excluding edge of glazing) are area-weighted to produce the whole product U-[value] (Curcija C. , Windows and Envelope Materials Group, Lawrence Berkeley National Laboratory, 2013)”. The CEN method uses the 2-D results for $U_{\text{frame-CEN}}$ and $U_{\text{edge-CEN}}$; the 1-D results are used for $U_{\text{cog-CEN}}$ and for linear thermal transmittance. The glazing U-value is treated as one dimensional by both methods, however, the CEN method takes into account the whole glazing area that is bordered by the sightline, whereas the NFRC method *only* takes into account the center-of-glazing area that is *adjacent* to the edge-of-glazing area (see Figure 2).

2.4.1 U_{frame} and Edge Effects

The NFRC and CEN whole window calculation methods are similar in that they both account for the thermal conductivity of the frame with the IGU; where the CEN method uses $U_{\text{frameIGU-NFRC}}$ in the Ψ -value calculation (see Equation 9). However, as reiterated in the RDH Building Engineering Ltd. (2014) study, the U_{frame} values of both methods are not comparable. One of the key differences between the CEN method and the NFRC method is that the CEN method uses a calibration panel, with an extremely low thermal conductivity (i.e. 0.035 W/mK), to determine $U_{\text{frame-CEN}}$; $U_{\text{frame-CEN}}$ is used in addition to $U_{\text{frameIGU-NFRC}}$ to derive the Ψ -value (see Equation 9). With the use of a calibration panel, the thermal transmittance of the frame itself is acquired without the influence of the thermal properties and configurations of the IGU. The use of a calibration panel to determine $U_{\text{frame-CEN}}$ gives a common standard element that can be used to compare frames on the same level (Wright G. , 2012). In addition, the calibration panel allows for the measurement and comparison of the incremental effect of the thermal performance of IGUs when combined with a frame configuration. Whereas in the NFRC method, the U_{frame} is determined by incorporating the simulated frame with the actual glazing system instead of a calibration panel (Gustavsen, Petter Jelle, Arasteh, & Kohler, 2007).

Simulating the actual glazing system in the frame, when determining the thermal transmittance of the frame in the NFRC method, results in a U_{frame} value that includes a portion of the edge effects that occur from the heat transfer interactions of the actual glazing, spacer and frame materials. In addition, ISO (2003) states that the difference between the $U_{\text{frame-NFRC}}$ and $U_{\text{frame-CEN}}$ is that $U_{\text{frame-NFRC}}$ incorporates “some of the heat transfer caused by the edge seal whereas $U_{\text{frame-CEN}}$ does not”. Thus, the edge effects are accounted for in the NFRC method by $U_{\text{edge-NFRC}}$ and $U_{\text{frame-NFRC}}$ and solely by the Ψ -value in the CEN method. $U_{\text{frame-NFRC}}$ therefore does not give the thermal transmittance of the frame by itself, whereas

the CEN method gives a more accurate U_{frame} value due to the calibration panel. Seeing that the two methods have different calculations and thus explanations for the thermal transmittance of the frame, in effect, the ISO (2003) suggests that the same calculation be used for window products in order to compare them on the same grounds.

The U_{edge} of both methods differ where $U_{\text{edge-NFRC}}$ uses a length of 63.5 mm and $U_{\text{edgeIGU-CEN}}$ uses 190 mm to account for the edge effects. A study conducted by Blanusa et al. (2007) found the two methods differ in the way in which they treat the spacer and its interactive effects on the heat transfer of the frame and edge-of-glazing area. Carpenter and Elmahdy (1994) and Elmahdy (2004) showed that a 63.5mm region gave sufficient results for ten different windows, however, Curcija and Goss (1994)'s study found that 100 mm accounted for the frame and spacer 2-D heat transfer effects on the glazing, in a wood-framed window, more accurately than the 63.5mm region. In addition, Weitzmann et al. (2000) found that the 63.5 mm rule did not sufficiently encompass the two dimensional edge-of-glazing effects between the spacer, frame and glazing for a typical Danish wood-framed window. Rather, this study concluded that an edge-of-glass length of 150 mm was more accurate.

ASHRAE (2009) acknowledged that due to the advance in technological innovations in the high performance window industry, the 63.5 mm value may not be sufficient for all windows. Determining the suitability of the 63.5 mm edge-of-glazing area by testing various high performance windows with a thermographic camera and measuring the edge effects of those captured images is acknowledged as an area that requires further research and is presently beyond the scope of this research.

In the CEN method, a 190 mm region is used in the example frame and spacer profile calculations to capture the heat transfer effects of the frame and spacer (Blanusa, et al., 2007). Weitzmann et al. (2000) concluded that by using the 150 mm edge-of-glazing length in the NFRC method and by including the corner effect (using 3-D modelling software Heat 3), the three dimensional point heat loss, in the CEN method, the two methods will give identical U-value results. However, simulations in Heat3 are not as detailed as THERM and thus key details in the configuration of the spacer, frame and glazing are neglected and therefore the heat transfer interactions are not accounted for as accurately.

2.4.2 Frame Cavity Methods

Heat transfer effects in the frame cavities are accounted for in THERM by applying an effective conductivity (k_{eff}) to these areas. Frame cavities are assumed to be a 'solid' and are assigned an effective conductivity value that incorporates radiative and convective heat transfer effects in that area.

The convective heat transfer coefficient in the k_{eff} equation, according to the NFRC and CEN methods, uses the conductivity of air as the primary conductivity of this ‘solid’ region (ISO, 2003; ISO, 2012; LBNL, 2012). The effective conductivity incorporates the geometry, heat flow direction, surface emissivity and temperature of the surrounding surfaces of the cavity region (LBNL, 2013).

The NFRC and CEN methods and THERM use the following equation to determine the effective conductivity of frame cavities:

$$k_{\text{eff}} = (h_c + h_r) \cdot d \quad (10)$$

Where:

k_{eff} = effective conductivity

h_c = convective heat transfer coefficient

h_r = radiative heat transfer coefficient ($h_r=0$ in the case when detailed radiation procedure is used)

d = thickness or width of the air cavity in the direction of heat flow
(ASHRAE Standards Project Committee SPC 142, 2000; ISO, 2003; ISO, 2012)

2.4.3 Radiation Models for Frame Cavities

2.4.3.1 NFRC Radiation Models

There are two types of radiation models for NFRC frame cavities, simplified and detailed; the simplified radiation model is most commonly used for the NFRC method.

1. **Simplified Radiation Model:** Based on the ASHRAE SPC 142P method, radiation heat transfer effects are modeled as “an effective conductance based on the temperature and emissivity of the two parallel [surfaces] perpendicular to the heat flow” (LBNL, 1998). The default values frame cavity surface temperatures are 7°C and –4°C and the emissivities of those surfaces are 0.90 (LBNL, 1998).
2. **Detailed Radiation Model:** Based on the computer program FACET, this model determines radiant heat transfer by incorporating the temperature and emissivity of the surrounding materials of a frame cavity and performs “an element-by-element view-factor calculation” (LBNL, 1998).

2.4.3.2 CEN Simplified Radiation Model

The CEN method has only one radiation model. The CEN simplified radiation model replaces frame cavities with a relatively equivalent rectangular cavity with walls that have a constant temperature (LBNL, 1998). The radiative heat transfer (h_r) is determined in this method using a view factor (F) for this section and a linear Stephan Boltzman law:

$$h_r = E \cdot F \cdot 4\sigma \cdot T_{avg}^3 \quad (11)$$

$$E = (\varepsilon_1^{-1} + \varepsilon_2^{-1} - 1)^{-1} \quad (12)$$

$$F = \frac{1}{2} \left(1 + \sqrt{1 + (L/H)^2} - L/H \right) \quad (13)$$

Where:

T = Temperature

ε = emissivity

L = the cavity dimension in the direction parallel to the heat flux

H = the cavity dimension in the direction perpendicular to the heat flux (ISO, 2012; LBNL, 1998)

The NFRC method uses the following calculation for the detailed radiation model (Roth, 1998):

$$h_r = \frac{4 \sigma T_{avg}^3}{\frac{1}{\varepsilon_{cold}} + \frac{1}{\varepsilon_{hot}} - 2 + \frac{1}{\frac{1}{2} \left[\left(1 + \left(\frac{L_h}{L_v} \right)^2 \right)^{\frac{1}{2}} - \frac{L_h}{L_v} + 1 \right]}} \quad \frac{W}{m^2 K} \quad (14)$$

The radiative heat transfer coefficient hr is calculated according to Roth (1998) which is referred to by the former working group ASHRAE SPC 142. Since these calculations and the CEN calculations are identical, this proves that the CEN simplified and NFRC detailed radiation models are the same.

The convective heat transfer coefficient in the CEN simplified radiation model uses a 10K temperature difference in its equation between the two frame cavity surfaces perpendicular to the heat flow; the thermal conductivity value of air at 10°C is used (ISO, 2012). The NFRC method uses different default temperatures for the frame cavity surfaces than ISO 15099 (2003): the ISO 15099 uses 0 and 10°C and the NFRC uses 7 and -4°C which is an 11°C temperature difference (LBNL, 1998). Although the difference in delta T between both methods is only 1°C, the different default temperatures used by both methods may influence the variations in U-value results.

The simplified radiation model used in the CEN method is only slightly different from the NFRC method. The CEN method incorporates the view factors of all the surfaces of a rectangular unventilated frame cavity to determine radiative heat flow, yet, the NFRC method only considers the emissivities of only the two surfaces that are perpendicular to the heat flow (ISO, 2012). The NFRC method only incorporates the temperatures and emissivities of the two walls that are perpendicular to the governing heat flow (LBNL, 1998).

Overall, based on the NFRC (ASHRAE 142) and CEN (ISO 10077-2) equations the CEN simplified radiation model is analogous to the NFRC detailed radiation model.

2.4.4 Unventilated and Ventilated Frame Cavity Models

The NFRC method refers to the cavity model as outlined in ISO 15099 and the CEN method refers to the cavity model outlined in ISO 10077-2.

2.4.4.1 NFRC Unventilated Frame Cavities

Cavities that are enclosed and those that have an opening to the exterior that is less than or equal to 2 mm, are considered to be unventilated cavities (ISO, 2003). The effective conductivity is calculated based on a rectangle that fully encloses the cavity (the specific correlations used can be found in ASHRAE SPC 142P) (LBNL, 1998). The NFRC method assumes that the heat flow direction flows linearly in a horizontal, up or down direction.

The NFRC method determines the direction of heat flow in unventilated cavities according to the following rules:

- Horizontal heat flow: the temperature difference between the vertical cavity surfaces is greater than the difference between the horizontal surfaces
- Vertical heat flow up: the temperature difference between the horizontal cavity surfaces is greater than the difference between the vertical cavity surfaces and the bottom cavity surface temperature is higher than the top surface temperature
- Vertical heat flow down: same as the vertical heat flow up except that the difference between the vertical cavity surfaces and the top cavity surface temperature is higher than the bottom surface temperature (ASHRAE Standards Project Committee SPC 142, 2000; ISO, 2003)

NOTE: Although the ASHRAE SPC 142 has been disbanded due to a lack of support and that there was an ISO standard on the same topic, their draft document is referenced by the THERM manual (ASHRAE, 2014; LBNL, 1998).

When the heat flow direction is horizontal, the effective conductivity is determined by incorporating the temperature difference and the average emissivity values of only the vertical surfaces that are perpendicular to the heat flow (LBNL, 1998). Thus the frame cavity wall temperatures and emissivities are based upon the temperature and emissivities of the surrounding materials.

2.4.4.2 CEN Unventilated Frame Cavities

The unventilated cavities according to the CEN method are defined as air cavities that are enclosed or slightly open to the interior or exterior with a slit that is less than or equal to 2 mm. The effective conductivity of the CEN unventilated cavity model is also based on a rectangle, however, the rectangle has the same aspect ratio as the cavity being analyzed (LBNL, 1998). This cavity model is used with the CEN simplified radiation model.

2.4.4.3 Slightly Ventilated Frame Cavities

The NFRC and CEN methods both have the same definition for slightly ventilated cavity spaces where cavities that have an opening to the exterior environment that is greater than 2 mm and less than or equal to 10 mm (ISO, 2003; ISO, 2012; LBNL, 2013). The slightly ventilated cavity models are only applicable to the side of the window that has an opening that faces and ventilates to the exterior environment.

2.4.4.4 Well-Ventilated Frame Cavities

The NFRC and CEN methods define a cavity with an opening to the exterior that is greater than 10 mm as a well-ventilated frame cavity and is considered to be fully exposed to the environment. Since a well-ventilated frame cavity is fully exposed to the environment, it is assumed that it has a surface film resistance; thus CEN uses a surface film coefficient as stated in ISO 10077-2 for surfaces with increased resistance for these cavity surfaces.

2.4.5 Impacts of these Differences on Whole Window U-values

When using different boundary conditions with the same calculation method, Roth (1998) showed that the NFRC boundary conditions give larger U-values than the CEN boundary conditions, primarily due to

the overall heat transfer coefficient value being larger. In other studies, Blanusa (2001) and Weitzmann et al. (2000) found that for both boundary conditions, the CEN method gave larger U-values than the NFRC method: Weitzmann et al. (2000) noted that the difference was due to the 2-D effects present in heights above 63.5 mm in the edge method. Furthermore, this study showed that the linear method gave more correct U-values when using 2-D and 3-D models.

Generally, the thermal transmittance of glazing is lower than the thermal transmittance of the frame for high performance windows. The frame to glazing area ratio changes with different sizes of windows. Thus, the influence of the different thermal transmittances of the frame and glazing on the overall window U-value increases with differently sized windows (Wright G. , 2012). More specifically, regarding the variation in window sizes, “The difference in U_w -values between the two calculation methods decreases as the total area of the window increases (Blanusa, 2001; Blanusa, et al, 2007). Blanusa (2001) found that the differences ranged from 1.4% for the smaller windows to 0.6% for the larger windows in the study. Despite using the same boundary conditions, Roth (1998) found that the two methods gave different results for the smaller windows in the study: a difference of 3.5% for a thermally broken aluminum framed window, 3% for a PVC framed window and 2.3% for a wood framed window. The agreement between the methods was found to be dependent upon the geometry of the window (Blanusa, et al., 2007). The different equations lead to the difference in the methods because of the way that the corner regions of the window frame and glazing are treated (Blanusa, et al., 2007)”.

It is also noted by ISO 15099 (2003) that the different whole window calculation methods may yield different U-values because the heat transfer that occurs on the frame and edge are not dealt with in the same way and due to the fact that these methods do not consider the three dimensional effects of heat transfer in these areas. In contrast to Blanusa’s findings regarding the larger differences in whole window U-values with larger window areas, the differences between the 3-D effects of both calculation methods are more evident when applied to smaller windows (ISO, 2003).

Gustavsen et al. (2008) suggests that the current methods in the ISO 15099 standard are not sufficient to model the heat transfer through low conductance frames, yet it is sufficient for modelling high conductance frames. Rather, more intricate algorithms are needed in order for current modelling programs are to be used for the design and improvement of low-conductance frames. Gustavsen et al. (2008) instead found that low conductance frames could be modeled accurately with computational fluid dynamic (CFD) models, in fact, CFD modeling was seen as necessary for analyzing convective heat transfer in vertical frame cavities. However, conducting CFD models and tests were quite time

consuming, “approximately 500 times longer than performing a 2D conduction run in THERM” (Gustavsen, Arasteh, Petter Jelle, & Curcija, 2008).

Since the CEN method uses a lower temperature difference, European windows tend to have a lower U-value calculation result (Young, 2012). In the window industry, some are of the opinion that the CEN method is more relevant for Canada, since the average temperature in Canada is approximately -3°C which is closer to CEN’s exterior boundary condition (0°C) than the NFRC’s (-18°C) (Gibson, 2012; RDH Building Engineering Ltd., 2014). In addition, in North America, the NFRC boundary conditions are more suited for sizing heating systems, whereas the CEN boundary conditions are more suited for determining the annual heating fuel consumption, (which is based on the average temperature of the year rather than extremes of temperature) (Gibson, 2012; RDH Building Engineering Ltd., 2014).

At the time of his report, Curcija (2005) identified some key problematic areas with regards to the differences between the two methods:

- Convective heat transfer correlations are inaccurate and outdated
- The assumption that there is a fixed temperature difference across the window system is incorrect and does not reflect what happens in reality
- A specified approach to irregular frame cavities, heat flow directions, frame cavity surface emissivities, etc. is lacking
- The radiation boundary condition is too simplified as it does not account for different emissivities and treats reduced radiation heat transfer in the corner regions as a constant
- “Simplified treatment of gas mixtures (Curcija C. , 2005)”
- Lack of g-factor (solar heat gain coefficient) calculations

The RDH Building Engineering Ltd. (2014) study looked at the differences between the CEN and NFRC calculation methods using two North American windows, vinyl and fiberglass-frames, and a vinyl-framed European window; all with argon gas infill and a thin-wall stainless steel, dual seal spacer. The following are some of the significant conclusions from this study:

- $U_{\text{cog-NFRC}}$ values were between zero and 23% higher than $U_{\text{cog-CEN}}$ values. Larger gap sizes gave the larger differences (14-23%).
- $U_{\text{window-NFRC}}$ values were found to be 14% lower to 18% higher than the CEN values.

- U_{frame} values differed where the NFRC U-values were found to be 5% lower to 24% higher than CEN values.
- SHGC values for the whole window were up to 50% lower than the center-of-glazing SHGC values.
- NFRC SHGC values for the center-of-glazing were between 1% and 8% lower than CEN SHGC values (RDH Building Engineering Ltd., 2014)

U_{frame} is a key component in the whole window U-value and thus discrepancies in how both calculation methods address this parameter has a significant impact on the overall window U-value (RDH Building Engineering Ltd., 2014). The study concluded that the difference in the U_{frame} values of each method is attributed to the fundamentally different U_{frame} calculation approaches (RDH Building Engineering Ltd., 2014).

Different thermal conductivities for the same materials are used in each method which also helps to account for some of the discrepancies between the U_{frame} values. Little difference was present between the fiberglass frame U-values of both methods due to the lower thermal conductivity value in the NFRC method than the CEN method which compensated for some of the differences when using the low thermal conductivity of the calibration panel in place of the actual glazing (RDH Building Engineering Ltd., 2014).

In addition, the RDH study (2014) concluded that the way in which these two methods approach the edge effects, i.e. Ψ -value (CEN) and $U_{\text{edge-NFRC}}$ are vastly differently and are therefore not comparable. Due to the use of a calibration panel, the whole insulated glazing unit, **and** a different calculation in the simulation, the CEN method approach is not the same as the NFRC calculation and method where only the whole insulated glazing unit is simulated to determine $U_{\text{edge-NFRC}}$.

Foremost, RDH's study suggests that the "NFRC and ISO U-values cannot be compared [because] they are based on different calculation procedures", instead, subscripts of each method for U-values are suggested to be used; i.e. U_{NFRC} and U_{ISO} (RDH Building Engineering Ltd., 2014). The climate-specific high performance window simulations conducted in the research may support this finding from the RDH study.

3 Methodology

3.1 Summary

Using 2-D simulation software, THERM and WINDOW, the effects of changing various parameters and boundary conditions upon the thermal transmittance of four high performance windows with various glazing combinations, were simulated and calculated according to the NFRC and CEN standard methods. The four frame cross-section types that were used are: an insulated fiberglass window frame, a thermally broken solid wood frame, a U-PVC frame and a solid wood frame (see Figures 5-8). U_{cog} was calculated using WINDOW and U_{frame} and U_{edge} values were calculated using THERM for both methods. The CEN method incorporates an Excel spreadsheet to calculate the U_{window} and the Ψ -value; whereas the NFRC method imports THERM results into WINDOW to configure the U_{window} , U_{cog} and SHGC results. WINDOW was used to calculate the SHGC for the CEN method and the NFRC method for glazing combinations without the frame.

The Lawrence Berkeley National Laboratory documentation that outlines how to model window units according to the NFRC method “THERM 6.3 / WINDOW 6.3 NFRC Simulation Manual”, and “Calculating Fenestration Product Performance in WINDOW 6 And THERM 6 according to EN 673 and EN 10077”, for the CEN method, were both adhered to for the NFRC and CEN simulations respectively (LBNL, 2009). The use of simulation programs is validated by national and international organizations whereby the “algorithms used by THERM and WINDOW, for the calculation of [the whole window U-value] and Solar Heat Gain Coefficient, are consistent with ASHRAE SPC142, ISO 15099, and the National Fenestration Rating Council (LBNL, 2013)”. THERM and WINDOW are on the NFRC’s approved software list. For a further discussion on the efficacy of computer simulations vs. lab testing see Section 7.

U_{window} , U_{cog} , U_{frame} and Ψ -values were evaluated by comparing the use of different boundary conditions and assumptions in the NFRC and CEN calculation methods in determining thermal transmittance by using variables in different combinations (see Section 4) from the following simulation matrix:

Table 6 Simulation Matrix

Exterior Temperature	Frame Material	Glazing Combination	Spacer	Material Thermal Conductivity	Frame Cavity	Wind Speed	Surface film coefficients	SHGC
NA 8 climate zones	Insulated fiberglass	Double IGU; high and low SHGC	Higher Performance: A	NFRC 101	NFRC	Inland	NFRC	NFRC
	Solid wood	Triple IGU; high and low SHGC	Standard: B	CEN (ISO 10077-2)	CEN	Coastal	CEN	CEN
	TBSW	Quad IGU; high SHGC	Higher Performance: C					
	U-PVC							

3.2 Window Type and Size

Operable single casement windows were simulated seeing that casement windows contain sashes, whereby the frame configuration is more intricate, than fixed windows. The NFRC standard size of casement windows is 1.5 m x 0.6 m (see Table 7); these dimensions were used for the NFRC method, even if the standard size differs from the actual window product size. Although the actual window product dimensions are used in the CEN method, the NFRC standard size for casements was used for the CEN simulations for the purpose of comparability of the same product. It is recommended that future studies simulate fixed high performance windows, as well as varying sizes.

Table 7 Product Type and Model Sizes (NFRC, 2010)

Product Type	Opening (X) Non-operating (O)	Model Size (width by height) (mm)
Casement – Double	XX, XO, OO	1200 mm x 1500 mm
Casement – Single	X	600 mm x 1500 mm
Dual Action	X	1200 mm x 1500 mm
Fixed (includes non-standard shapes)	O	1200 mm x 1500 mm

3.3 Frame Materials

The four simulated frame materials are as follows: a thermally broken wood frame (TBSW), insulated fiberglass frame, U-PVC frame and a solid wood frame. These are representative of the frame materials

used in high performance windows in North America (see Figures 5-8). These frames are sourced from various North American certified PHIUS windows.

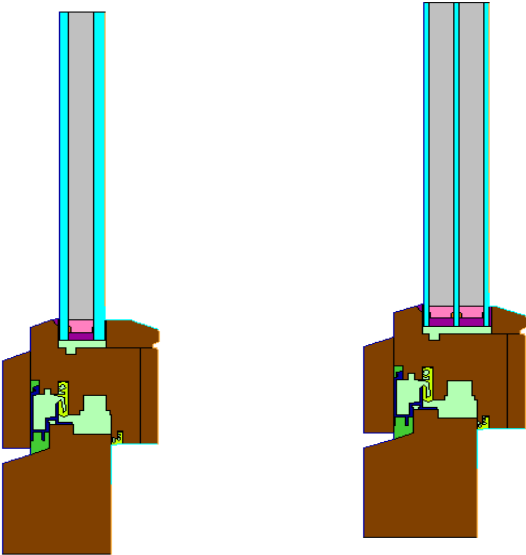


Figure 5 Solid Wood Frame with Double and Triple IGUs

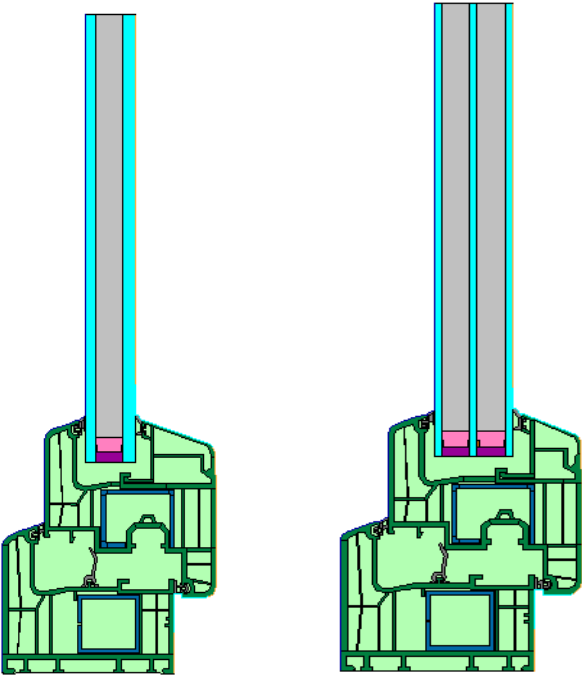


Figure 6 U-PVC Frame with Double and Triple IGUs

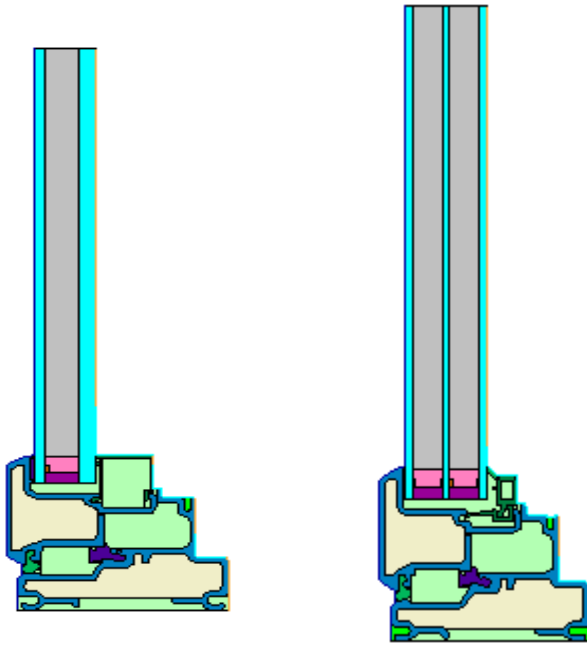


Figure 7 Fiberglass Frame with Double and Triple IGUs

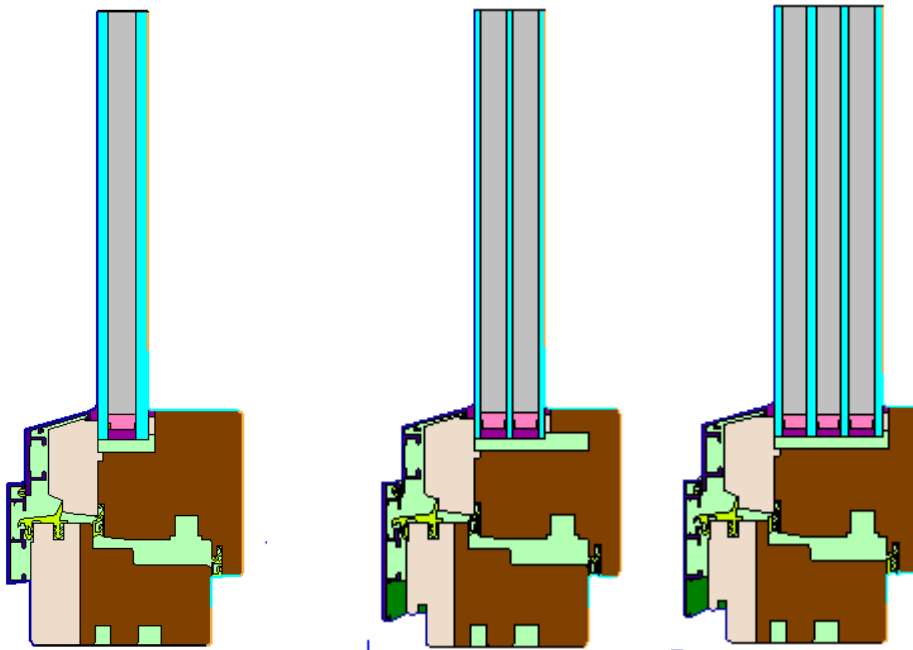


Figure 8 TBSW Frame with Double, Triple and Quad IGUs

3.4 Spacer Materials

The spacers of all of the high performance windows have different materials, configurations and thermal conductivities. Various combinations of the double, triple and quad insulated glazing units were paired with each frame type in the simulations; the U_{window} , U_{frame} and Ψ -values of window units with higher conductive spacers were compared with windows with lower conductive spacers. The three primary simulated spacers used are from different manufacturers and are labeled A, B and C. The simulated spacers used are those of the original product, as detailed by the manufacturer. With a height of 12 mm, Spacer A primarily comprises of an insulating plastic composite material with a stainless steel gas tight barrier foil. With a height of 7.874 mm, Spacer B comprises a stainless steel, dessicant, a primary polyisobutylene (PIB) seal and a silicone secondary seal. With a height of 12 mm, Spacer C comprises silicone foam with a dessicant pre-fill, a polyisobutylene primary seal and a silicone secondary seal. For the high performance windows that incorporate Heat Mirror™ technology, the required thermally-broken metal spacers are used to provide structural support for the thin plastic film/heat mirror.

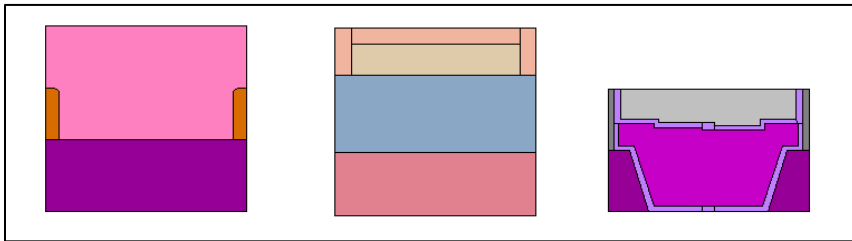


Figure 9 Spacers: A, B and C

3.5 Glazing Configurations

The glazing configurations were chosen based on the technical specifications of several high performance North American window manufacturers. For each glazing configuration, Surface #1 refers to the glazing surface that faces the exterior environment and the ID numbers of each glazing type used in the WINDOW software are included. The gas infill in each of the triple and quadruple glazing configurations comprised 90% krypton and 10% air. This is the typical percentage that manufacturer's achieve and is the amount that NFRC simulations require (LBNL, 2013). Lawrence Berkeley National Laboratory documentation, which outlines how to model according to the CEN method in THERM, also uses these air and krypton gas percentages (LBNL, 2009). For the NFRC method, the NFRC thermal conductivity values for krypton and air were used and for the CEN method, the CEN thermal conductivity values were used for the simulations. The glass thickness was based on the standard size of 3 mm, however, for specific glazing configurations such as the quadruple glazing, a 4 mm glass thickness was

used according to the manufacturer’s product. In order to adhere to the manufacturer’s drawings, the insulated glazing unit was 34 mm in order to fit each frame; except for the quadruple glass pane window, which is 52 mm. The overall glazing cavity width for the window units were based on the manufacturers’ technical specifications for each insulated glazing unit.

The following glazing configurations were simulated:

3.5.1 Double IGU

The double pane glazing combinations were used as a base case scenario for high performance glazing and were compared to other glazing combinations.

Overall glazing cavity width: 24.2 mm

Table 8 Double IGU High SHGC

	ID	Name	Mode	Thick	Flip	Tsol	Rsol1	Rsol2	Tvis	Rvis1	Rvis2	Tir	E1	E2
Glass 1 ▶▶	4117	OptifloatClear5mm.NSG	#	5.0	<input type="checkbox"/>	0.804	0.073	0.073	0.890	0.081	0.081	0.000	0.840	0.840
Gap 1 ▶▶	206	NFRC Argon/Krypton 9C		13.2										
Glass 2 ▶▶	9924	LOW-E_6.LOF	#	6.0	<input type="checkbox"/>	0.662	0.113	0.100	0.819	0.108	0.102	0.000	0.157	0.840

Table 9 Double IGU Low SHGC

	ID	Name	Mode	Thick	Flip	Tsol	Rsol1	Rsol2	Tvis	Rvis1	Rvis2	Tir	E1	E2
Glass 1 ▶▶	2156	LoE366-5.CIG	#	5.0	<input type="checkbox"/>	0.270	0.379	0.548	0.707	0.065	0.043	0.000	0.840	0.022
Gap 1 ▶▶	206	NFRC Argon/Krypton 9C		13.2										
Glass 2 ▶▶	4118	OptifloatClear6mm.NSG	#	6.0	<input type="checkbox"/>	0.783	0.071	0.071	0.884	0.080	0.080	0.000	0.840	0.840

3.5.2 Triple IGU

Overall glazing cavity width: 34 mm

Table 10 Triple IGU High SHGC

	ID	Name	Mode	Thick	Flip	Tsol	Rsol1	Rsol2	Tvis	Rvis1	Rvis2	Tir	E1	E2
Glass 1 ▶▶	2191	LoE180-3.CIG	#	3.0	<input type="checkbox"/>	0.689	0.164	0.189	0.871	0.091	0.078	0.000	0.840	0.068
Gap 1 ▶▶	208	NFRC Krypton/Air 90/10		12.5										
Glass 2 ▶▶	2001	Clr-3.CIG	#	3.0	<input type="checkbox"/>	0.848	0.076	0.076	0.904	0.082	0.082	0.000	0.840	0.840
Gap 2 ▶▶	208	NFRC Krypton/Air 90/10		12.5										
Glass 3 ▶▶	2191	LoE180-3.CIG	#	3.0	<input checked="" type="checkbox"/>	0.689	0.189	0.164	0.871	0.078	0.091	0.000	0.068	0.840

Table 11 Triple IGU Low SHGC

	ID	Name	Mode	Thick	Flip	Tsol	Rsol1	Rsol2	Tvis	Rvis1	Rvis2	Tir	E1	E2
Glass 1	2154	LoE366-3.CIG	#	3.0	<input type="checkbox"/>	0.275	0.429	0.549	0.713	0.066	0.044	0.000	0.840	0.022
Gap 1	208	NFRC Krypton/Air 90/10		12.5										
Glass 2	2001	Clr-3.CIG	#	3.0	<input type="checkbox"/>	0.848	0.076	0.076	0.904	0.082	0.082	0.000	0.840	0.840
Gap 2	208	NFRC Krypton/Air 90/10		12.5										
Glass 3	2191	LoE180-3.CIG	#	3.0	<input checked="" type="checkbox"/>	0.689	0.189	0.164	0.871	0.078	0.091	0.000	0.068	0.840

3.5.3 Quadruple IGU

Overall glazing cavity width: 52 mm

Table 12 Quadruple IGU High SHGC

	ID	Name	Mode	Thick	Flip	Tsol	Rsol1	Rsol2	Tvis	Rvis1	Rvis2	Tir	E1	E2
Glass 1	11333	PLT ULTRA N 4mm.SGI	#	4.0	<input checked="" type="checkbox"/>	0.585	0.240	0.293	0.884	0.048	0.045	0.000	0.837	0.037
Gap 1	208	NFRC Krypton/Air 90/10		12.0										
Glass 2	11004	PLANILUX 4mm.SGG	#	4.0	<input type="checkbox"/>	0.825	0.074	0.074	0.896	0.081	0.081	0.000	0.837	0.837
Gap 2	208	NFRC Krypton/Air 90/10		12.0										
Glass 3	11333	PLT ULTRA N 4mm.SGI	#	4.0	<input type="checkbox"/>	0.585	0.293	0.240	0.884	0.045	0.048	0.000	0.037	0.837
Gap 3	208	NFRC Krypton/Air 90/10		12.0										

3.5.4 Triple IGU (with Heat Mirror™)

Overall glazing cavity width: 25.4 mm

Table 13 Triple IGU (with Heat Mirror™) High SHGC

	ID	Name	Mode	Thick	Flip	Tsol	Rsol1	Rsol2	Tvis	Rvis1	Rvis2	Tir	E1	E2
Glass 1	2001	Clr-3.CIG	#	3.0	<input type="checkbox"/>	0.848	0.076	0.076	0.904	0.082	0.082	0.000	0.840	0.840
Gap 1	208	NFRC Krypton/Air 90/10		9.5										
Glass 2	1506	HM88.SwT	#	0.1	<input type="checkbox"/>	0.625	0.268	0.249	0.875	0.057	0.063	0.000	0.110	0.760
Gap 2	208	NFRC Krypton/Air 90/10		9.5										
Glass 3	2191	LoE180-3.CIG	#	3.0	<input checked="" type="checkbox"/>	0.689	0.189	0.164	0.871	0.078	0.091	0.000	0.068	0.840

Table 14 Triple IGU (with Heat Mirror™) Low SHGC

	ID	Name	Mode	Thick	Flip	Tsol	Rsol1	Rsol2	Tvis	Rvis1	Rvis2	Tir	E1	E2
Glass 1 ▶▶	2154	LoE366-3.CIG	#	3.0	<input type="checkbox"/>	0.275	0.429	0.549	0.713	0.066	0.044	0.000	0.840	0.022
Gap 1 ▶▶	208	NFRC Krypton/Air 90/10		9.5										
Glass 2 ▶▶	1506	HM88.SWT	#	0.1	<input checked="" type="checkbox"/>	0.625	0.249	0.268	0.875	0.063	0.057	0.000	0.760	0.110
Gap 2 ▶▶	208	NFRC Krypton/Air 90/10		9.5										
Glass 3 ▶▶	5009	CLEAR_3.PPG	#	3.0	<input type="checkbox"/>	0.827	0.076	0.077	0.898	0.086	0.086	0.000	0.840	0.840

3.5.5 Quadruple IGU (with Heat Mirror™)

Overall glazing cavity width: 35 mm

Table 15 Quadruple IGU (with Heat Mirror™) High SHGC

	ID	Name	Mode	Thick	Flip	Tsol	Rsol1	Rsol2	Tvis	Rvis1	Rvis2	Tir	E1	E2
Glass 1 ▶▶	2001	Clr-3.CIG	#	3.0	<input type="checkbox"/>	0.848	0.076	0.076	0.904	0.082	0.082	0.000	0.840	0.840
Gap 1 ▶▶	208	NFRC Krypton/Air 90/10		9.5										
Glass 2 ▶▶	1506	HM88.SWT	#	0.1	<input type="checkbox"/>	0.625	0.268	0.249	0.875	0.057	0.063	0.000	0.110	0.760
Gap 2 ▶▶	208	NFRC Krypton/Air 90/10		9.5										
Glass 3 ▶▶	1506	HM88.SWT	#	0.1	<input type="checkbox"/>	0.625	0.268	0.249	0.875	0.057	0.063	0.000	0.110	0.760
Gap 3 ▶▶	208	NFRC Krypton/Air 90/10		9.5										

Table 16 Quadruple IGU (with Heat Mirror™) Low SHGC

	ID	Name	Mode	Thick	Flip	Tsol	Rsol1	Rsol2	Tvis	Rvis1	Rvis2	Tir	E1	E2
Glass 1 ▶▶	2156	LoE366-5.CIG	#	5.0	<input type="checkbox"/>	0.270	0.379	0.548	0.707	0.065	0.043	0.000	0.840	0.022
Gap 1 ▶▶	208	NFRC Krypton/Air 90/10		8.0										
Glass 2 ▶▶	1506	HM88.SWT	#	0.1	<input checked="" type="checkbox"/>	0.625	0.249	0.268	0.875	0.063	0.057	0.000	0.760	0.110
Gap 2 ▶▶	208	NFRC Krypton/Air 90/10		8.4										
Glass 3 ▶▶	1506	HM88.SWT	#	0.1	<input checked="" type="checkbox"/>	0.625	0.249	0.268	0.875	0.063	0.057	0.000	0.760	0.110
Gap 3 ▶▶	208	NFRC Krypton/Air 90/10		8.4										

3.6 Gas Infill Mixtures

The CEN method refers to EN 673 and ISO 10292 for the thermal conductivities of all gases; the standard temperature that is used for the thermal conductivity is 10°C (see Table 17).

Table 17 Thermal Conductivity of Pure Gases- EN 673

	-10°C	0°C	10°C	20°C
Air (W/mK)	0.02336	0.02416	0.02496	0.02576
Krypton (W/mK)	0.00842	0.00870	0.00900	0.00926

However, in THERM the thermal conductivity of air and krypton at 0°C, at standard temperature and conditions (STP), are used instead of at 10°C (see Table 18).

Table 18 NFRC and CEN Infill Gas Thermal Conductivities - THERM

	NFRC	CEN (EN673)
Air (Pure) (W/mK)	0.024070	0.024169 (-0.000791)
Krypton (Pure) (W/mK)	0.008663	0.008707 (-0.000293)

The thermal conductivity values used in the THERM gas library for the CEN method are slightly less than what the ISO standards recommend and may contribute to differences in center-of-glazing results. Since EN 673 does not provide the various conductivity, viscosity and specific heat coefficients that THERM requires to determine the thermal conductivity of the gases, the THERM default values for the pure gases were used for all simulations.

The krypton/air gas mixtures that are typically used by manufactures are:

1. air (5%) and krypton (95%)
2. air (10%) and krypton (90%)

The NFRC method uses the thermal conductivity of krypton at 0°C for the -18°C boundary condition. In order to verify the thermal conductivity of the two krypton and air gas mixtures at -18°C, the gas property calculator from WINDOW was used. The gas property calculator is limited to thermal conductivity values with three decimal places. The thermal conductivities of infill gas mixtures of krypton gas were simulated for nine temperatures ranging from -40 to 40°C. Tables 19 and 20 show that the thermal conductivities of the krypton and air gas mixtures are identical at 0°C. Thus, the thermal conductivity of the air/krypton gas mixtures that THERM uses are consistent for the NFRC and CEN methods.

In comparison to the value at 0°C, for the 5%/95% gas mixture, the thermal conductivities slightly decrease by 0.001 W/mK at -30°C for both methods and increase at 10 and 20°C for the CEN and NFRC methods respectively (see Table 19). For the 10%/90% gas mixture, the thermal conductivities increase by 0.001 W/mK at 30°C, decrease by 0.001 W/mK at -10°C, and by 0.002 at -40°C (see Table 20).

Table 19 Gas property calculator (WINDOW), air 5%/krypton 95%, NFRC and CEN Thermal Conductivities

	-40°C	-30°C	-20 (-18°C)	-10°C	0°C	10°C	20°C	30°C	40°C
NFRC (W/mK)	0.008	0.008	0.009	0.009	0.009	0.009	0.010	0.010	0.010
CEN (EN673) (W/mK)	0.008	0.008	0.009	0.009	0.009	0.010	0.010	0.010	0.010

Table 20 Gas property calculator (WINDOW), air 10%/krypton 90%, NFRC and CEN Thermal Conductivities

	-40°C	-30°C	-20 (-18) °C	-10°C	0°C	10°C	20°C	30°C	40°C
NFRC (W/mK)	0.008	0.009	0.009	0.009	0.010	0.010	0.010	0.011	0.011
CEN/ISO 10292(W/mK)	0.008	0.009	0.009	0.009	0.010	0.010	0.010	0.011	0.011

It is acknowledged that further research could involve obtaining the conductivity, viscosity and specific heat coefficients for the gases taken from EN 673 and inputting these values in THERM. The thermal conductivities of the gas mixtures for each change in the temperature boundary condition could be simulated to see how the change in thermal conductivity, according to temperature, affects the thermal transmittance of the glazing (Ug).

Although some of the manufacturers use 95% krypton and 5% air (according to EN673) in their simulations, for this research the krypton/air gas percentage mixture of 90/10 was used in the simulations in order to adhere to the NFRC standard.

3.7 Interior Temperature Boundary Conditions

For the eight climate zones, an indoor temperature of 21°C for exterior temperatures that are below 30°C, were used to concur with the NFRC's and ASHRAE's indoor standard design temperatures. For the exterior temperatures that are 30°C and above, an indoor temperature of 24°C was used for the U_{cog} simulations; this coincides with the NFRC summer boundary conditions (see Table 22). Since there is a minute change in U-values when the NFRC and CEN standard interior temperatures were used, the U_{window} , U_{frame} and Ψ -value simulations use the NFRC and CEN standard interior temperature of 21°C and 20°C in order to normalize the results rather than the summer design interior temperatures for the 30°C and 40°C exterior temperature simulations.

3.8 Exterior Temperature Boundary Conditions of North America's Climate Zones

The insulated glazing units (IGUs) were simulated in the IECC's eight climate zones of North America (U.S. Dept. of Energy, 2009). Simulating in the 8 climate zones highlighted potential differences and patterns of thermal transmittance observed for the four test windows. The four windows were tested using the average annual, winter and summer design temperatures specific to each zone as the exterior temperature boundary conditions, according to ASHRAE (ASHRAE, 2009).

Using the NFRC and CEN calculation methods, the U_{window} , U_{cog} and U_{frame} values were derived from the simulations and compared. It will be determined if there are any significant differences between these U-values and the extent of influence that the exterior temperatures in each climate zone have on the U-values.

3.9 Winter and Summer Design Conditions

Standard winter boundary conditions were specified for the NFRC method and CEN method (ISO 10077-1) (see Table 21).

Considering that the CEN method does not have specified summer boundary conditions, the summer boundary conditions as outlined by ISO 15099, Section 8.2, were used in the simulations as a baseline case for the CEN method (see Table 22). The NFRC has specified summer boundary conditions as stated in NFRC 200-2010: Procedure for Determining Fenestration Product Solar Heat Gain Coefficient and Visible Transmittance at Normal Incidence (See Table 22). Chen and Wittkopf (2011) use 7.7 W/m²K for the interior convective surface film coefficient for the summer conditions in their simulations. This value

was derived from the NFRC test conditions according to the winter interior temperature of 21°C from NFRC 102-2010.

Table 21 NFRC and CEN Winter Boundary Conditions

	North America (NFRC)	Europe (CEN)
ISO Standard Used	ISO 15099	ISO 10077
Interior Temperature	21.1°C	20°C
Exterior Temperature	-18°C	0°C
Exterior Wind Velocity	5.5 m/s	4 m/s
Exterior Radiant Mean Temperature	$T_{r,m} = T_{\text{exterior}}$	$T_{r,m} = T_{\text{exterior}}$
Interior Radiant Mean Temperature	$T_{r,m} = T_{\text{interior}}$	$T_{r,m} = T_{\text{interior}}$

Table 22 Summer Boundary Conditions according to the NFRC and ISO 15099, Section 8.2

	NFRC	CEN
Standard	NFRC 200-2010	ISO 15099
Interior temperature	24°C	25°C
Exterior temperature	32°C	30°C
Interior convective surface heat transfer coefficient, hcv, int	7.7 W/(m ² K) (NFRC 102 hc int and ASTM E1423)	2.5 W/(m ² K)
Exterior convective surface heat transfer coefficient, hcv, ext	15 W/(m ² K)	8 W/(m ² K)
Radiant Mean Temperature, Tr,m	Tex	Tex
Solar irradiance, Is	783 W/m ²	500 W/m ²
Wind Velocity	2.75 m/s	4 m/s

3.10 North America's Climate Zones: Inland and Coastal locations

The 99% dry bulb temperature (i.e. defined as the January 1% in Canada) was used for the winter design temperature (ASHRAE, 2009). For the summer design temperature, the July 1% dry bulb temperature was used (ASHRAE, 2009). The winter frequency of 99.6% and the summer frequency of 0.4% was used for designing for extreme weather conditions which is not suited to this research.

3.11 Climate Specific U-values

In order to obtain an overall measure of the annual energy performance of a window, the average temperature of each climate zone was required. As mentioned earlier, the summer and winter design temperatures are primarily used to size heating and cooling systems, therefore, the summer and winter design temperatures were used to set the range of climate temperature ranges for each climate zone. To highlight the average annual energy performance, the average annual high and low temperatures and the average temperatures of each climate zone (as obtained from Environment Canada) were used to define the average annual climate zone temperature range. The average temperature of each climate zone was not chosen to define each climate zone considering the variability of temperature in each climate zone. In order to accommodate for this variability, a specified range was defined for each climate zone based on the chosen location. For example, for Toronto, the annual average temperature is 9.2°C and the average annual high and low temperatures are 5.6 and 12.7°C respectively. Based on this, the average annual temperature range for Toronto was defined as being between 5.6 and 12.7°C. The annual average temperatures and the annual average high and low temperatures were based on average monthly temperatures over a 30 year period (Environment Canada, 2013) (Environment Canada, 2007).

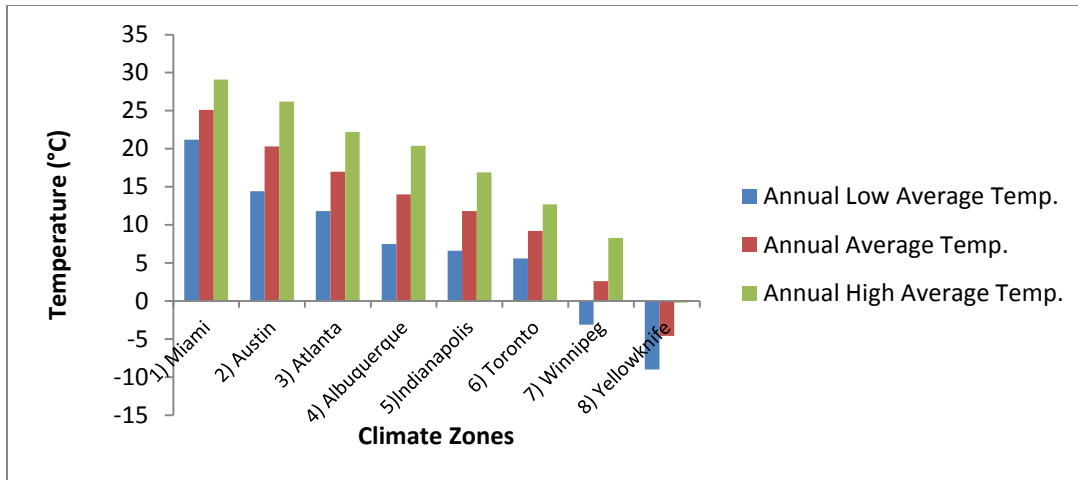


Figure 10 Annual Average Temperatures of North America's 8 Climate Zones

For the U.S. locations, the average annual high and low temperatures were obtained from normalized data from several public domain sources including the Southeast, High Plains, Midwestern and Western Regional Climate Centers and the National Climatic Data Center (NCDC Clim81 1981-2010) (Canty and Associates LLC, 2014).

The climate specific annual average U_{window} values and the standard $U_{\text{window-NFRC}}$ value that is assigned to the North American continent were compared to see the applicability of the NFRC standard boundary conditions in the eight climate zones.

3.12 Solar Heat Gain Coefficient

The fraction of incident solar radiation that enters the building interior through a window unit is defined as the solar heat gain coefficient (SHGC) (Efficient Windows Collaborative, 2012). The fraction of solar radiation that a window allows to pass through itself does not change therefore despite the different levels of incident solar radiation in the 8 climate zones, the SHGC remains the same. For example, an SHGC of 0.3 will allow 30% of the solar radiation (i.e. 500 or 700 W/m², see Table 22) to pass through itself no matter the location of the window and the amount of incident solar radiation in that location.

The Solar Heat Gain Coefficient of the CEN and NFRC methods are calculated differently and were compared for several glazing combinations. Considering the NFRC standard method requires that the frame characteristics be incorporated into the SHGC calculation; high and low SHGCs for the double and triple IGUs, and the quad IGU with a high SHGC were simulated with each frame type. In addition, without the influence of the frame, the NFRC and CEN SHGC calculation methods were compared for several IGU combinations.

Table 23 North American Climate Zones: Inland Locations

Climate Zones (inland)	Winter Design Temp. (°C)	Summer Design Temp. (°C)	Annual Low Average Temp. (°C)	Annual Average Temp (°C)	Annual High Average Temp. (°C)	Wind Velocity (m/s)
1 **						
2 Austin, TX	-1	37	14.4	20.3	26.2	7.6
3 Atlanta, GA	-4	33	11.8	17.0	22.2	7.7
4 Albuquerque, NM	-6	34	7.5	14.0	20.4	9.3
5 Indianapolis, IN	-14	32	6.6	11.8	16.9	8.4
6 Toronto, ON	-16	29	5.6	9.2	12.7	9.1
7 Winnipeg, MB	-30	29	-3.1	2.6	8.3	9.8
8 Yellowknife, NT	-40	24	-9	-4.6	-0.2	7.7

**Note: Climate zone 1 does not have an inland location since it is located solely on the southern tip of Florida.

Table 24 North American Climate Zones: Coastal Locations

Climate Zones (coastal)	Winter Design Temp. (°C)	Summer Design Temp. (°C)	Annual Low Average Temp. (°C)	Annual Average Temp. (°C)	Annual High Average Temp. (°C)	Wind Velocity (m/s)
1 Miami, FL	11	33	21.2	25.1	29.1	7.7
2 Jacksonville, FL	0	34	14.3	20.3	26.3	7.3
3 San Francisco, CA	5	26	10.6	14.1	17.6	10.6
4 New York City,	-8	30	8.3	12.3	16.2	9.6

NY (JFK airport)						
5 Vancouver, BC	-4	24	6.5	10.1	13.7	7.6
6 St. John's, NFLD	-14	23	0.6	4.7	8.7	12.3
7 Whitehorse, YT	-35	23	-5.9	-0.7	4.5	8.4
8 Iqaluit, NU	-38	14	-13.6	-9.8	-6.0	11.1

3.13 Gap Sizes

U_{cog} is calculated differently by the NFRC and CEN method; the CEN method is considered more simplified. The U_{cog} values of the test high performance windows with different gap sizes were simulated according to the exterior temperature boundary conditions of each climate zone for the NFRC and CEN methods, to see the effect of various temperature ranges on different gap sizes. For the double and triple glazing units, the U_{cog} values were simulated using the NFRC and CEN methods and standard boundary conditions as a base case scenario. The gap size range was between 6-20 mm in increments of 2mm for a single spacer, as drawn from RDH Building Engineering Ltd. (2014) and LBNL studies (Kohler, 2012).

3.14 Location Specific Wind Velocities in North America's Climate Zones

To determine the impact of wind velocity on the U_{window} and U_{cog} , the wind velocities of coastal cities in each climate zones were simulated. It is important to note that the wind velocity can be changed in WINDOW however, in THERM, the wind velocity is accounted for in the surface film coefficient on the exterior side. In the NFRC method, each frame material is assigned a convective surface heat transfer coefficient that has a constant value and is temperature dependent as outlined by each method (see Section 3.16) (LBNL, 2013).

Given that wind velocities are greatest during the winter months and weakest in the summer, the lowest value given for the extreme annual wind velocities, where the wind speed is higher than the stated speed 5% out of all the hours of the year, and the winter design temperatures were used according to ASHRAE's climatic design conditions. The smaller percentage values (1 and 2.5%) were not chosen for they are used for extreme design conditions for "estimating peak loads to account for infiltration" (ASHRAE, 2009). Instead, this research takes a more conservative approach to account for the high

variability and unpredictability of the wind speed year round, noting that the results give a measurable extreme case scenario since winter design temperatures were used.

The U_{window} values were compared to the inland locations of each climate zone to see the effect of different wind velocities (see Tables 23 and 24).

It is important to note that the direction and velocity of the wind are largely influenced by the nature of the geographical surface features and the slope of the land. ASHRAE's wind data (extreme annual design conditions) was taken from locations that have a relatively flat terrain and an open exposure. Thus various conditions that may affect the results include areas that have more convoluted geographical features where the wind speed and direction may be quite different from the wind data that has been taken from airport locations. In these locations, a year-long site specific wind study would need to be conducted to properly assess the local wind conditions (ASHRAE, 2009). This area is beyond the scope of this research.

3.15 Material Thermal Conductivities

Some of the thermal conductivity values of the materials that are referenced to in each calculation method have been assigned different values. This difference may have a significant effect on the U_{window} , U_{frame} and U_{cog} . For each calculation method, the values of the materials that have different thermal conductivities for each test window were drawn from the following documents: *ISO 10077-2*, *the NFRC 101-2010* and *Procedure for Determining Thermophysical Properties of Materials for Use in NFRC-Approved Software*. For a list of the material thermal conductivities used in the simulated frame types, see Table 25. The primary materials that have significant different thermal conductivities are fiberglass and typical softwood; these values were used in the simulations.

Each test window was simulated according to:

- the NFRC method with NFRC thermal conductivities and compare with the CEN method using ISO thermal conductivities (using standard boundary conditions)
- the NFRC and CEN method using NFRC thermal conductivities
- the NFRC and CEN method using CEN thermal conductivities

Table 25 Different NFRC and CEN Material Thermal Conductivities

Frame Type: Material	NFRC (W/mK)	CEN (ISO 10077-2) (W/mK)
Solid wood: Douglas fir*	0.111	0.13
Fiberglass: PE Resin	0.3	0.4
TBSW: Meranti (hardwood)	0.16	0.18 general; 0.13 light red, 0.16 dark red
Pine (softwood)*	0.14 (general)	0.13 scots-EU; 0.11 lodgepole NA

3.16 Surface Film Coefficients (Boundary Conductances)

The surface film coefficients used in each of the calculation methods were assigned different values (see Table 26). The degree of influence of these different surface film coefficients on the U_{window} and U_{frame} were evaluated for each of the test high performance windows. The CEN method's surface film coefficients combine the convective and radiation coefficients; whereas the NFRC method does not include the radiation component in the surface film coefficient value as it is included in the radiation model in the simulations. Therefore, when replacing CEN surface film coefficient values with NFRC values, the radiation component is being neglected and thus this is only a theoretical scenario to determine the effect of various surface film coefficient values upon U_{window} and U_{frame} .

Each test window was simulated according to:

- the NFRC and CEN method using NFRC surface film coefficients
- the NFRC and CEN method using CEN surface film coefficients

Note: It was found that switching the surface film coefficients of both methods was not possible in real terms due to the radiation coefficient calculation being temperature dependent according to the EN ISO 6946 (2007) (see Equations 18 & 19). The NFRC radiation coefficient is slightly lower than the CEN radiation coefficient due to the lower exterior temperature used in the NFRC method. Although the convective coefficients are interchangeable, a small difference of 1.5 m/s in the wind speeds of both methods (i.e. NFRC = 5.5 m/s; CEN = 4 m/s) was not considered a significant influence on U_{window} simulations. Representative simulations of the inland and coastal locations, as discussed in Section 3.10, which use the various winter design temperatures and wind velocities specific to each location, gives a more accurate comparison of surface film coefficient values for each method.

Table 26 Surface Film Coefficients used by the NFRC and CEN methods

Calculation Method	Position	External, R_{se} (W/m^2K)	Internal, R_{si} (W/m^2K)
ISO 10077-2 (CEN)	Normal (plane surface)	25	7.69
	Reduced radiation/convection [in edges between two surfaces]	25	5
NFRC	Vertical (convection only)		
Aluminum frame		26	3.29
Thermally broken frame		26	3.00
Thermally improved frame		26	3.12
Wood/Vinyl frame		26	2.44

For this research the surface film coefficients of the NFRC and CEN methods were used for all climate zone simulations. It is acknowledged that the surface film coefficient can significantly change with various wind velocities which can in turn affect a window’s overall U-value. Hutcheon and Handegord (1995) give some examples of equivalent total surface film conductances used for different wind velocities (see Table 27).

Table 27 Equivalent Total Surface Film Conductances (ASHRAE, 1981)

Surface Position	Flow Direction	Conductance ($W/m^2 \cdot K$)
Indoors		
Vertical	Horizontal	8.3
Outdoors		
Breeze 3.4 m/s (summer)	Any	23
Stormy 6.7 m/s (winter)	Any	34

Hence, further research is required to see how the whole window U-values are affected by surface film coefficients that are determined according to the wind velocities that are climate zone specific.

The surface film coefficients were used to account for the heat transfer characteristics that occur at the interior and exterior glazing and frame surfaces. An equivalent conductance or resistance is assigned as the surface film coefficient at these surfaces, and it incorporates the radiative and convective heat transfer coefficients (Straube J. , 2003). Seeing that convective heat transfer is significantly impacted by wind velocity and that it is a substantial factor in determining the exterior surface film coefficient, the exterior surface film coefficient is highly influenced by the velocity and the direction of the wind (LBNL, 2013; Straube J. , 2003).

In determining U_{frame} , THERM considers emissivity, temperature and a constant convective heat transfer coefficient (LBNL, 2013). On the exterior side, the convective heat transfer coefficient is dependent on the wind velocity (LBNL, 2013). Since U_{frame} can incorporate the different wind velocities of the climate zones with the use of the convective heat transfer coefficient on the exterior side, U_{frame} can give an indication of the impact of these wind velocities on the frame's thermal transmittance.

3.16.1 NFRC Exterior Convective Film Coefficient

Section 8.3.3.3 of ISO 15099 gives a convective heat transfer coefficient calculation for the exterior side for comparing and rating window products:

$$h_{\text{cv,ex}} = 4 + 4V_s$$

Where: (15)

$h_{\text{cv,ex}}$ = convective heat transfer coefficient ($\text{W}/\text{m}^2\text{K}$)

V_s = free stream velocity near the fenestration surfaces (m/s)

The NFRC method uses this calculation to determine the exterior convective film coefficient:

Given: $V_s = 5.5 \text{ m}/\text{s}$ (NFRC standard wind velocity)

$h_{\text{cv,ex}} = 4 + 4(5.5) = 26 \text{ W}/\text{m}^2\text{K}$ (NFRC standard exterior convective film coefficient)

In order to account for the effect of the different wind velocities on the exterior convective film coefficient in each climate zone, the exterior convective film coefficient was calculated according to ISO 15099 for the NFRC method (see Table 28).

Table 28 NFRC Exterior Convective Film Coefficients for Inland and Coast Locations in NA Climate Zones

Climate Zone	Inland Exterior Surface Film Coefficient (W/m ² K) (no decimal place)	Coastal Exterior Surface Film Coefficient (W/m ² K) (no decimal place)
1	-----	35
2	34	33
3	35	46
4	41	42
5	38	34
6	40	53
7	43	38
8	35	48

3.16.2 CEN Exterior Surface Film Coefficient

The CEN method uses surface film coefficients according to ISO 6946. The exterior surface film coefficient is determined by the addition of the convective and radiative heat transfer coefficient and inverting that value. The inverse of the surface film resistance (R_s) was used as the surface film coefficient (h_{cr}) in order to equate the metrics of W/m²K used in THERM and the NFRC method. The wind velocities of the eight climate zone locations were inputted into this calculation to determine the exterior surface film coefficients that are specific for each climate zone (see Tables 23 and 24). The calculation is as follows:

$$R_s = \frac{1}{h_c + h_r} \quad (16)$$

And:

$$h_{cr} = \frac{1}{R_s} \quad (17)$$

Where:

h_{cr} = surface film coefficient (W/m²K) (no decimal places)

R_s = surface film resistance (m²K/W) (rounded to two decimal places)

h_c = convection heat transfer coefficient (W/m²K)

h_r = radiative heat transfer coefficient (W/m²K) (German Institute for Standardization, 1999)

$$h_r = \epsilon \cdot h_{r0} \quad (18)$$

$$h_{r0} = 4 \cdot \sigma \cdot T_m^3 \quad (19)$$

Where:

σ = Stefan-Boltzmann constant (5.67 x 10⁻⁸ W/m²K)

ϵ = surface emissivity (0.9)

h_{r0} = blackbody radiation heat transfer (rounded to one decimal place)

T_m^3 = average thermodynamic temperature of the surface and its surroundings (K) (German Institute for Standardization, 1999)

For the internal surface where the heat flow is horizontal, the convective heat transfer coefficient used was: $h_c = 2.5$ W/m²K. For an external surface, the convective heat transfer coefficient calculation is the same as the ISO 15099/NFRC method:

$$h_c = 4 + 4V_s \quad (20)$$

Where:

V_s = free stream velocity near the fenestration surfaces (m/s) (German Institute for Standardization, 1999)

Using these equations, the standard exterior surface film coefficient used in the CEN method was calculated as follows:

Given: $V_s = 4$ m/s and the exterior temperature = 0°C = 273.15 K

$$R_s = 1 / [4+4(4)] + [0.9(4)(5.67 \times 10^{-8})(273.15^3)]$$

$$= 1 / (20) + 0.9(4.6)$$

$$= 1 / 24.14$$

$$= 0.04 \text{ m}^2\text{K/W}$$

$$h_{cr} = 1 / 0.04 = \mathbf{25 \text{ W/m}^2\text{K}} \text{ (CEN standard exterior surface film coefficient)}$$

Tables 29 and 30 outline the different variables calculated according to the CEN/ISO 6946 surface film coefficient calculation (see Equations 16-20) for the inland and coastal locations in the eight climate zones. Calculating the surface film coefficient (h_{cr}) according to CEN/ISO 6946 resulted in values with little variation. Due to the limitation of decimal places for the blackbody radiation heat transfer (h_{ro}) and surface film resistance (R_s), the variation in the surface film coefficient values at different temperatures are normalized and account for the little variation of values (i.e. 33 and 50 $\text{W/m}^2\text{K}$) for all climate zones. In order to show the variation of surface film coefficients and how they are impacted by the different wind velocities, the surface resistance (R_s) was rounded to three decimal places and then placed in Equation 17. These new values are given in Tables 29 and 30 under h_{cr} (new method).

Table 29 CEN/ISO 6946 Exterior Surface Film Coefficients Calculation Table – Inland Locations

Inland Climate Zones	Annual Avg Temp (°C)	Annual Avg Temp. (°K)	h_{ro} ($\text{W/m}^2\text{K}$)	h_r ($\text{W/m}^2\text{K}$)	h_c ($\text{W/m}^2\text{K}$)	R_s ($\text{m}^2\text{K/W}$)	h_{cr} ($\text{W/m}^2\text{K}$) ISO 6946 procedure	h_{cr} ($\text{W/m}^2\text{K}$) New Method
1								
2	-1	272.15	4.6	4.14	34.4	.03/.026	33	38
3	-4	269.15	4.4	3.96	34.8	.03/.026	33	38
4	-6	267.15	4.3	3.87	41.2	.02/.022	50	45
5	-14	259.15	3.9	3.51	37.6	.02/.024	50	42
6	-16	257.15	3.9	3.51	40.4	.02/.023	50	43
7	-30	243.15	3.3	2.97	43.2	.02/.022	50	45

8	-40	233.15	2.9	2.61	34.8	.03/.027	33	37
---	-----	--------	-----	------	------	----------	-----------	-----------

Table 30 CEN/ISO 6946 Exterior Surface Film Coefficients Calculation Table – Coastal Locations

Coastal Climate Zones	Winter design Temp (°C)	Winter design temp (°K)	h_{ro} (W/m ² K)	h_r (W/m ² K)	h_c (W/m ² K)	R_s (m ² K/W)	h_{cr} (W/m ² K)	h_{cr} (W/m ² K)
							ISO 6946 procedure	New Method
1	11	284.15	5.2	4.68	34.8	.03/.025	33	40
2	0	273.15	4.6	4.14	33.2	.03/.027	33	37
3	5	278.15	4.9	4.41	46.4	.02	50	50
4	-8	265.15	4.2	3.78	42.4	.02/.022	50	45
5	-4	269.15	4.4	3.96	34.4	.03/.026	33	38
6	-14	259.15	3.9	3.51	53.2	.02/.018	50	56
7	-35	238.15	3.1	2.79	37.6	.02/.025	50	40
8	-38	235.15	2.9	2.61	48.4	.02	50	50

It is more evident in the new values how the surface film coefficient values reflect the impact of the variations in wind velocities for each climate zone. These values are similar to the variation seen in ASHRAE’s values according to wind velocity in Table 27. Table 28 gives the NFRC exterior surface film coefficients (h_{cr}) specific to the eight climate zones based on the CEN/ISO 6946 surface resistance calculation method. These values were used for the NFRC simulations accounting for the different wind velocities for the eight climate zones.

The surface film coefficients used in the CEN method are higher than the NFRC method because they are based on different calculations. The CEN method incorporates the radiative and the convective heat transfer, whereas the NFRC method just includes the convective heat transfer for the surface film

coefficient. The NFRC method accounts for radiation in its view-factor based radiation methods as outlined in ISO 15099.

3.17 NFRC and CEN Interior Surface Convective and Surface Film Coefficients

The interior surface film coefficient incorporates the difference between the interior room temperature, the interior surface temperature of the window, and the height of the window (LBNL, 2013). It was assumed that the interior surface was primarily subject to natural convection and that the surface temperature was influenced by the material properties and configuration (LBNL, 2013). For all the simulations, since the interior room conditions were consistent, the interior convective and surface film coefficients were used for each method (see Table 26).

3.18 Frame Cavity Methods

The way in which the two calculation methods treat frame cavities are complex. ISO 15099 (NFRC reference) is similar to ISO 10077-2 in determining what is ventilated and what is not, however, they differ in the way equivalent simplified geometries are given in order to give an equivalent thermal conductivity to the cavities. ISO 15099 is generally more complex than ISO 10077-2 (see Section 2.4.2). The differences of these two calculation methods were analyzed with the high performance windows that have frame cavities.

The surface film coefficients and frame cavity methods were simulated using winter boundary conditions for all test simulations seeing that in smaller temperature differentials, there is less opportunity for thermal transmittance by radiation, convection and conduction.

3.19 Ψ -Values

Given that the NFRC method does not use a Ψ -value, Graham (2012) postulated the following equation to configure an NFRC Ψ -value:

$$\Psi_{EDGE}^{NFRC} = (U_{EDGE} - U_{COG}) \cdot I_{EDGE} \quad (\text{Graham, 2012}) \quad (21)$$

However, this equation does not take into account the additional thermal transmittance that occurs in the frame, seeing that the edge effects in the NFRC method are incorporated for the most part in U_{edge} , but also slightly in U_{frame} . Also, the U_{edge} height value is only 63.5 mm and it's not analogous to the CEN method's minimum glazing height (i.e. 150 mm). Therefore, to determine the thermal bridging potential in each of the eight climate zones, the Ψ -value used in the CEN method was calculated.

- NFRC and CEN boundary conditions for the CEN method

- Boundary conditions of North American climate zones in the CEN method

Average temperature ranges for each climate zone were used for the Ψ -value simulations to measure potential thermal bridging through the frame junctions; seeing that larger temperature differentials have a greater impact on the conduction in frames.

4 Summary and Justification of Simulations

Table 31 Summary of Simulations

Results Reported	Parameter	Description	Outcome
SHGC	NFRC and CEN Standard Methods	Compare SHGC values of both methods for 9 IGU units with high and low SHGC	Percentage differences for both methods
	NFRC and CEN: IGU Only	Compare SHGC values of both methods for 9 IGU units with high and low SHGC	Possibility of harmonization
U _{window}	NFRC and CEN Standard Methods	Compare four frame types with double, triple and quad IGUs with high and low SHGC using both methods	Percentage differences of both methods
	Climate Zones	Compare four frame types with double, triple and quad IGUs with high and low SHGC using different exterior temperatures of the climate zones	Impact of exterior temperature on U _{window}
	Material Thermal Conductivity	Compare NFRC and CEN material thermal conductivities for fiberglass, TBSW and solid wood frames with double, triple and quad IGUs	Impact of thermal conductivity on U _{window} differences
	Frame Cavity Method	Compare NFRC and CEN frame cavity methods for four frame types with double, triple and quad IGUs	Impact of frame cavity methods on U _{window}
	Surface Film Coefficients	Compare NFRC and CEN surface film coefficients for four frame types with double, triple and quad IGUs	Effect of surface film coefficients on U _{window}
	Spacers	Compare Spacers A, B and C	Impact of spacers on U _{window} ; compare spacer's thermal conductivity
	Inland and Coastal	Compare wind velocities and winter design exterior temperatures of locations in each climate zone	Impact of exterior temperature and coef. sets on U _{window}
	Exterior Temp. Symmetry	Compare NFRC and CEN U _{window} values using the standard exterior temperature for both methods (i.e. -18°C and 0°C)	Harmonization of both methods

Results Reported	Parameter	Description	Outcome
U _{cog}	NFRC and CEN	Compare double, triple and quad IGUs with a high and low SHGC using both methods	Percentage differences of both methods
	Climate Zones	Compare double, triple and quad IGUs with high and low SHGC using different exterior temperatures of the climate zones	Effect of exterior temperature on U _{cog}
	Gap Spacing Sizes	Compare gap sizes of four IGUs (high and low SHGC) in climate zones	Impact of gap sizes on U _{cog} differences in climate zones
U _{frame}	NFRC (with IGU), CEN (with IGU and calibration panel)	Compare three frame calculation methods for four frame types	Establish differences in U _{frame} methods and influential factors
	CEN	Compare four frame types with calibration panel (U _{frame-CEN})	Establish highest and lowest conductive frames
	Material Thermal Conductivity	Compare NFRC and CEN material thermal conductivities for fiberglass, TBSW and solid wood frames	Impact of different thermal conductivities on U _{frame}
	Frame Cavity Method	Compare NFRC and CEN frame cavity methods for four frame types using U _{frame-CEN}	Impact of different FCMs on U _{frame}
	Surface Film Coefficients	Compare NFRC and CEN surface film coefficients for four frame types	Impact of different surface film coefficients on U _{frame}
ψ-Value	CEN	Determine linear thermal transmittance for four frame types with double, triple and quad IGUs with high and low SHGC	Measure edge effects; impact of IGUs and frames
	Climate Zones	Compare four frame types with double, triple and quad IGUs with high and low SHGC using different exterior temperatures of the climate zones	Effect of exterior temperature on the ψ-Value
	Spacers	Compare Spacers A,B and C, using four frame types with double, triple and quad IGUs	Measure thermal efficiency of spacers in each climate zone

5 Results and Discussion

The results of this study aid in identifying and explaining the percentage change between both methods, as well as, determining how each method defines and utilizes various parameters; and defining the most influential parameters in the percentage change differences.

5.1 Solar Heat Gain Coefficient Simulations

The Solar Heat Gain Coefficient varies for different frame materials when calculated according to the NFRC method. The NFRC standard method takes into account the frame of the actual window unit with the glazing when calculating the SHGC, whereas, the CEN method only considers the glazing by itself at a 1000 mm height and width. The NFRC method is unique in that the solar radiation absorbed and transmitted through the frame is included in the SHGC calculation. The NFRC method also takes into account the glazing at the height of the actual window unit rather than the default 1000 mm height in WINDOW: for example, for a casement window, a height of 1500 mm and 600 mm width is used in the SHGC calculation. Including the solar radiation transmission through the frame and the actual glazing height results in a large discrepancy between NFRC and CEN SHGC values.

Table 32 NFRC and CEN SHGC: IGU only

	NFRC	CEN	% Change
Double High SHGC	0.69	0.65	6%
Double Low SHGC	0.27	0.25	8%
Triple High SHG Heat Mirror	0.54	0.52	4%
Triple Low SHG Heat Mirror	0.24	0.23	4%
Triple High SHG Glass	0.56	0.54	4%
Triple Low SHG Glass	0.24	0.23	4%
Quad High SHGC Heat Mirror	0.46	0.45	2%
Quad Low SHGC Heat	0.22	0.21	5%

Mirror			
Quad Glass High SHGC	0.42	0.41	2%

Table 33 Fiberglass SHGC according to the NFRC and CEN Methods

	NFRC	CEN	% Change
Double High SHGC	0.48	0.65	-26%
Double Low SHGC	0.19	0.25	-24%
Triple High SHGC	0.39	0.54	-28%
Triple Low SHGC	0.17	0.23	-26%

Table 34 Thermally Broken Solid Wood SHGC according to the NFRC and CEN Methods

	NFRC	CEN	% Change
Double High SHGC	0.37	0.65	-43%
Double Low SHGC	0.15	0.25	-40%
Triple High SHGC	0.3	0.54	-44%
Triple Low SHGC	0.13	0.23	-43%
Quad High SHGC	0.22	0.41	-46%

Table 35 Solid Wood SHGC according to the NFRC and CEN Methods

	NFRC	CEN	% Change
Double High SHGC	0.36	0.65	-45%
Double Low SHGC	0.15	0.25	-40%
Triple High SHGC	0.3	0.54	-44%
Triple Low SHGC	0.13	0.23	-43%

Table 36 U-PVC SHGC according to the NFRC and CEN Methods

	NFRC	CEN	% Change
Double High SHGC	0.35	0.65	-46%
Double Low SHGC	0.14	0.25	-44%
Triple High SHGC	0.29	0.54	-46%
Triple Low SHGC	0.13	0.23	-43%

All four frame types were simulated using double and triple IGUs with Spacer C (see Tables 33-36). The NFRC SHGC values were found to be 24- 46% lower than CEN SHGC values due to the inclusion of the frame and the actual IGU product dimensions in the NFRC SHGC method. This is similar to the findings of the RDH Building Engineering Ltd. (2014) study where the NFRC SHGC values were up to 50% lower than CEN values. Seeing that the SHGC measures the solar radiation transmittance between the exterior and interior surfaces, the height and width of the frame is a significant influence on the amount of solar

radiation transmitted through the window where the larger the glazing area the more solar radiation transmission occurs and would therefore contribute to a higher SHGCs. Since much less solar radiation is absorbed and transmitted through the frame, those window units with larger frame surface areas result in a lower SHGC value. This observation is demonstrated in the simulation results where the fiberglass frame NFRC SHGC values had the lowest percentage change in comparison to the CEN values because, out of all the frames, the fiberglass frame had the smallest height (from the sightline to the outer edge of the frame) of 73 mm. The small height of the fiberglass also resulted in larger NFRC SHGC values than the other three frames. The U-PVC frame had the lowest NFRC SHGC values of all the frames; they were slightly lower than the solid wood and TBSW SHGC values, because the height differences between them were minimal. In contrast, the U-PVC frame had the largest height at 122 mm, which was only slightly higher than the solid wood and TBSW frames (117 and 114 mm respectively). Thus, the higher the height of the frame, the larger the frame surface area, the lower the percentage change between the NFRC and CEN SHGC values; and the higher the NFRC SHGC value in comparison to other NFRC SHGC values of different frame types. The high SHGC IGUs had slightly larger percentage change differences for all the frame types; this may be attributed to surface area of the glazing with a higher solar transmittance is referenced in the SHGC calculation is much smaller than the CEN SHGC calculation. Glazing that has lower solar transmittance characteristics, (i.e. low SHGC), is less affected by the decreased surface area when using the NFRC SHGC calculation method.

The default height and width of 1000mm was used for both simulation methods for nine glazing IGUs with high and low SHGCs: double IGUs with glass panes, triple IGUs with glass panes, triple IGUs with heat mirrors, quad IGUs with heat mirrors, and a quad IGU with a high SHGC and glass panes. The frame was not included in the SHGC results. The results showed that the NFRC SHGC values were 2-8% higher than CEN values (see Table 32). The double IGUs with a high and low SHGC, as well as the Quad IGU with a low SHGC and heat mirrors, had the largest percentage change whereas the Quad IGU with glass panes had the lowest percentage change between the two methods.

The observation of larger differences between both methods with high SHGC IGUs is multifaceted. An IGU with a low SHGC decreases the thermal transmittance of the glazing more efficiently than an IGU with a high SHGC. Portions of long wave radiation are reflected by the low-E layers present on low SHGC glazing. Due to this occurrence, combine with increasing interior and temperature differences, less heat is transferred towards the frame. The frame temperature can thus be lower than for a frame with a high SHGC, depending on the thermal efficiency of the frame. The low-E layer adds more material to the

glazing allowing more heat transfer through conduction to place. In addition, more thermal transmittance occurs for the double IGUs at increasing temperature differentials due to the larger gap width size. The larger the gap width size, the more temperature plays a role in increasing the effect of heat transfer through convection.

There was a minor discrepancy between the NFRC and CEN SHGC values when the glazing, by itself, was analyzed in the U_{cog} simulations (see Table 32). In using the default height and width of 1000 mm, and by considering the glazing by itself, this approach narrowed the differences between the NFRC and CEN methods in determining the solar transmittance through the glazing. The primary factors that attribute to these differences are the following boundary conditions: the interior and exterior temperatures, wind speed, and solar irradiance.

In the NFRC method, when the exterior temperatures for the SHGC boundary conditions are changed, the center-of-glazing SHGC changes. Increasing the wind speed (and thus the surface film coefficient) to 5 m/s decreases the SHGC by 0.002, wind speeds in the summer are generally very low therefore this factor is negligible. Changing the SHGC exterior temperature in the eight climate zones only results in 0-0.005 decrease where the greatest change in value only occurs for the lowest summer design temperature of 14°C in Iqaluit, however, the SHGC only changes by 0-0.01 when rounded to two decimal places. Likewise, in the CEN method there are minimal changes.

With an interior temperature of 20°C, EN 673 determines the solar transmittance across a temperature difference of 15K and does not outline summer boundary conditions. For the CEN simulations, the summer boundary conditions outlined in ISO 15099 are used for the SHGC calculations (see Table 22). The NFRC SHGC values were 2-8% higher due to the NFRC's larger interior and exterior temperature difference of 8°C, and a higher exterior temperature by 2°C (see Table 22). Although the NFRC surface film coefficients are higher than the CEN values and increasing those alone decreases the SHGC value, the effect of the higher NFRC exterior temperature, the greater difference between interior and exterior temperatures, and the greater difference between the interior and exterior surface film coefficients, contribute to the higher NFRC center-of-glazing SHGC values.

Furthermore, the NFRC method's higher solar irradiance also contributes to larger NFRC center-of-glazing SHGC values in (i.e. 783 vs 500 W/m²). Lowering the solar irradiance value to 500 W/m² in the NFRC method in effect lowers the SHGC by 0.01. In addition, raising the wind speed to 4 m/s in the NFRC method lowers the SHGC by 0.004 which is significant when combined with other factors that

slightly change the SHGC value (i.e. surface film coefficients). Thus, the cumulative effect of the different irradiances, interior and exterior temperatures and surface film coefficients of both methods, account for the higher NFRC center-of-glazing SHGC values.

5.2 U_{cog} Simulations

5.2.1 U_{cog-NFRC} and U_{cog-CEN} Comparison in the 8 Climate Zones

Double, triple and quad IGUs with high and low SHGCs were simulated within the eight climate zones. The larger differences at 30 and 40°C in the CEN method are again due to the different summer boundary conditions, particularly the lower surface film coefficients and higher interior temperature (see Table 22) that were used at those temperatures. To normalize the results, the temperatures that lie 20°C and below that used the standard boundary conditions is discussed.

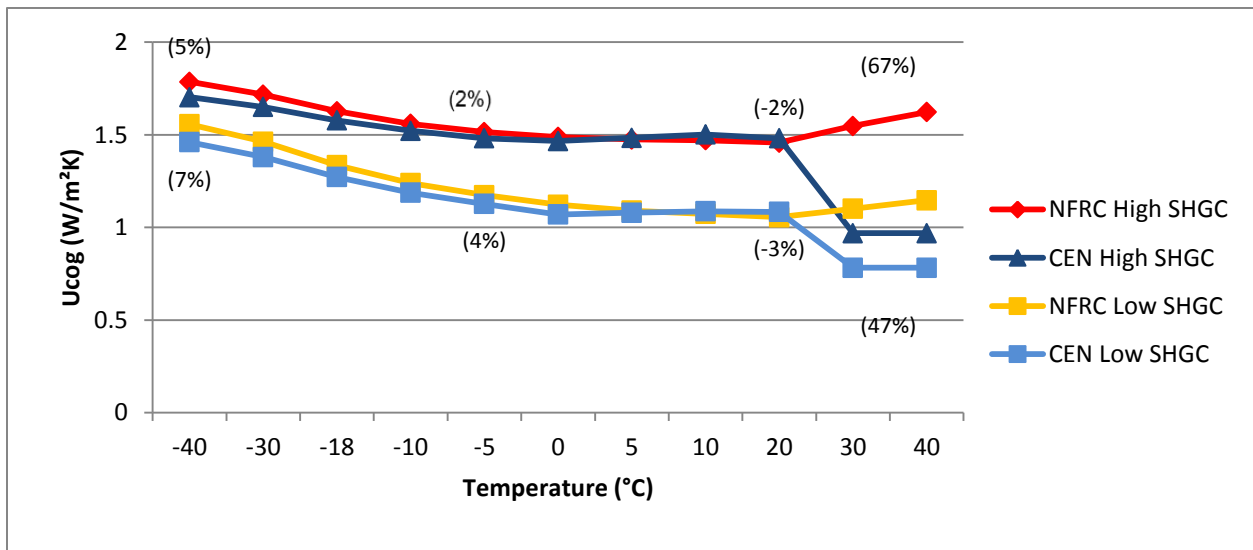


Figure 11 High and Low SHGC Double IGUs: NFRC vs CEN U_{cog} values (Percentage Change)

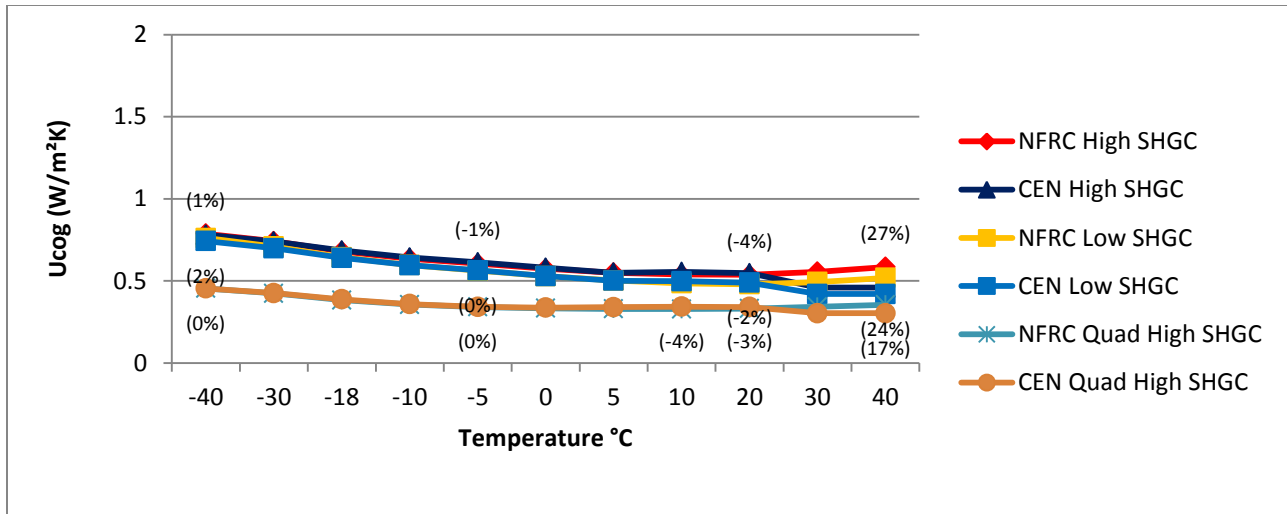


Figure 12 High and Low SHGC Triple and Quad IGUs: NFRC vs CEN U_{cog} Values (Percentage Change)

The trend in Figures 34 and 35 shows that the higher the IGU's thermal performance, the less differences that occur between both U_{cog} methods. This supports the possible harmonization of these methods as discussed in Section 5.7.

Examining the heat transfer equations for the U_{cog} value, the interior and exterior temperature differential is integral in formulating the radiative and convective heat transfer coefficients. The heat transfer coefficients measure the thermal conductance of the gas spacing and glazing materials. Temperature values are placed in the majority of calculations that formulate the heat transfer coefficients, as seen, for example, in the radiation conductance equation, and the Grashof number in the Nusselt equations which are part of the gas conductance equation: the radiation and gas conductance equations form the total thermal conductance of the glazing (CEN, 1997). For windows with double IGUs, the mean temperature difference across the gas space is 15K and the mean temperature is 10°C (CEN, 1997) (RDH Building Engineering Ltd., 2014). Thus, a degree incremental change can change the U_{cog} significantly for each standard.

The NFRC method according to ISO 15099 is more detailed than the CEN method in several ways. The external and internal facing surface temperature of each glazing layer is calculated using a meshing sequence at finite intervals (ISO, 2003). Temperature values are integral in the radiative component of the thermal transmittance of the glazing in the NFRC method as well (ISO, 2003). The 15K mean temperature difference between bounding glazing surfaces is also true for double IGU windows in the NFRC method when analyzing the isothermal lines in THERM simulations of this study. Therefore, the different thermal conductivities of the gas infill mixtures slightly contribute to the different U_{cog} results.

See Section 3.6 for further discussion of the impact of temperature on the gas thermal conductivities of each method.

Foremost, the different surface film coefficient sets (see Section 3.16); the effect of the exterior and interior temperature boundary conditions (see Section 3.9) upon these sets and upon the material and gas properties of the IGU; and the different U_{cog} calculation methods, altogether significantly contributes to the difference in the U_{cog} values of both methods.

The IGU combinations were simulated across the climate zone exterior temperature range. The trend showed that the higher the difference between interior and exterior temperatures, the higher the U_{cog} values. The change in exterior temperature in both calculation methods directly influences the thermal conductivity of the gas infill in the IGU. In addition, the thickness of the layers of the low-E coatings also influences the convective and conductive heat transfer effects of the gas infill (see Section 5.1). This demonstrates the influence of the variances of the exterior and interior boundary condition temperature differences upon the U_{cog} value of both methods.

5.2.2 $U_{\text{cog-NFRC}}$ in Reference to -18°C

The $U_{\text{cog-NFRC}}$ in reference to the NFRC standard temperature of -18°C were 16% lower to 34% higher in the exterior temperature range of -40 to 40°C . Larger differences occurred at 20°C . The double IGU with a high SHGC had the least differences compared with the standard value specific to each IGU, followed by the quad IGU.

5.2.3 $U_{\text{cog-CEN}}$ in Reference to 0°C

The $U_{\text{cog-CEN}}$ in reference to the CEN standard temperature of 0°C were 29% lower to 51% higher in the exterior temperature range of -40 to 40°C . Larger differences were seen at larger temperature differences and with the double IGUs. The least differences occurred for the quad IGU.

All of the IGUs in Section 5.2.1 with a lower SHGC had higher differences in U_{cog} values for both methods due to the increased conductive heat transfer through the presence of more low-E coatings (than high SHGC IGUs), as well as the effect of the various temperatures differences (in the exterior temperature range); where the greater the temperature difference, the greater conductive transfer.

5.2.4 U_{cog} Values with Different Gap Spacing Sizes in the 8 Climate Zones

The U_{cog} values of double and triple glazing IGUs with high and low SHGCs were simulated in the annual average temperatures of locations within the eight climate zones. Figures 36 and 37 represent the standard NFRC and CEN U_{cog} values with different gap spacing sizes; which were used as a baseline.

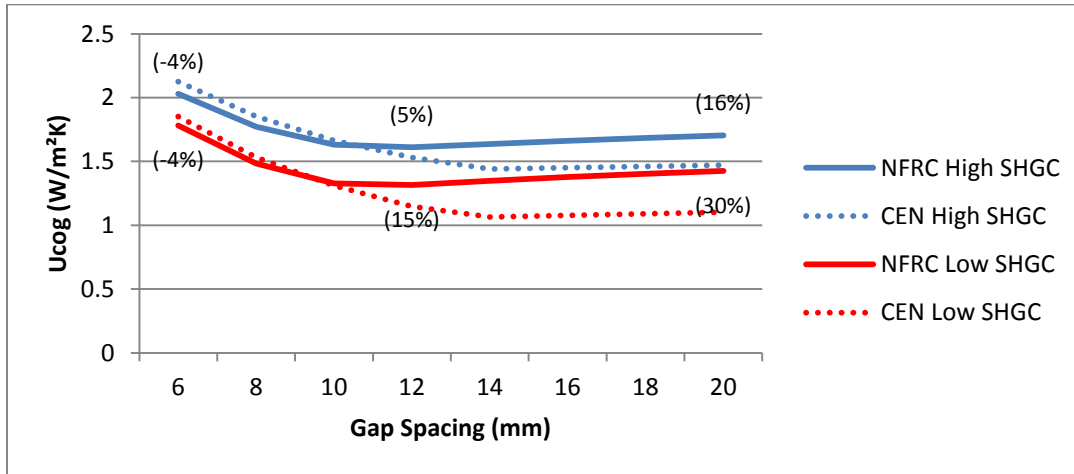


Figure 13 $U_{cog-NFRC}$ and $U_{cog-CEN}$ with Double IGUs: Various Gap Spacing Widths

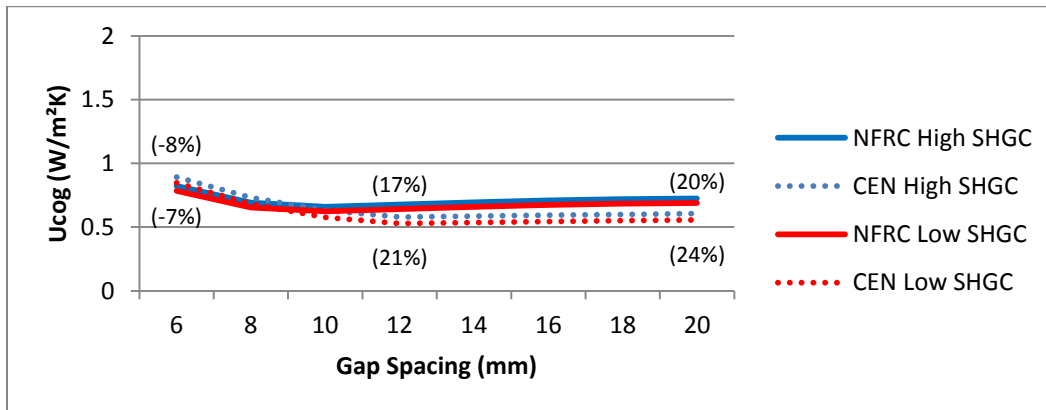


Figure 14 $U_{cog-NFRC}$ and $U_{cog-CEN}$ with Triple IGUs: Various Gap Spacing Widths

$U_{cog-NFRC}$ values for the double high SHGC IGU are 5% lower to 4% higher than $U_{cog-CEN}$ values in the 8 climate zones. $U_{cog-NFRC}$ values for the double low SHGC IGU are 28% lower to 7% higher than $U_{cog-CEN}$ values in the 8 climate zones (see Tables D-44 & D-45). $U_{cog-NFRC}$ values for the triple high SHGC IGU are 6% lower to 6% higher than $U_{cog-CEN}$ values in the 8 climate zones. $U_{cog-NFRC}$ values for the triple low SHGC IGU are 6% lower to 3% higher than $U_{cog-CEN}$ values in the 8 climate zones see (Tables D-46 & D-47).

Therefore, the trend shows that for higher performing IGUs the differences in U_{cog} values for both methods are less.

The $U_{\text{cog-NFRC}}$ values ranged from 16% lower to 34% higher than the standard NFRC value in the climate zones for different gap widths (see Tables D-44-D-47). Similarly, $U_{\text{cog-CEN}}$ values ranged from 29% lower to 51% higher than the standard CEN value in the climate zones for different gap widths. Therefore, depending on the climate zone location, the annual average U_{cog} values for both methods can potentially be 16% lower to 34% higher than an NFRC rated window; and 29% lower to 51% higher for a CEN rated window in North America.

The results show that the locations within the climate zones with higher extremes in temperature, in reference to the same interior temperature of 21°C, thermal transmittance increases with larger gap widths. Seeing that the larger gap widths entail larger volumes of infill gas, there is more potential for heat transfer to occur through convection and radiation with higher temperature extremes. Therefore, depending on the climate zone location, larger gap widths do not always give lower U_{cog} values. In effect, there is potential for more variance in gap spacing size within design processes using average annual U_{cog} values for each climate zone (Speier F. , 2014).

The double IGUs showed a slightly greater difference between the two SHGCs than the triple IGUs due to the larger gap spacing size and thus greater thermal transmittance through convection. The IGUs with a low SHGC had greater differences due to increased conduction through the presence of more low-E coatings and their effect on the thermal conductivity of the gas infill. There were negligible differences between the U_{cog} values of the double IGUs for both methods. For the triple IGUs, the largest percentage change between both methods occurs in climate zones 7 and 8 with gap widths from 14-20 mm due to larger gap widths and larger interior and exterior temperature differences result in increased conductive and radiative heat transfer.

5.3 Uframe Simulations

5.3.1 $U_{\text{frame-NFRC}}$, $U_{\text{frame-CEN}}$ and $U_{\text{frameIGU-CEN}}$ Calculation Methods

The results showed that the $U_{\text{frame-NFRC}}$ values are 7% lower to 1% higher than the $U_{\text{frame-CEN}}$ values with the IGU for all the frames. The trend showed that greater differences in $U_{\text{frame-CEN}}$ values of both methods occurred for the solid wood and TBSW compared with the U-PVC and fiberglass frames (see Figures 15-18). The greater the length of the sightline to the edge of the frame, and the greater the frame width, the greater the differences in $U_{\text{frame-CEN}}$ values (See Table 39 and Section 5.5 for further

discussion). Different thermal conductivities, frame cavity methods, surface film coefficients and calculation methods contribute to the variation in values. The different exterior temperatures of both methods do not impact the U_{frame} seeing that the results showed that U_{frame} did not change between the temperatures of -40 to 40°C.

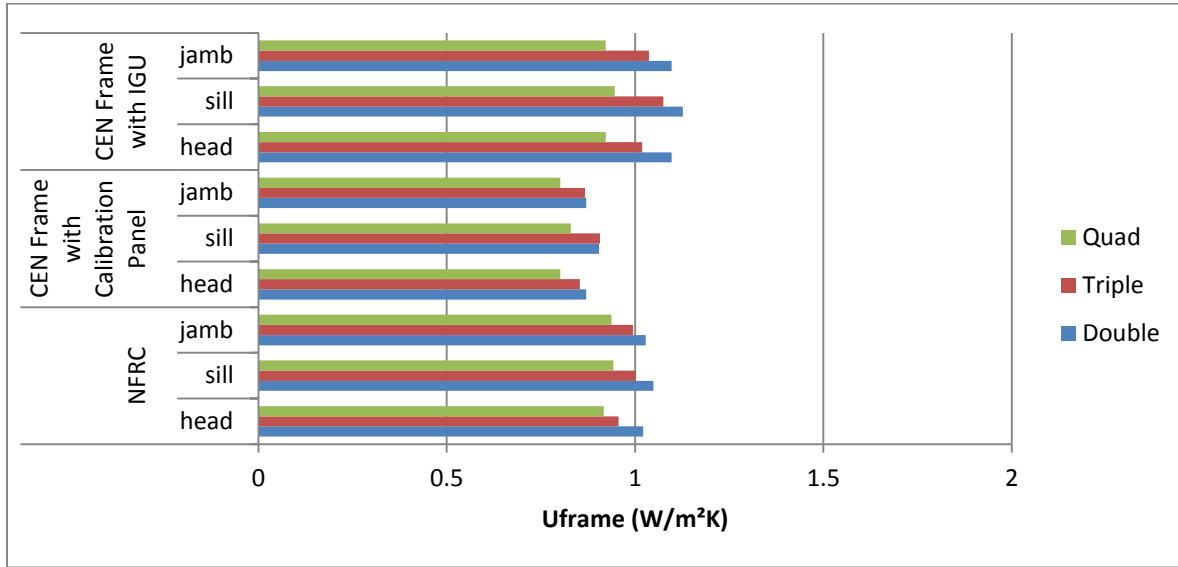


Figure 15 TBSW U_{frame} : NFRC and CEN Frame Methods

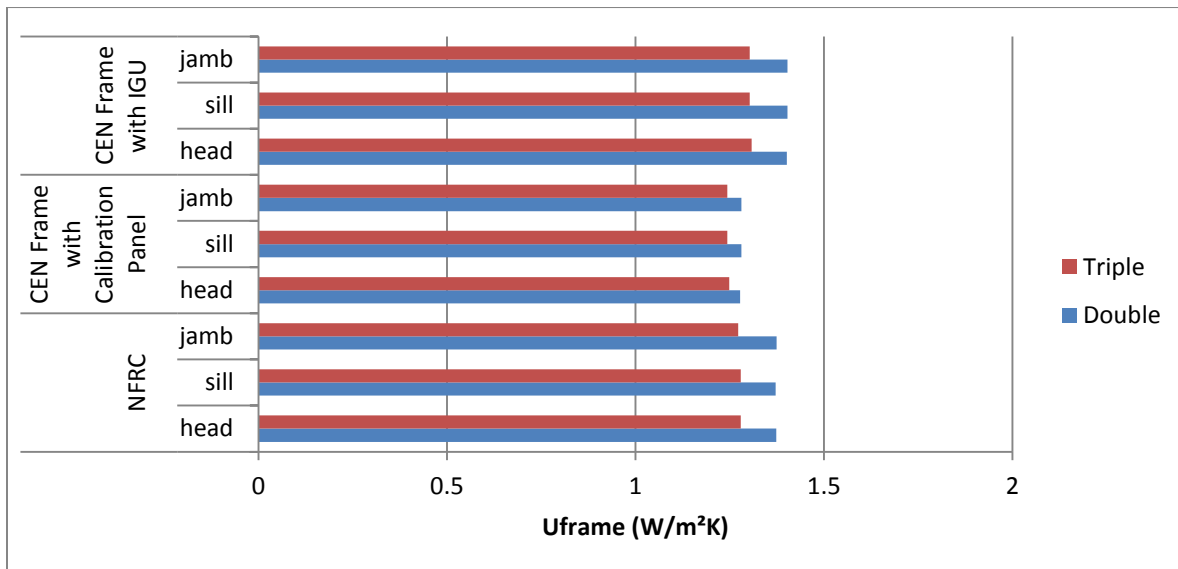


Figure 16 U-PVC U_{frame} : NFRC and CEN Frame Methods

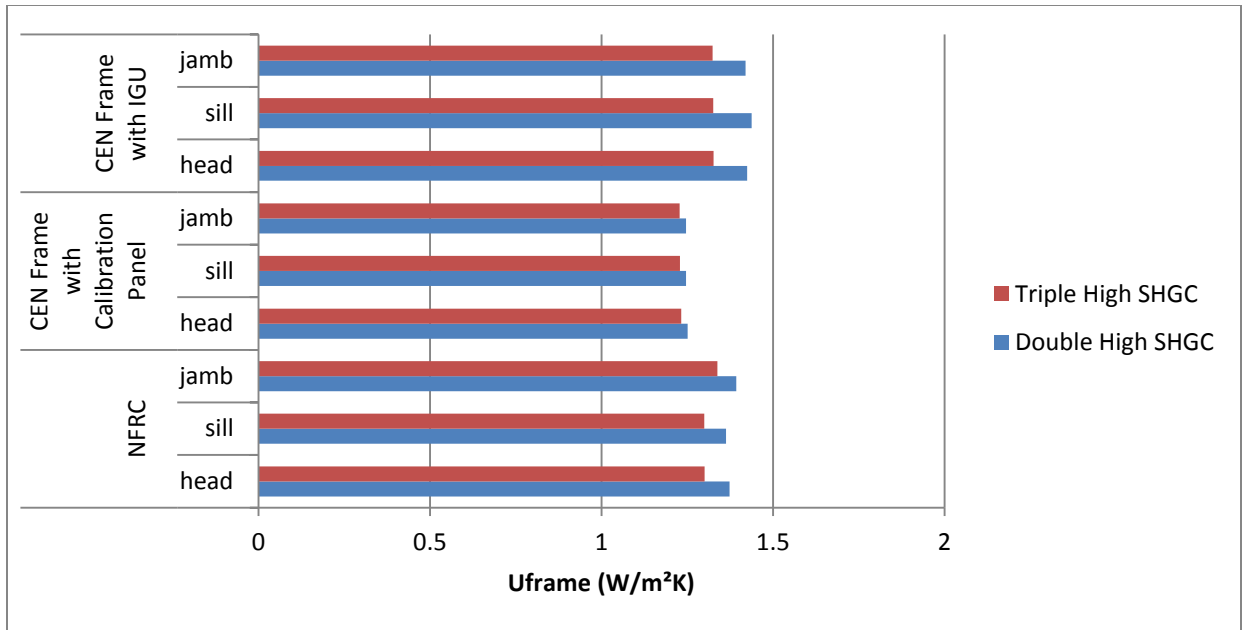


Figure 17 Fiberglass Frame: $U_{\text{frame-NFRC}}$ vs $U_{\text{frame-CEN}}$ and $U_{\text{frameIGU-CEN}}$

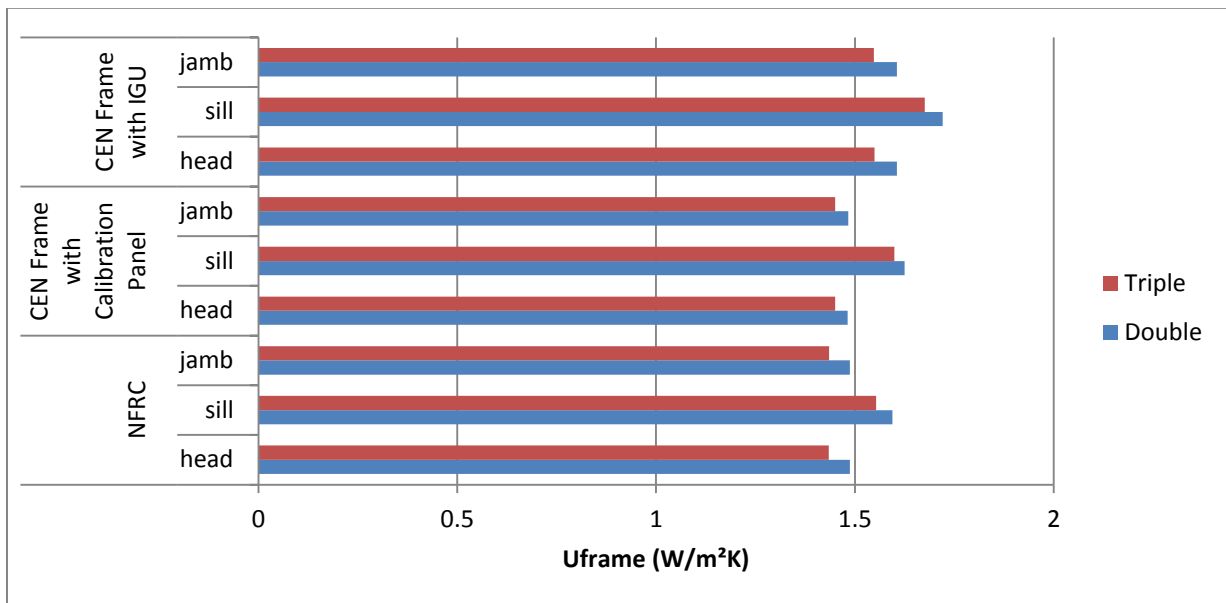


Figure 18 Solid Wood Frame: $U_{\text{frame-NFRC}}$ vs $U_{\text{frame-CEN}}$ and $U_{\text{frameIGU-CEN}}$

Although $U_{\text{frame-CEN}}$ and $U_{\text{frameIGU-CEN}}$ (from Equation 8) are modeled differently, $U_{\text{frameIGU-CEN}}$ is typically higher than $U_{\text{frame-CEN}}$. $U_{\text{frameIGU-CEN}}$ is higher because it is determined using the actual glazing insert which includes the thermal transmittance effects of the glazing and spacer (which typically contain

materials with a higher thermal conductivity). That in effect raises the thermal transmittance of the frame. Whereas the $U_{\text{frame-CEN}}$ is typically lower since it uses a calibration panel with a very low thermal conductivity (i.e. 0.035 W/mK). For high performance glazing and spacers, the NFRC and CEN U_{frame} values with the IGU would be more similar, since there is less heat transfer interactions taking place from the frame towards the spacer and glazing than a lower performing window unit. The primary differences here are in the boundary conditions, such as, the edge effects lengths are 65 and 190 mm for the NFRC and CEN methods respectively and different surface film coefficients. Overall, the $U_{\text{frame-CEN}}$ can give a fair comparison of frames due to the use of a calibration panel, which also allows for various IGU combinations to be compared and the incremental effect of their thermal performance can be measured when combined with the frame. $U_{\text{frame-CEN}}$ thus gives a more in depth picture of the thermal interactions that are responsible for the degree of differences between both methods.

5.3.2 $U_{\text{frame-CEN}}$ with CEN and NFRC Frame Cavity Methods

Seeing that the $U_{\text{frame-CEN}}$ method gives the thermal transmittance value of the frame without the influence of the IGU, the $U_{\text{frame-CEN}}$ method was used to simulate the four frame types with different boundary conditions. The effect of using different frame cavity methods, thermal conductivities and surface film coefficients were simulated with triple IGUs with a high SHGC and Spacer C. The results showed that using the CEN frame cavity method gave $U_{\text{frame-CEN}}$ values that were 3% lower to 4% higher than the $U_{\text{frame-CEN}}$ using the NFRC frame cavity method (see Figure 19). For the fiberglass head and sill simulations there was no change in $U_{\text{frame-CEN}}$ values. The TBSW and solid wood frames ranged from 0-3% percentage change between the two methods. The U-PVC frame showed the larger percentage change out of all the frames at 4% higher $U_{\text{frame-CEN}}$ value than when using the NFRC frame cavity method.

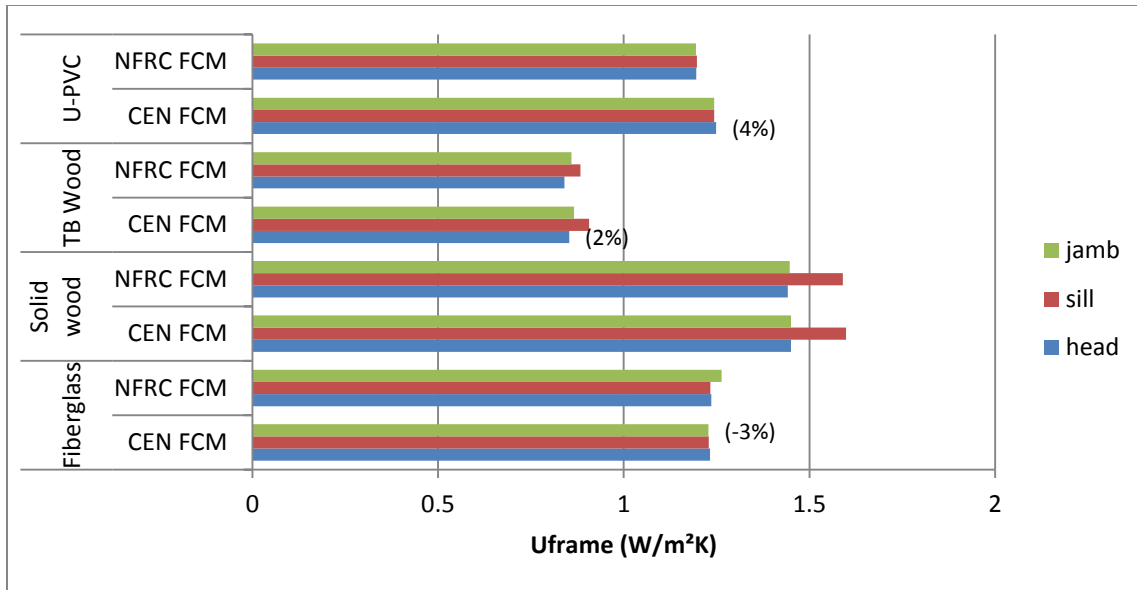


Figure 19 CEN U_{frame} : CEN vs NFRC Frame Cavity Methods (FCM)

Considering that the CEN frame cavity method takes into account the surface temperatures of each side of a rectangular cavity, the thermal conductivity of more surfaces are taken into account. Structural reinforcement, such as galvanized steel, with a 62 W/mK thermal conductivity, compared with U-PVC's lower conductivity of 17 W/mK, can contribute to increased heat flows in the frame cavities when all surfaces are considered. The NFRC frame cavity method only takes into account two facing frame cavity surface temperatures, therefore, higher conductive materials surrounding the frame cavities have a slightly less effect on the frame's thermal transmittance.

The TBSW frame had the second highest percentage change and this may be due to the effect of the oxidized aluminum siding placed on the exterior, with a thermal conductivity of 237 W/mK. This high thermal conductivity influences the thermal transmittance in the frame cavity areas next to it, however, the extremely low conductivity of the insulation foam and EPDM efficiently reduce the impact of the aluminum's conductivity upon the entire frame.

The fiberglass frame had no percentage change between the two methods for the head and sill due to the low thermal conductivity of fiberglass, U-PVC and weather stripping components, combined with insulation foam which has an extremely low conductivity (see Section 3.15). The placement of the insulation foam and other components with a low thermal conductivity impedes the thermal transmittance across frame cavities from various directions, thus stabilizing frame cavity surface temperatures. The CEN frame cavity method gave a 3% lower $U_{\text{frame-CEN}}$ value than the NFRC frame

cavity method for the jamb due to the effect of gravity and the frame cavity configuration within the jamb. The frame cavities are elongated in the downward direction, which is the same direction as the heat flow and gravity. Therefore, since air at a lower temperature in the frame cavities sinks with the gravitational pull, and that the NFRC method only accounts for the two surface temperatures, there is a slightly higher temperature differential between the top and bottom of the jamb.

The solid wood frame had 0-1% differences between the two methods since there are a minimal number of frame cavities and their size is extremely small.

Overall, when comparing the $U_{\text{frame-CEN}}$ values for all of the frame types with a calibration panel, the TBSW frame had the lowest U-value and in ascending order, the fiberglass, U-PVC and solid wood frames (see Figures 20 & 21). Without the influence of the thermal interactions of the actual IGU, this $U_{\text{frame-CEN}}$ value allows for a fairer comparison between the frame types than when the IGU is included.

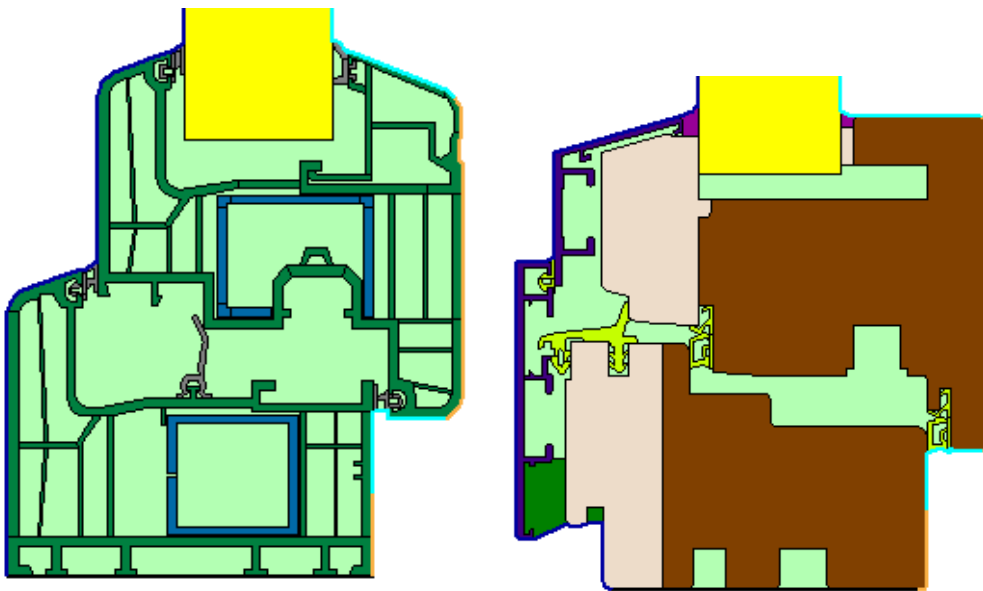


Figure 20 U-PVC and TBSW Frames with a Calibration Panel

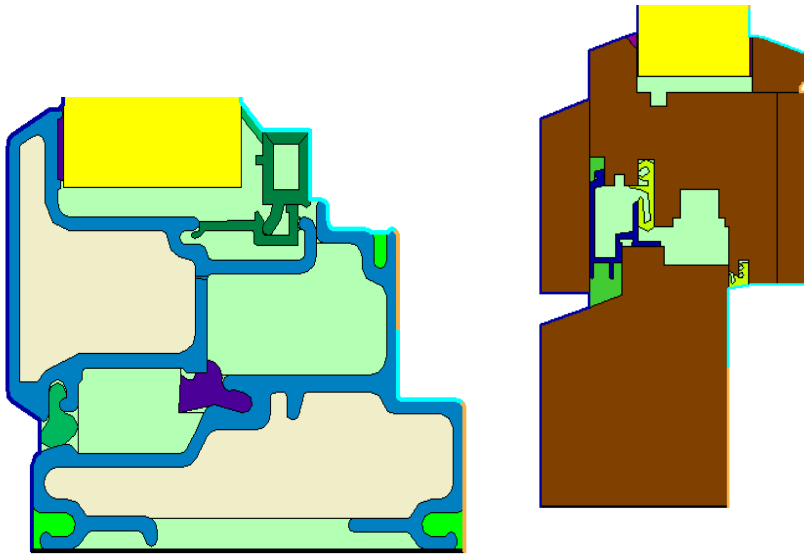


Figure 21 Fiberglass and Solid Wood Frames with a Calibration Panel

5.3.3 $U_{\text{frame-CEN}}$ Comparison with CEN and NFRC Surface Film Coefficients

The surface film coefficients, which combine convection and radiation, have a large impact on the $U_{\text{frame-CEN}}$. As stated in Section 3.16, the CEN method includes the radiation and convective components in the surface film coefficient values, whereas the NFRC method does not include the radiation component, as it is included in the radiation model in the simulations. Therefore, when replacing CEN surface film coefficients with NFRC values, the radiation component is being neglected and thus this is only a theoretical scenario. However, this was an experiment to investigate how different surface film coefficient values impacted the $U_{\text{frame-CEN}}$ values. The different surface film coefficients used in the NFRC and CEN methods had a large impact on the $U_{\text{frame-CEN}}$ values. The $U_{\text{frame-CEN}}$ values were 19-34% higher than the $U_{\text{frame-CEN}}$ values using the NFRC surface film coefficients. The largest impact in descending order was for the solid wood, U-PVC, fiberglass and TBSW frames. The effect of different surface film coefficients upon $U_{\text{frame-CEN}}$ values depends upon the thermal performance of the frame. The results showed that the higher the thermal performance of the frame, the less of an impact that the surface film coefficients had upon $U_{\text{frame-CEN}}$. The NFRC surface film coefficients had the most impact on the U-PVC frame and the least impact on the TBSW frame due to its higher thermal performance.

5.3.4 $U_{\text{frame-CEN}}$ of Four Frame Types with a Calibration Panel

To rate the four frame types from the least to the most conductive, $U_{\text{frame-CEN}}$ simulations were conducted. Figure 22 shows that the TBSW frame is the least conductive and in ascending order;

fiberglass, U-PVC and solid wood. The solid wood sill simulations were slightly more conductive than the other frames, due to the longer length of the sightline to the edge of the frame.

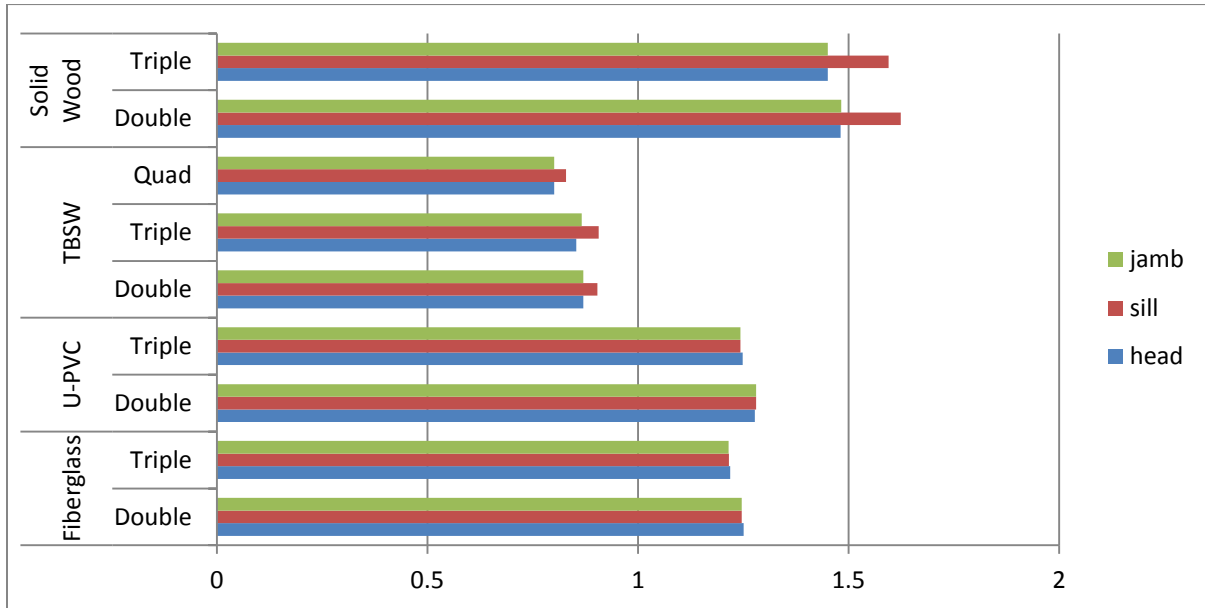


Figure 22 $U_{frame-CEN}$ with Four Frame Types

5.3.5 $U_{frame-CEN}$ Comparisons with Various Material Thermal Conductivities

$U_{frame-CEN}$ comparisons were conducted for the fiberglass, TBSW and solid wood frames with a calibration panel for the frames that fit a triple IGU (see Figure 23). These simulations demonstrate the effect of different thermal conductivities of the frame materials on the $U_{frame-CEN}$.

Using CEN thermal conductivities for softwood for the TBSW frame resulted in 5% higher $U_{frame-CEN}$ values than values with NFRC thermal conductivities. The solid wood $U_{frame-CEN}$ values were 10-11% higher than U-frame values using NFRC thermal conductivities.

Different thermal conductivities of the frame material result in a 5-11% difference for softwood materials (see Figure 23).

The $U_{frame-CEN}$ values for the fiberglass frame showed that the higher NFRC thermal conductivity for fiberglass gave 9% higher $U_{frame-CEN}$ values than when the CEN thermal conductivity values was used.

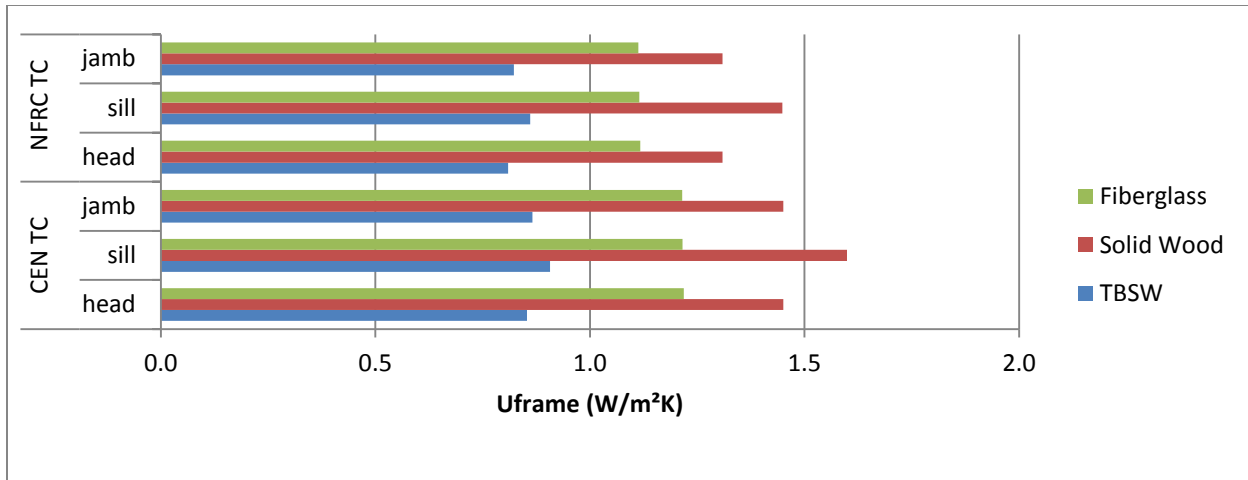


Figure 23 $U_{\text{frame-CEN}}$: CEN and NFRC Thermal Conductivities

5.4 U_{window} Simulations

5.4.1 $U_{\text{window-NFRC}}$ and $U_{\text{window-CEN}}$ Standard Comparison

All of the window configurations, listed in Section 3.5, were simulated using Spacer C in the standard CEN and NFRC methods. Results from the SHGC, U_{cog} and U_{frame} simulations in Sections 5.1-5.3 were utilized to aid in the explanation of the U_{window} results found in this section. As a result of simulations performed in Sections 5.5 and 5.6.4, Spacer C was the highest performing spacer and was thus chosen for the U_{window} comparisons. It is acknowledged that using Spacers A and B in all of the U_{window} simulations would give different results. This is beyond the scope of this research. The quad IGU was only simulated with the TBSW frame as per the manufacturer’s specifications since it is not typically installed in other frame types.

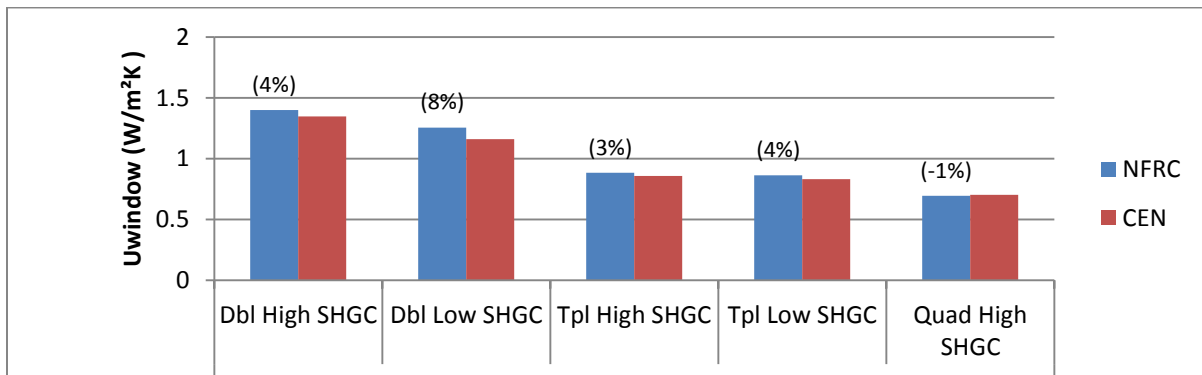


Figure 24 TBSW Frame: NFRC and CEN U_{window} Values (Percentage Change)

For the TBSW frame, the $U_{\text{window-NFRC}}$ value results were 1% lower to 8% higher than $U_{\text{window-CEN}}$ values. The IGUs with a low SHGC showed the greater differences between the methods (see Figure 24 and Table B-42).

The $U_{\text{window-NFRC}}$ values for the double and triple IGU combinations with the solid wood frame were 1% lower to 3% higher than CEN values (see Figure 25 and Table B-42). The lower $U_{\text{window-NFRC}}$ values are attributed to the lower NFRC thermal conductivity (see Section 3.15). The higher $U_{\text{window-NFRC}}$ values are attributed to the influence of higher $U_{\text{cog-NFRC}}$ values (see Table 37) and the weighting of the U_{cog} value in the $U_{\text{window-NFRC}}$ calculation method.

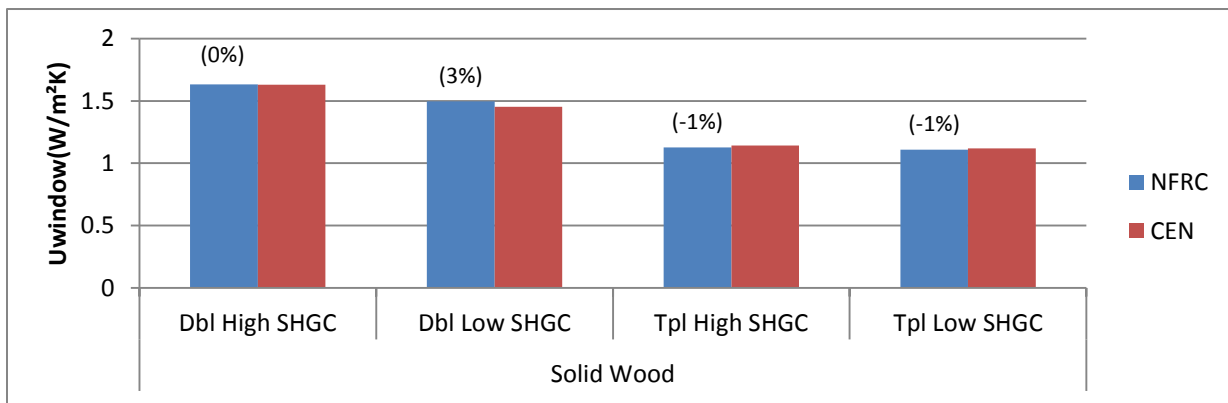


Figure 25 Solid Wood Frame: NFRC and CEN U_{window} Values (Percentage Change)

The $U_{\text{window-NFRC}}$ values of the double and triple IGU combinations for the fiberglass frame were 5-11% higher than CEN values (see Figure 26 and Table B-42).

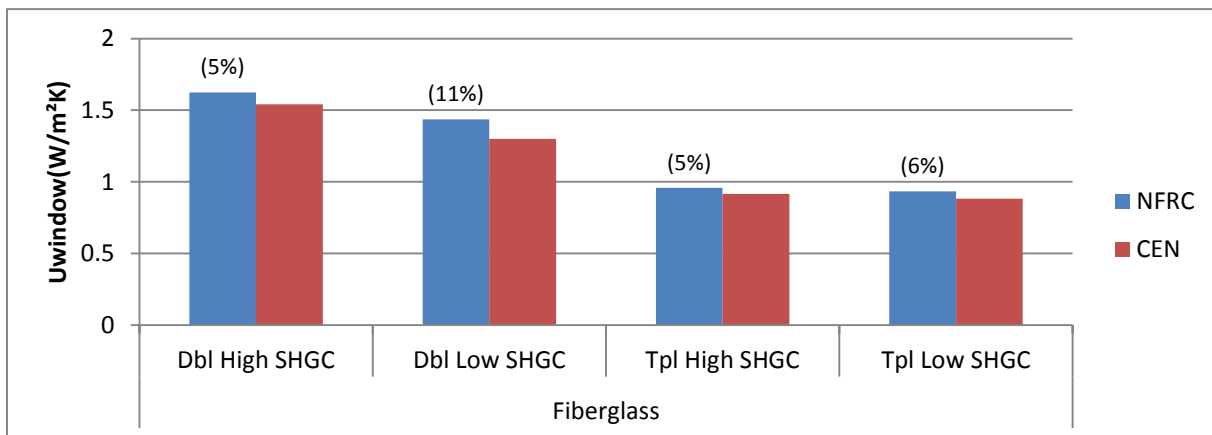


Figure 26 Fiberglass Frame: NFRC and CEN U_{window} Values (Percentage Change)

The $U_{\text{window-NFRC}}$ values for the double and triple IGU combinations for the U-PVC frame were found to be 2-7% higher than CEN values (see Figure 27 and Table B-42).

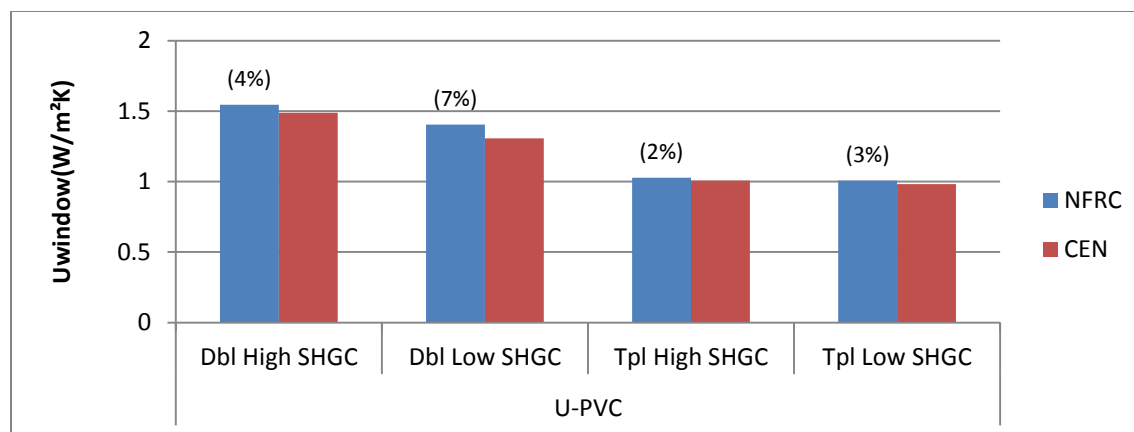


Figure 27 U-PVC Frame: NFRC and CEN U_{window} Values (Percentage Change)

The $U_{window-NFRC}$ values range from 1% lower to 6% higher for the triple and quad high performance window combinations. For all of the frame types, the trend shows that $U_{window-NFRC}$ values are primarily larger than $U_{window-CEN}$ values for most of the IGU combinations and the differences between both methods decrease as the thermal performance of the IGU improves. Therefore, the methods can be harmonized for higher performing frames and IGUs. The greater differences seen in the double IGU combinations suggest that the differences in U_{cog} procedures are accentuated in lower performing window combinations.

Since the U_{cog} is highly variable with the exterior temperatures and are increasingly variable with larger temperature differences between the interior and exterior environments, the longer the length of the sightline to the edge of the frame, the lesser the differences that occur between the NFRC and CEN U_{window} values. The solid wood frame had the highest conductivity, and in descending order: U-PVC, fiberglass and TBSW (see Section 5.3.4). This occurrence is partially due to the thermal interactions of the higher IGU U-value transferring to the frame. The larger frame surface area and width of the solid wood frame (see Table 39) contributes more conductive heat transfer through the frame. Therefore, the discrepancies in U_{cog} NFRC and CEN values are reduced by the thermal interactions of the IGU being transferred through the frame. Although the TBSW frame is less conductive than the fiberglass frame, the TBSW frame had lesser differences between both methods due to the longer length from the sightline to the edge of the frame. Again, the transfer of the thermal interactions of the IGU is less effective the longer the length of the high performance frame between the sightline and frame edge.

Out of all the frames simulated, the fiberglass frame showed the larger differences where $U_{window-NFRC}$ values were between 5-11% higher than CEN values. From the thermal conductivity comparative results

of both methods for fiberglass frames in Section 5.3.4, it would be assumed that the $U_{\text{window-NFRC}}$ results would be lower than the CEN values given CEN's lower thermal conductivity for fiberglass (i.e. 0.3 vs 0.4 W/mK). However, since the NFRC values are higher, other boundary conditions are influential here. Specifically, the different exterior temperatures, surface film coefficients, frame cavity and center-of-glazing approaches specific to each method all contribute to the discrepancies in the U_{window} results.

The result of changing CEN simulation's exterior temperature to the NFRC value of -18°C (see Table B-43), was an $U_{\text{window-NFRC}}$ value that was 1% higher than the CEN value for the double IGUs and a 2% lower value for the triple IGUs. Therefore, for the double IGUs, the difference in exterior temperatures used in both methods gives a minimal contribution to a higher $U_{\text{window-NFRC}}$ value. For the triple IGUs, the difference in exterior temperatures slightly lowers the $U_{\text{window-NFRC}}$ value and thus doesn't explain the higher NFRC values.

The effect of using different surface film coefficients of both methods does not explain the higher $U_{\text{window-NFRC}}$ values. The surface film coefficient comparative results show that for the fiberglass frame, the $U_{\text{window-NFRC}}$ values were 4-5% lower than the $U_{\text{window-NFRC}}$ values using CEN surface film coefficients. Therefore, the effect of using different surface film coefficients of both methods does not explain the higher $U_{\text{window-NFRC}}$ values. See Section 5.4.3 for further discussion.

From the frame cavity method comparison results (see Section 5.4.4), the $U_{\text{window-NFRC}}$ values of the fiberglass frame combinations were 1% higher than the NFRC values using the CEN frame cavity method. The $U_{\text{window-CEN}}$ values were 1% lower than when using the NFRC frame cavity method. Similarly, the $U_{\text{frame-CEN}}$ frame cavity method comparison isolated the effect of the different frame cavity methods on the frame by itself, and the results showed that for a triple IGU with a high SHGC, the $U_{\text{window-NFRC}}$ value for the jamb was 3% higher than the $U_{\text{window-CEN}}$ value. Thus, there is a slight difference between the frame cavity methods and this difference does contribute slightly to the higher $U_{\text{window-NFRC}}$ values.

The center-of-glazing approaches of both methods yields results where the $U_{\text{cog-NFRC}}$ values of the IGUs used in this study were found to be 11-22% higher than $U_{\text{cog-CEN}}$ (see Table 37). The larger differences were seen for the IGUs with a low SHGC due to the presence of higher conductive low-E coatings (see Section 5.2.1 for further discussion). Seeing that the glazing constitutes the majority of the window area and, in addition, is a large component of the thermal transmittance calculations, the thermal transmittance of the glazing is integral and highly influential in the final U_{window} value. The higher $U_{\text{cog-NFRC}}$ values significantly lowers the U_{window} values and thus explains and largely accounts for the higher

$U_{\text{window-NFRC}}$ values for the fiberglass frame and IGU combinations. The potential effect of the thermal conductivity differences between both methods will be discussed further.

Table 37 NFRC and CEN U_{cog} Values

IGU	NFRC	CEN	% Change
Double High SHGC	1.627	1.466	11%
Double Low SHGC	1.336	1.071	25%
Triple High SHGC	0.681	0.58	17%
Triple Low SHGC	0.645	0.53	22%

Although the NFRC $U_{\text{cog-NFRC}}$ values for the double and triple IGUs were considerably higher than the CEN values, the higher performing triple IGUs had less of an impact on the U_{window} value than the double IGUs.

Lower performing insulated glazing units influence the thermal transmittance of the frame if the frame is poorly insulated. If the frame is well insulated, it improves U_{window} by impeding the thermal transmittance from the glazing to the frame which could further lower a poorly insulated frame.

5.4.2 $U_{\text{window-NFRC}}$ and $U_{\text{window-CEN}}$ with Various Material Thermal Conductivities

The $U_{\text{window-NFRC}}$ values of the fiberglass frames with the double and triple IGUs were compared using the NFRC and CEN thermal conductivity values of 0.3 and 0.4 W/mK. All simulations used Spacer C. Using the NFRC thermal conductivity resulted in 2-3% lower $U_{\text{window-NFRC}}$ values than $U_{\text{window-NFRC}}$ values when the CEN thermal conductivity was used. These results show that harmonizing the fiberglass thermal conductivity values, by utilizing the NFRC value (for example) for both methods, will result in 2-3% lower $U_{\text{window-CEN}}$ values. This drop in values would accentuate the differences in $U_{\text{window-NFRC}}$ and $U_{\text{window-CEN}}$ values seen in Figure 28. Although using the same material thermal conductivities would accentuate the differences in U_{window} values of both methods, it is important to use the same thermal conductivities for a material and focus on other influential parameters in order to harmonize the two methods.

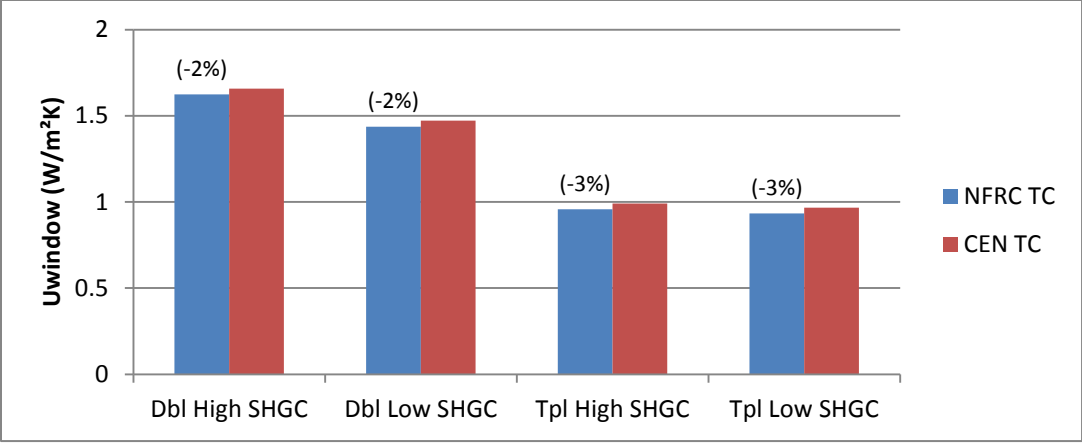


Figure 28 Fiberglass Frame: NFRC U_{window} : NFRC and CEN Thermal Conductivities (TC) (Percentage Change)

For the TBSW frame, the $U_{window-NFRC}$ values were 2-4% lower than when the CEN thermal conductivity was used (see Figure 29).

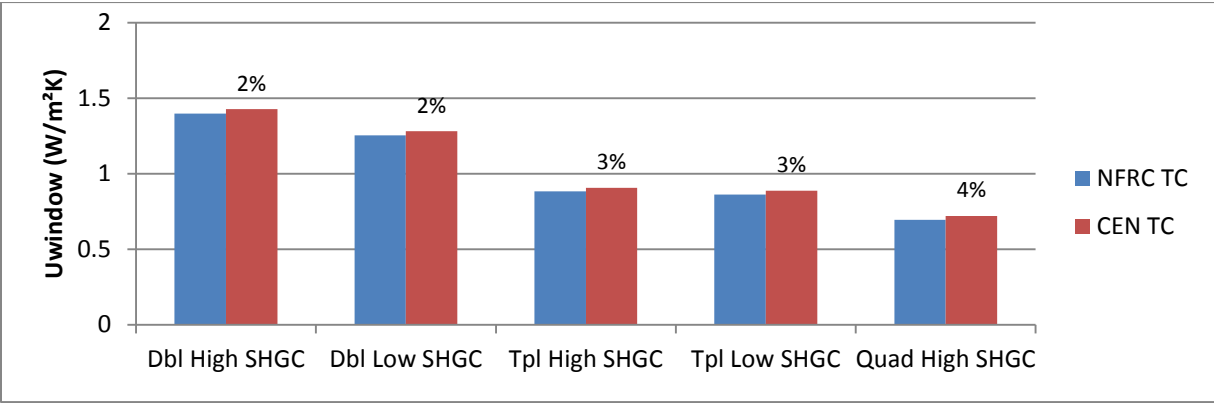


Figure 29 $U_{window-NFRC}$ TBSW Frame: NFRC and CEN Thermal Conductivities (TC) (Percentage Change)

For the solid wood frame, $U_{window-NFRC}$ values, with the NFRC thermal conductivity for softwood, were 4-6% lower than when using the CEN thermal conductivity. The percentage change is higher than for the TBSW frame due to the larger area of solid wood within the frame (See Figure 30).

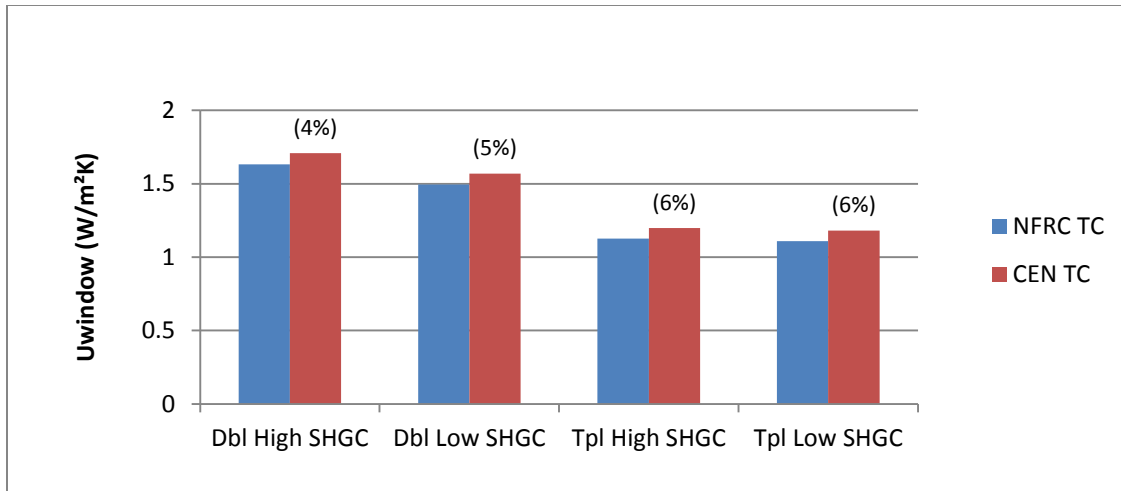


Figure 30 U_{window-NFRC} Solid Wood Frame: NFRC and CEN Thermal Conductivities (TC) (Percentage Change)

Table 38

Frame Material	NFRC (W/mK)	CEN (W/mK)	Percentage Change
Fiberglass	0.3	0.4	-25%
Softwood	0.11	0.13	-15%

Overall, using thermal conductivities that are 15-25% higher in each method can potentially give 2-6% lower U_{window-NFRC} values (see Table 38).

Harmonizing the thermal conductivity values of both methods results in lower U_{window-NFRC} values; whereby the magnitude of the increase is dependent upon the increase in thermal conductivity and the area of that material within the frame. When identical thermal conductivities are used in both methods, the differences in U_{window} values are analogous for the TBSW and solid wood frames (see Figures 29 & 30). The differences are less for the TBSW frame due to the less volume of solid wood and the use of lower conductive insulation foam, EPDM and frame cavities, which function as a thermal break between the higher conductive solid wood and aluminum siding. The TBSW frame also does not expose the solid wood to the exterior environment and is thus the other materials mentioned serve as a protective thermal barrier. Seeing that there are lesser differences in the higher performing frames, this supports the possibility of harmonizing the material thermal conductivities of both methods.

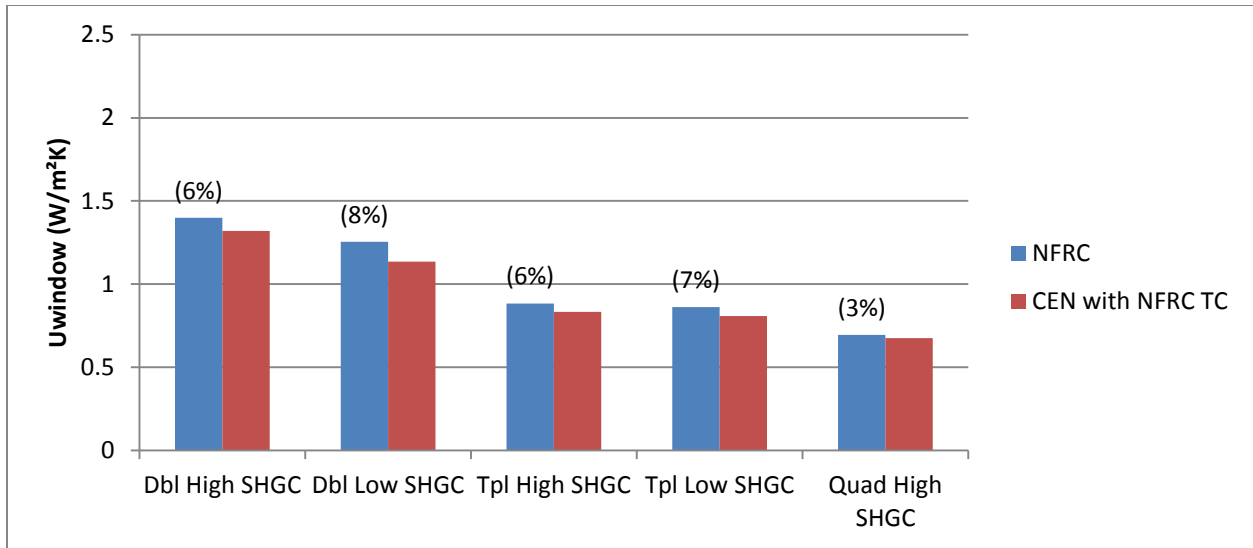


Figure 31 $U_{\text{window-NFRC}}$ and $U_{\text{window-CEN}}$ TBSW Frame: NFRC Material Thermal Conductivities (Percentage Change)

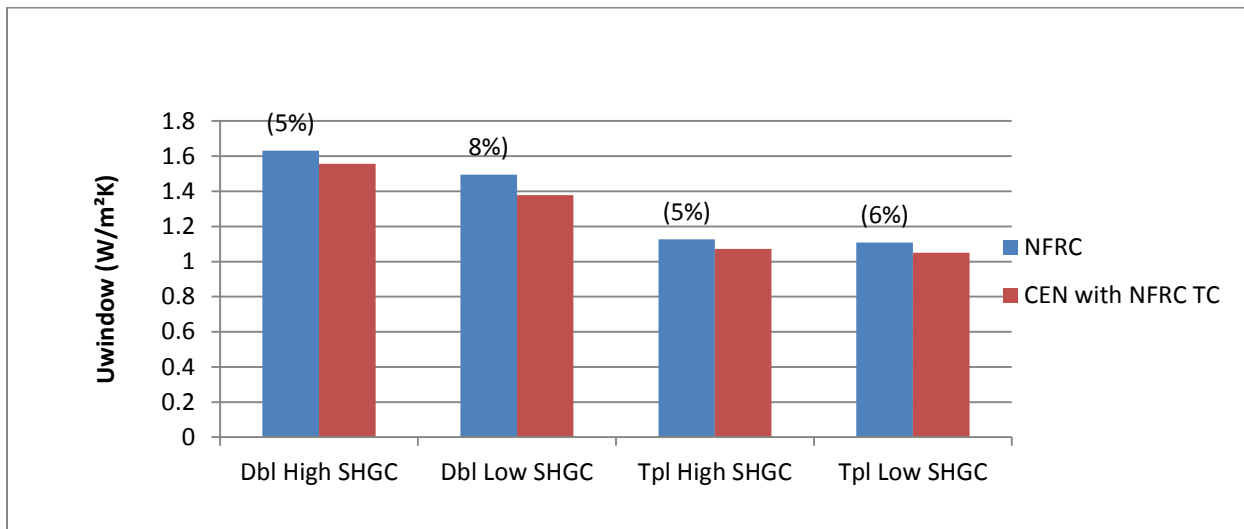


Figure 32 $U_{\text{window-NFRC}}$ and $U_{\text{window-CEN}}$ TBSW Frame: NFRC Material Thermal Conductivities (Percentage Change)

5.4.3 $U_{\text{window-NFRC}}$ and $U_{\text{window-CEN}}$ with NFRC and CEN Surface Film Coefficient Sets

It was assumed that fiberglass had the same surface film coefficient as NFRC does not yet specify one for fiberglass. All frame and glazing combinations used Spacer C, and were simulated with the $U_{\text{window-NFRC}}$ calculation method using NFRC and CEN surface film coefficients (see Figures 33-36). The same window combinations were simulated with the $U_{\text{window-CEN}}$ calculation method using CEN and NFRC surface film coefficients.

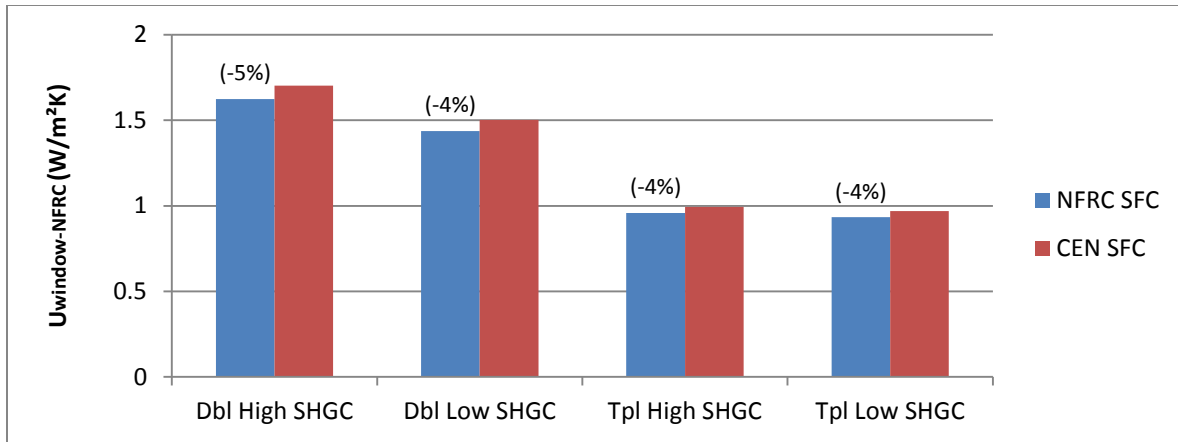


Figure 33 Fiberglass Frame: NFRC vs CEN Surface Film Coefficients using the NFRC Method

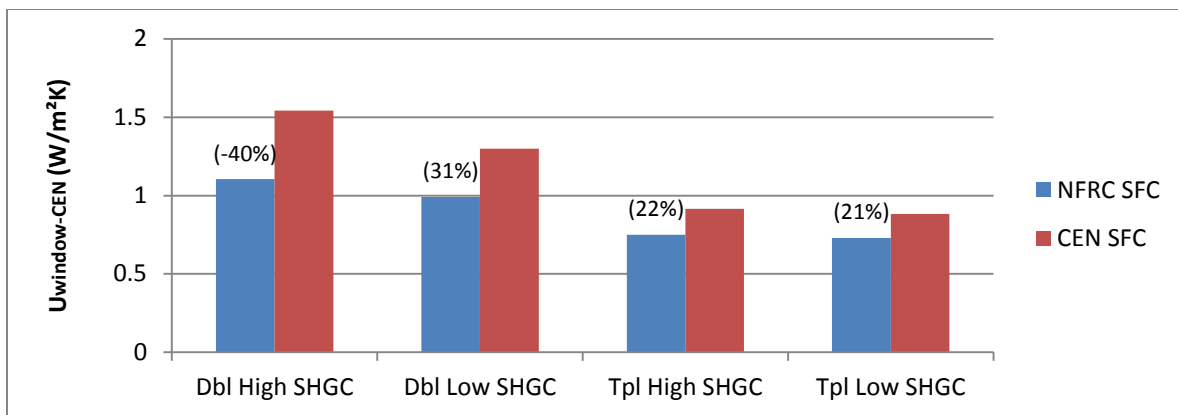


Figure 34 Fiberglass Frame: NFRC vs CEN Surface Film Coefficients using the CEN Method (Percentage Change)

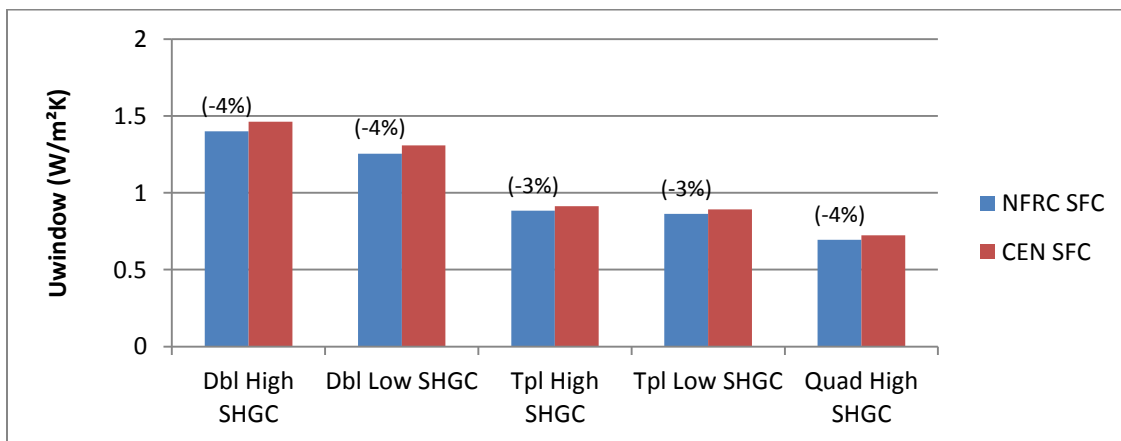


Figure 35 TBSW Frame: NFRC vs CEN Surface Film Coefficients using the NFRC Method (Percentage Change)

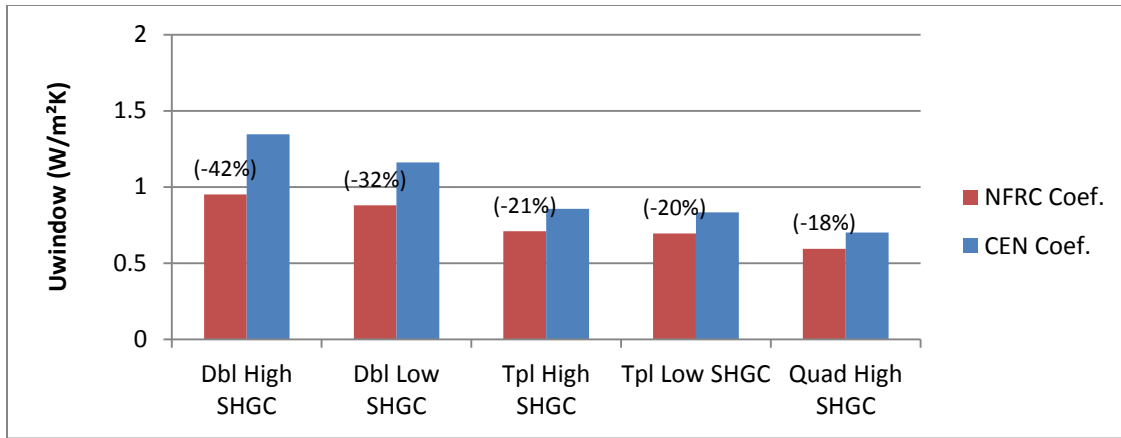


Figure 36 TBSW Frame: NFRC vs CEN Surface Film Coefficients using the CEN Method (Percentage Change)

The largest discrepancy for all the window combinations and frame types was for the double IGUs; particularly the double IGU combinations with a high SHGC due to the effect of the different interior and exterior temperature boundary conditions. The trend showed that there are greater differences in the U_{window} values of both methods for the most conductive frame, i.e. solid wood. For the remaining three frames, the deeper the inset of the IGU (i.e. sightline to the bottom of the IGU), and the longer the length between the sightline to the edge of the frame, as well as the conductivity of the frame components all contribute to the lower differences in U_{window} values between both methods.

Overall, the NFRC method's lower surface film coefficient values result in lower $U_{\text{window-CEN}}$ values. Larger discrepancies were seen in the CEN simulations due to the omissions of the radiation component in the NFRC surface film coefficient sets as stated in Section 3.16.

5.4.4 $U_{\text{window-NFRC}}$ and $U_{\text{window-CEN}}$ using NFRC and CEN Frame Cavity Methods

The $U_{\text{window-NFRC}}$ value using the NFRC frame cavity method is 1% lower to 1% higher than the $U_{\text{window-NFRC}}$ values that use the CEN frame cavity method for all of the frames. For the fiberglass frame simulations with double and triple IGUs, the $U_{\text{window-NFRC}}$ values when using the NFRC frame cavity method were all 1% higher than the NFRC values using the CEN frame cavity method. There was no change in $U_{\text{window-NFRC}}$ values using both frame cavity methods for the TBSW and solid wood frames. The U-PVC $U_{\text{window-NFRC}}$ values using the NFRC frame cavity method were 1% lower than values using the CEN frame cavity method (see Figure 37). There are thus negligible differences between both frame cavity methods when using the NFRC method. This supports the harmonization of the frame cavity procedures of both the NFRC and CEN methods.

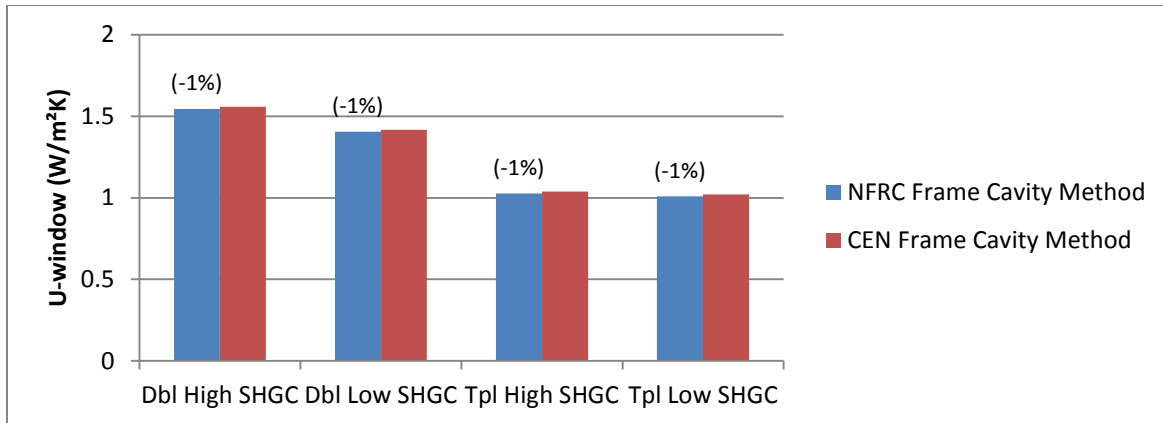


Figure 37 U-PVC Frame: NFRC vs CEN Frame Cavity Methods using the NFRC Method (Percentage Change)

The $U_{\text{window-CEN}}$ value using the CEN frame cavity method is 1% lower to 3% higher than the $U_{\text{window-CEN}}$ values that use the NFRC frame cavity method for all the frames. All of the TBSW frame combinations and the double IGU solid wood simulations showed no difference in U_{window} values. The triple IGU solid wood frame $U_{\text{window-CEN}}$ values were 1% higher than CEN values using the NFRC frame cavity method. The $U_{\text{window-CEN}}$ values for the fiberglass frame combinations were 1% lower than the $U_{\text{window-CEN}}$ values using the NFRC frame cavity method. The $U_{\text{window-CEN}}$ values of the U-PVC frame combinations were 2-3% higher than the values using the NFRC frame cavity method; the triple IGU combination showed the higher results (see Figure 38). The U-PVC frame had the larger differences since it has the most frame cavities out of all the frames. Since the NFRC frame cavity method only considers two surfaces in the direction of the heat flow, there is a slightly larger difference between the frame cavity surface temperatures which result in a higher $U_{\text{window-CEN}}$ value (see Section 3.18).

Overall, the two frame cavity methods produce negligible differences in U_{window} for all frame types and thus amalgamating this parameter supports the harmonization of these methods.

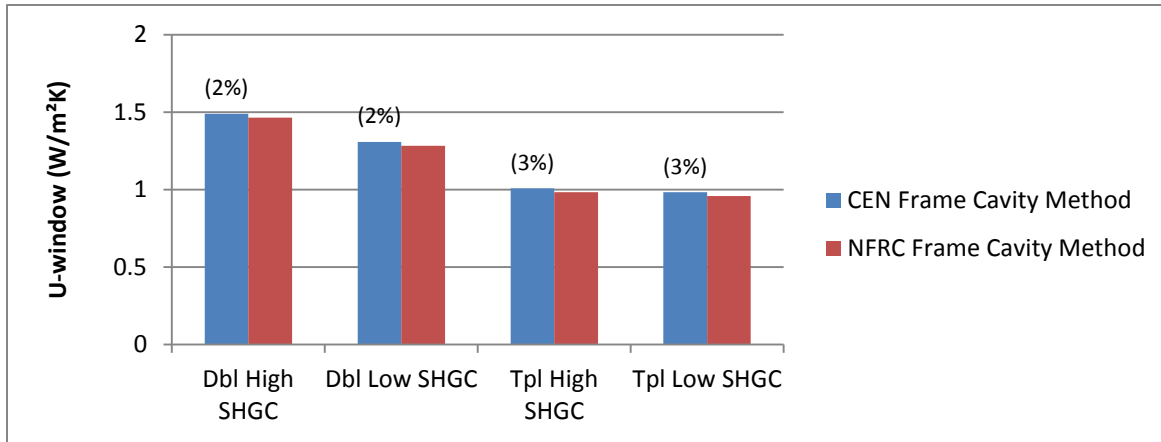


Figure 38 U-PVC Frame: $U_{\text{window-CEN}}$ using NFRC and CEN Frame Cavity Methods (Percentage Change)

5.4.5 $U_{\text{window-NFRC}}$ and $U_{\text{window-CEN}}$ Comparison with 4 Frame Types

The comparative results of the four frame types with double IGUs, with a low SHGC, showed that the TBSW frame had the lowest $U_{\text{window-NFRC}}$ values and in ascending order: fiberglass, U-PVC and solid wood. For the double IGUs with a high SHGC, the TBSW frame had the lowest $U_{\text{window-NFRC}}$ and in ascending order: U-PVC, fiberglass and solid wood (see Figure 39).

For the four frame types with a triple IGU for both methods, the TBSW frame with the high and low SHGC had the lowest U_{window} value and in ascending order: fiberglass, U-PVC and solid wood (see Figure 40). These results are identical to the $U_{\text{frame-CEN}}$ simulations in Section 5.3.3.

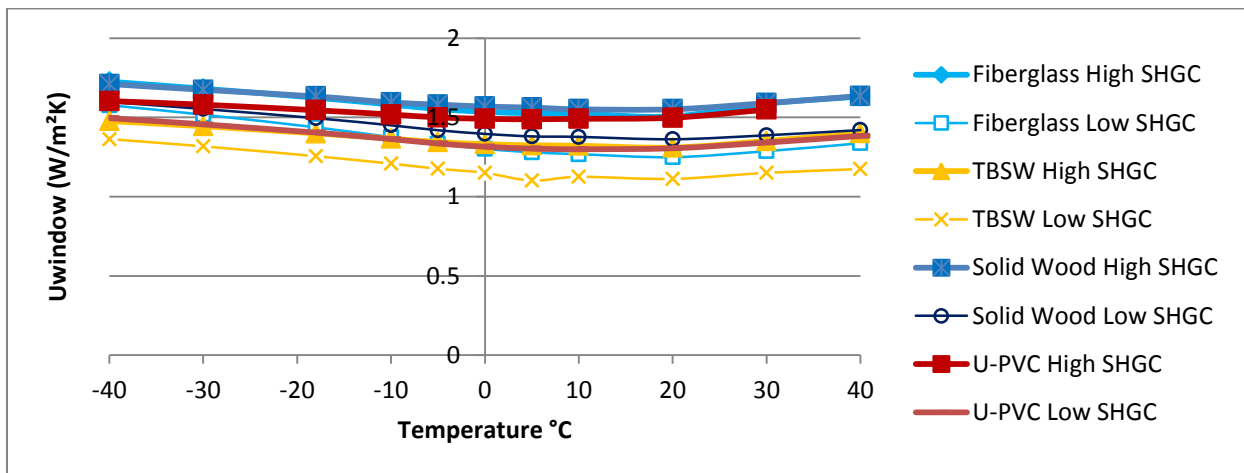


Figure 39 Frame Types with Double IGUs: $U_{\text{window-NFRC}}$ (Percentage Change)

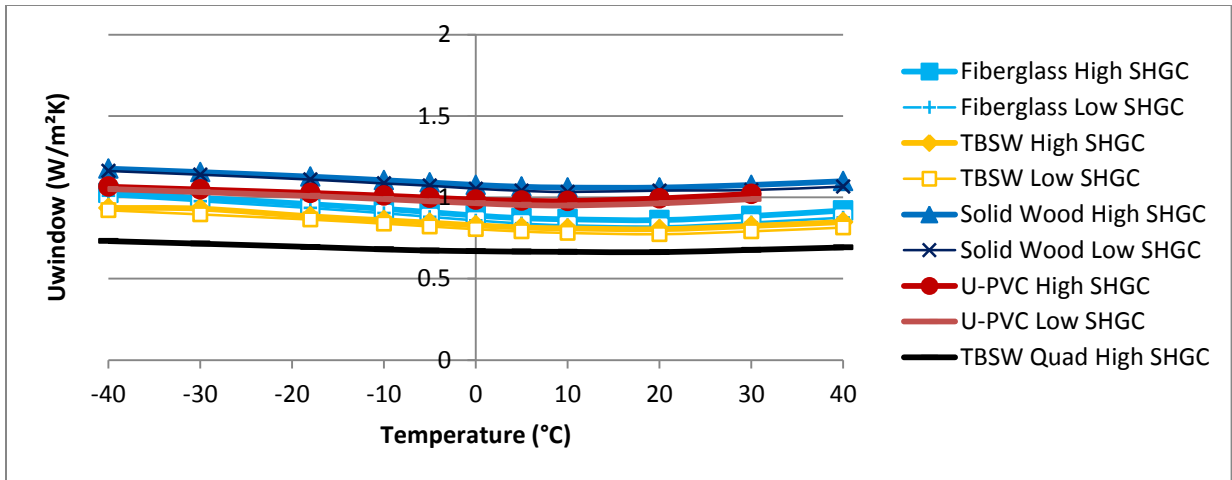


Figure 40 Frame Types with Triple IGUs: $U_{\text{window-NFRC}}$ (Percentage Change)

The $U_{\text{window-CEN}}$ values for the double IGU with high and low SHGC combinations, the U_{window} values were as follows, in ascending order: TBSW low SHGC, fiberglass low SHGC, U-PVC low SHGC, TBSW high SHGC, solid wood low SHGC, U-PVC high SHGC, fiberglass high SHGC and solid wood high SHGC (see Figures 41).

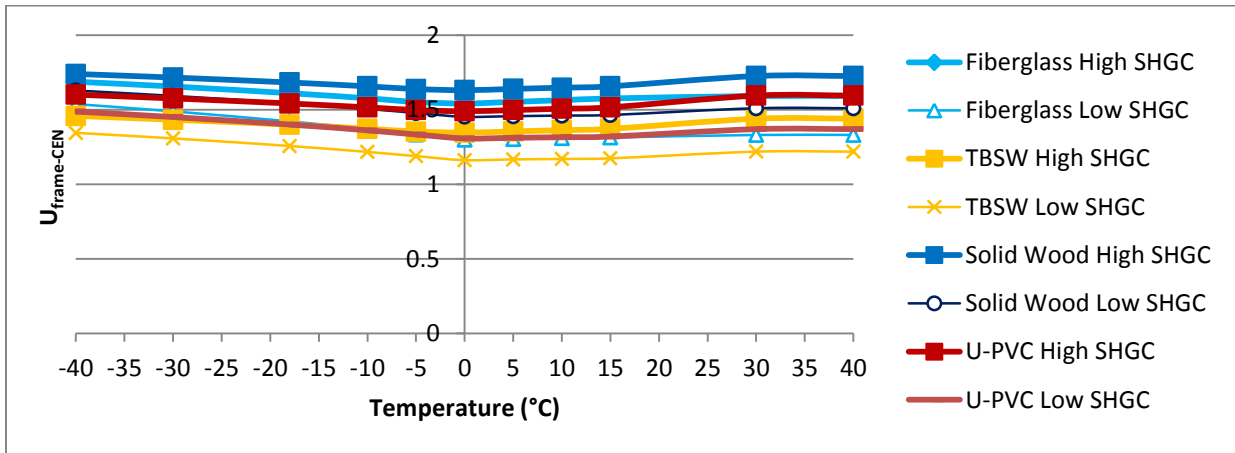


Figure 41 Frame Types with Double IGUs: $U_{\text{window-CEN}}$

For the $U_{\text{window-CEN}}$ values for the triple IGU with high and low SHGC combinations, the TBSW frame types had the lowest U_{window} values and in ascending order; fiberglass, U-PVC and solid wood.

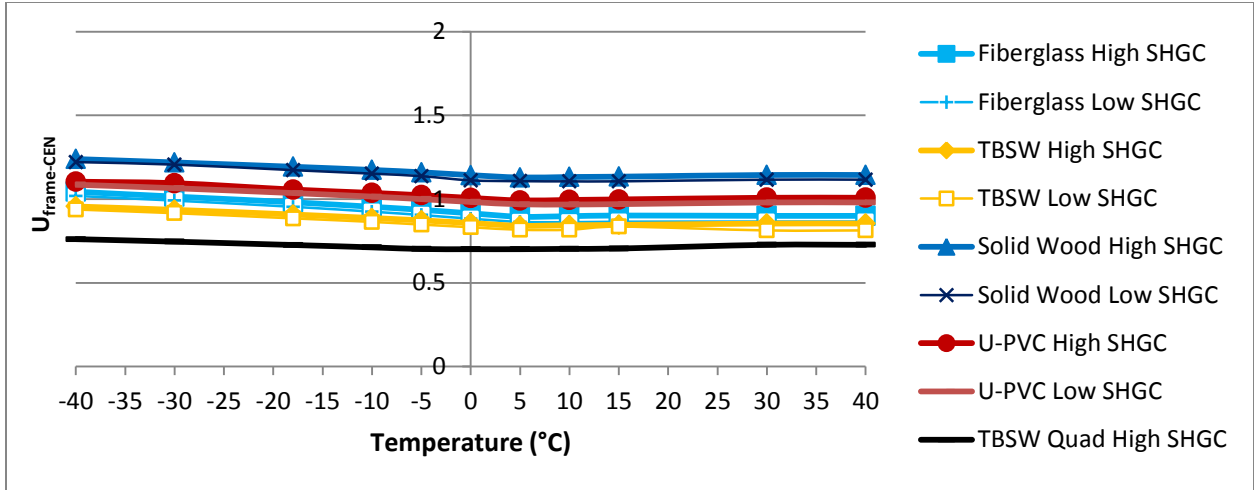


Figure 42 Frame Types with Triple IGUs: $U_{\text{window-CEN}}$

5.5 Ψ -Value Comparison with Various Frame and Spacer Types

Results from the SHGC, U_{cog} , U_{frame} and U_{window} simulations in Sections 5.1-5.4 were utilized to aid in the explanation of the U_{window} results found in this section. Simulations were conducted for double, triple and quad IGUs for all the frame types with three different spacers are as follows (see Figures 43-51):

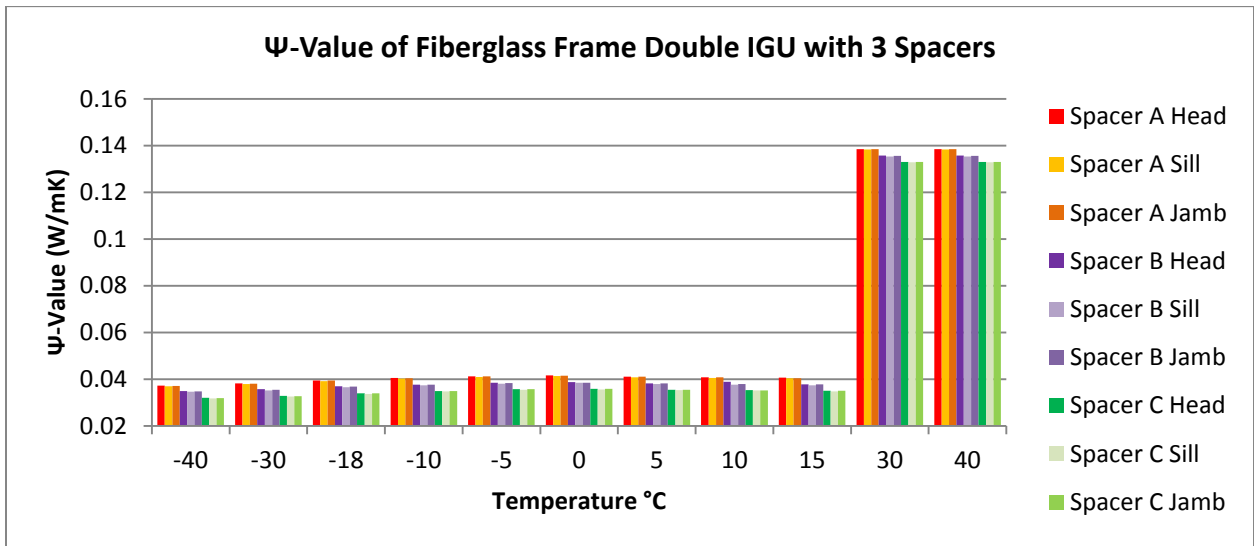


Figure 43 Fiberglass Frame with Double IGU (High SHGC) Ψ -Values: Spacer Comparison

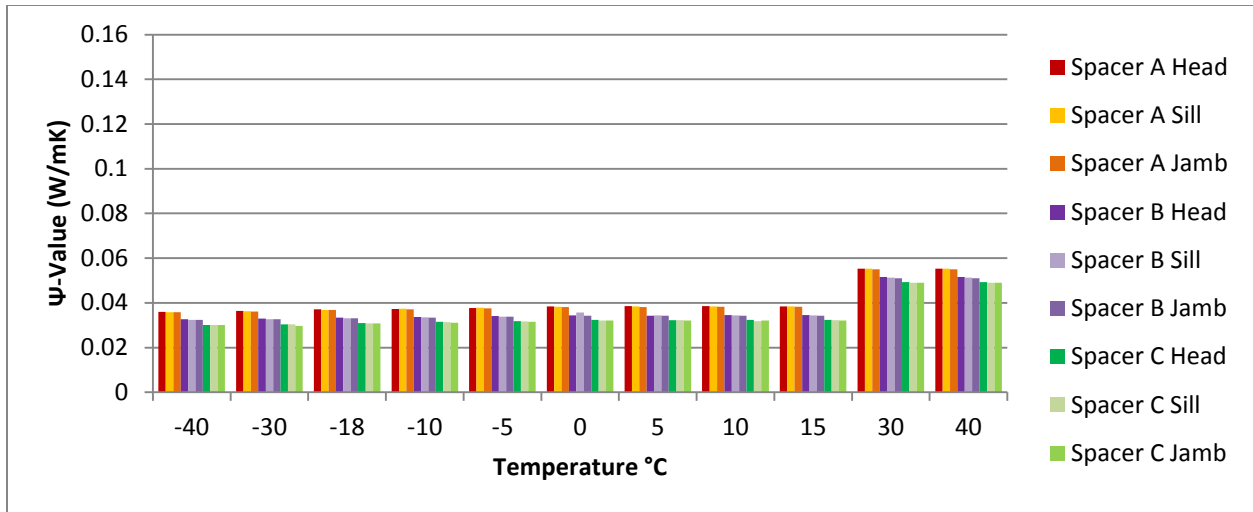


Figure 44 Fiberglass Frame with Triple IGU (High SHGC) Ψ -Values: Spacer Comparison

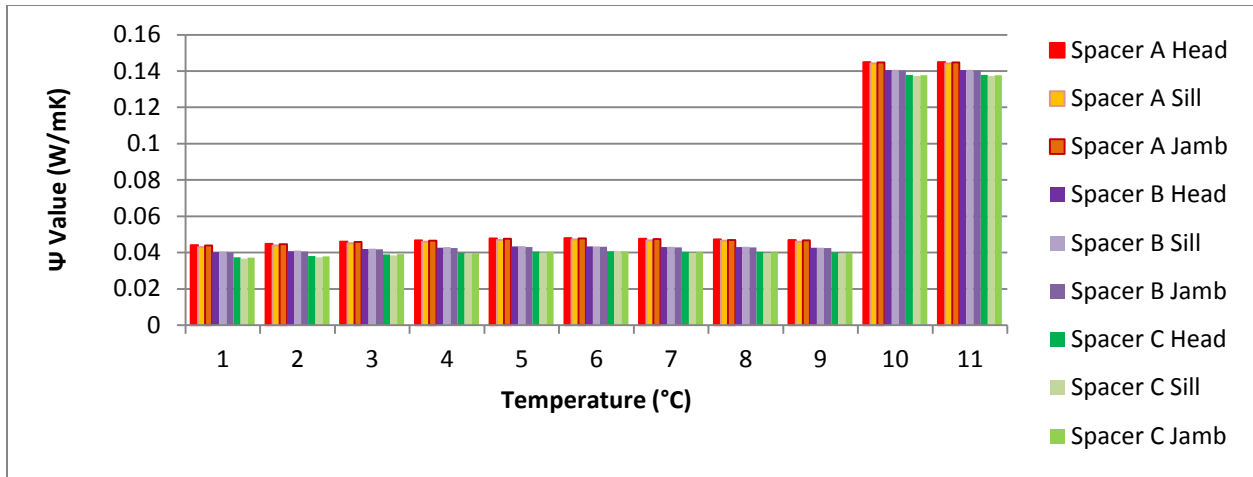


Figure 45 Ψ -Values of Solid Wood with Double IGUs: Spacer Comparison

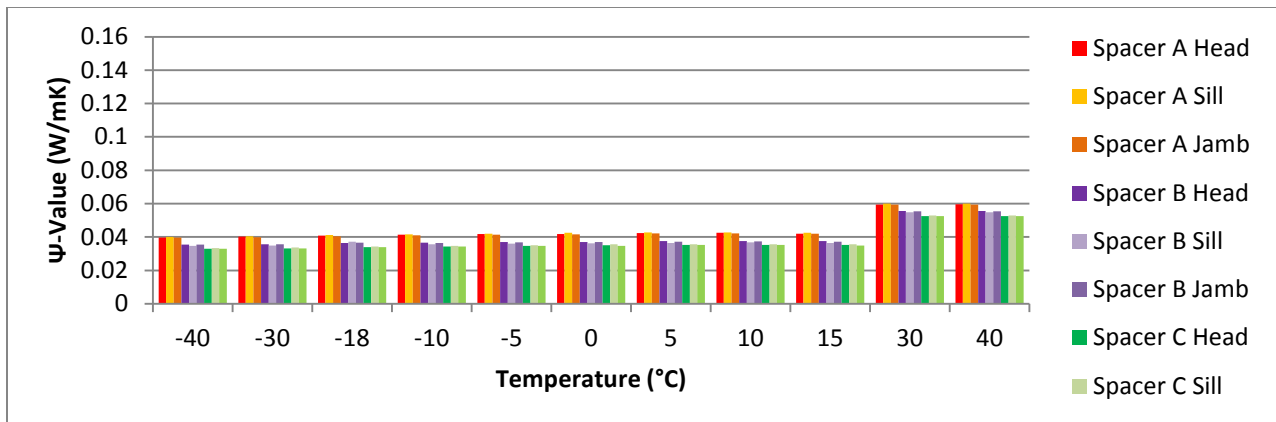


Figure 46 Ψ -Values of Solid Wood with Triple IGUs: Spacer Comparison

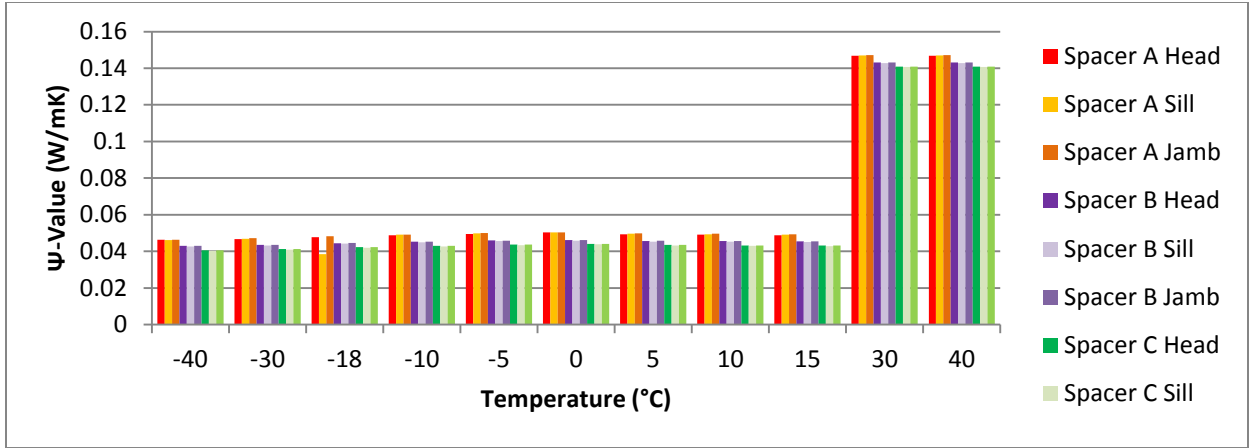


Figure 47 Ψ -Values of TBSW Frame with Double IGUs: Spacer Comparison

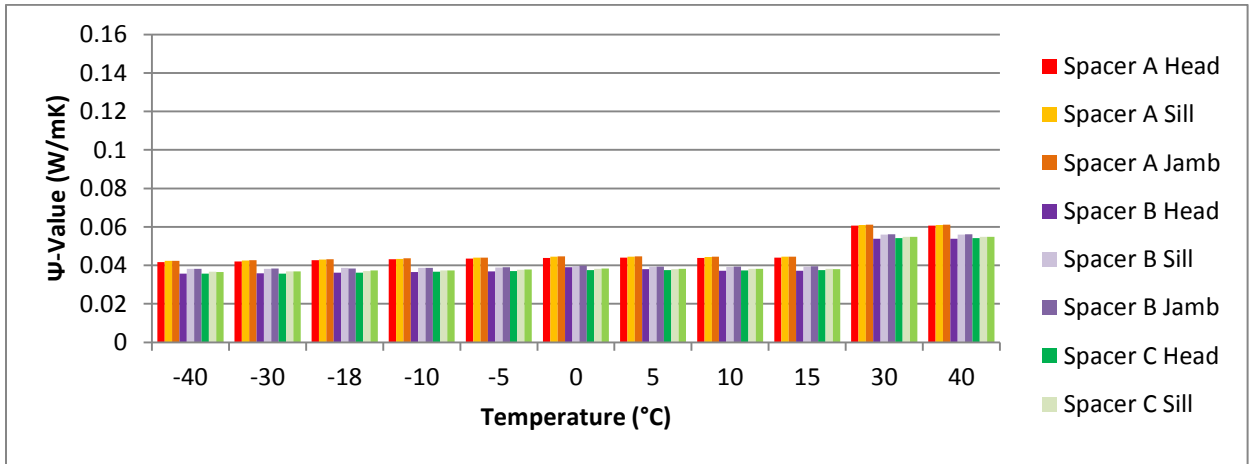


Figure 48 Ψ -Values of TBSW Frame with Triple IGUs: Spacer Comparison

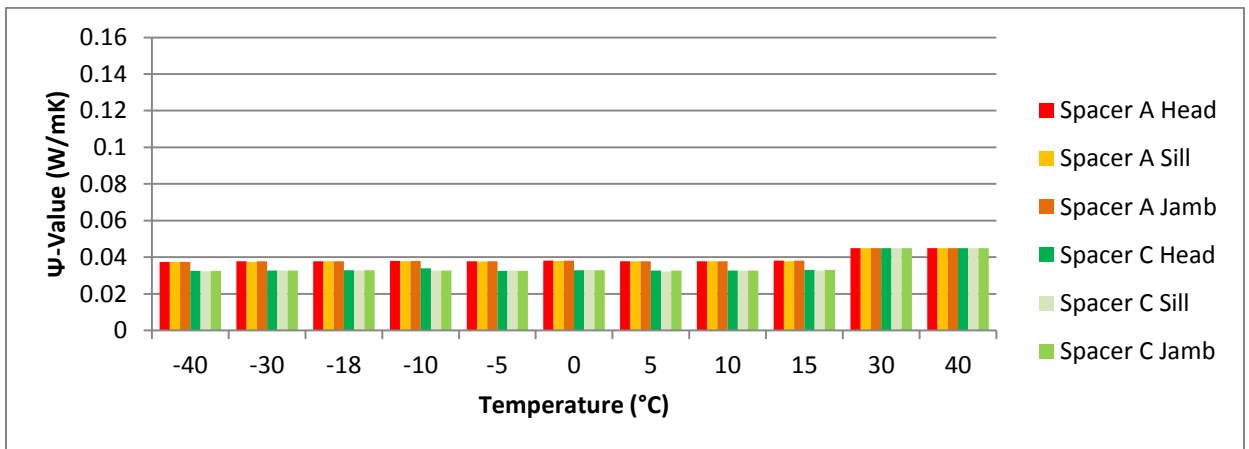


Figure 49 TBSW Frame with Quad IGU (High SHGC) Ψ -Values: Spacer Comparison

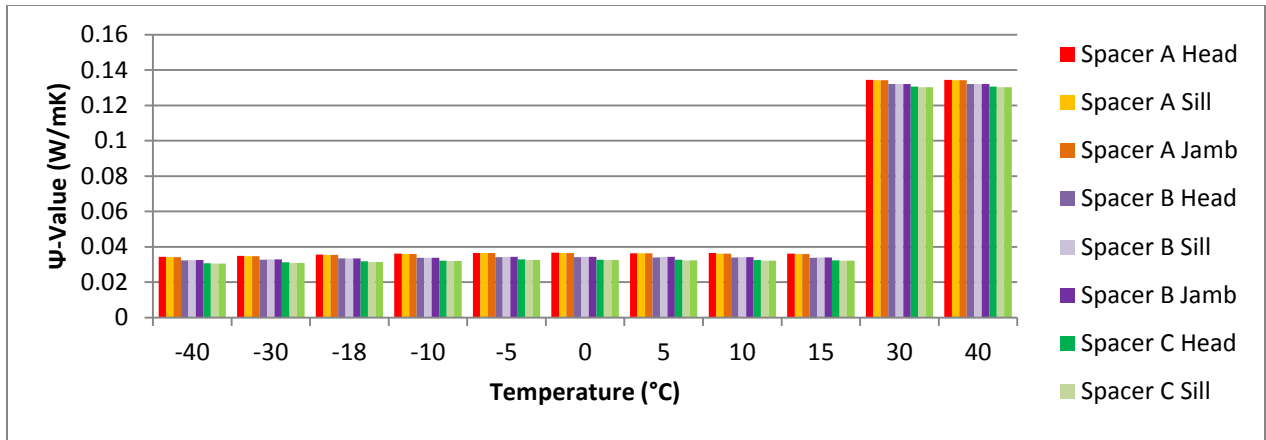


Figure 50 Ψ -Values of U-PVC Frame with Double IGUs: Spacer Comparison

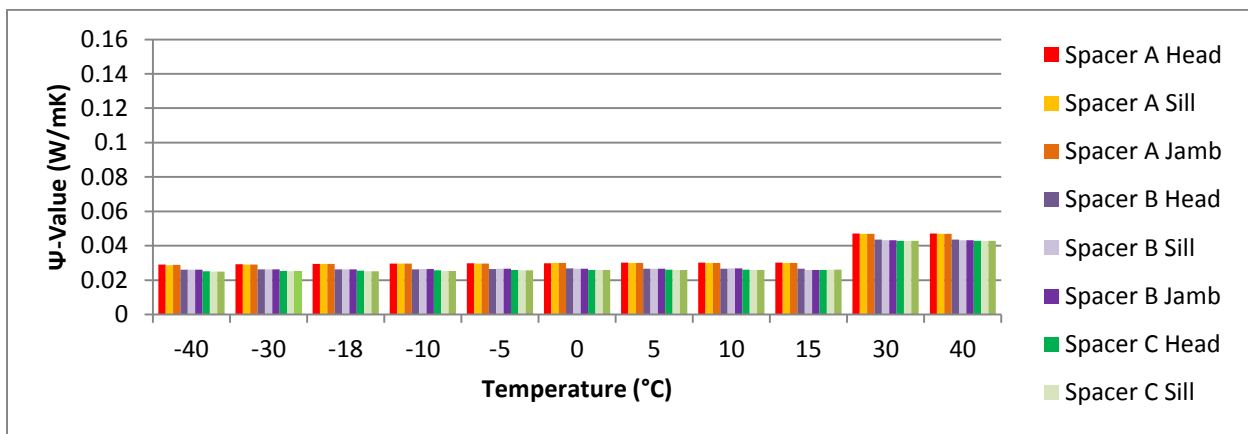


Figure 51 Ψ -Values of U-PVC Frame with Triple IGUs: Spacer Comparison

Spacer C had the lowest Ψ -values and Spacer A had the largest Ψ -values across the temperature range of -40 to 40°C for all window combinations. There were no significant changes of the Ψ -values between -40 to 15°C. As stated before, the largest Ψ -values were at 30 and 40°C due to the CEN summer boundary conditions used for those two temperatures.

The Ψ -values of each frame type with double, triple and quad IGUs were compared across the exterior temperature range from -40 to 40°C and are as follows:

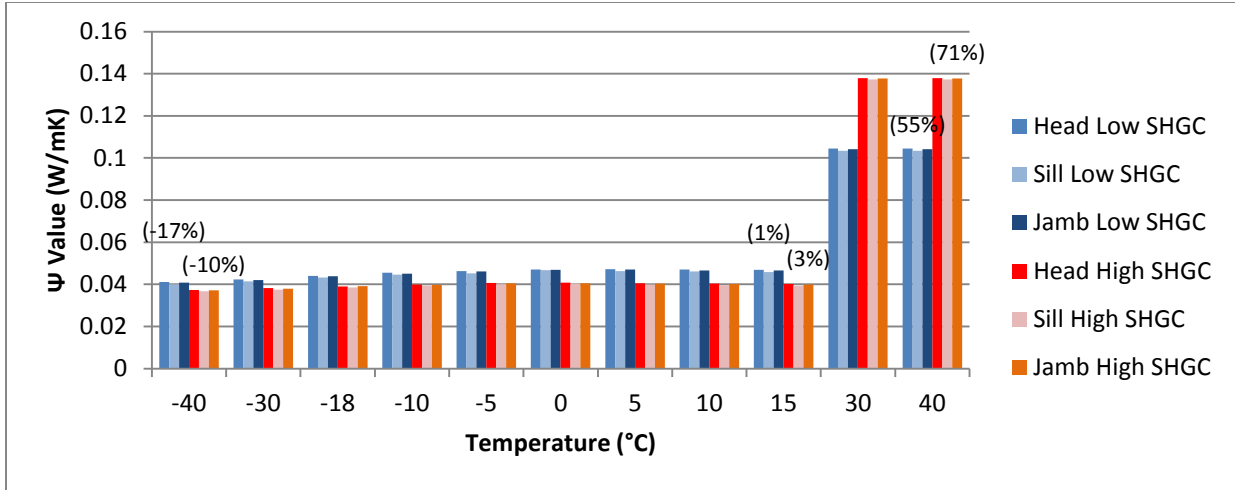


Figure 52 Solid Wood Frame with Double IGU and Spacer C: High vs Low SHGC (Percentage Change)

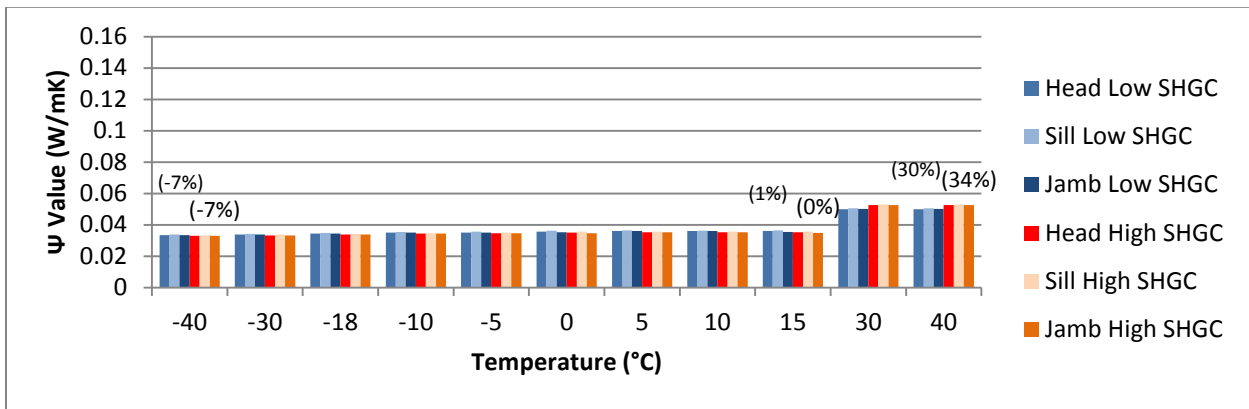


Figure 53 Solid Wood Frame with Triple IGU and Spacer C: High vs Low SHGC (Percentage Change)

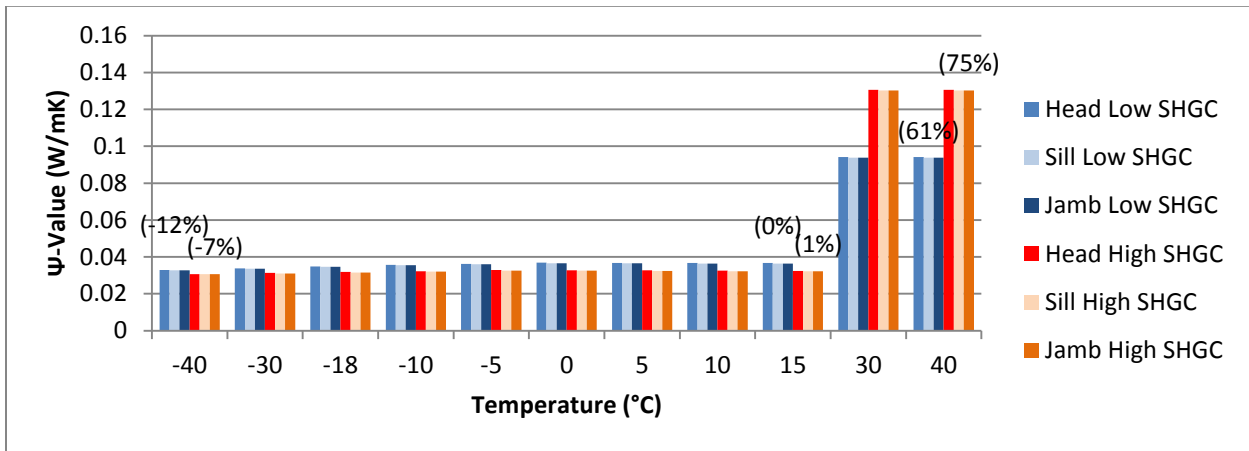


Figure 54 U-PVC Frame with Double IGU and Spacer C: High vs Low SHGC (Percentage Change)

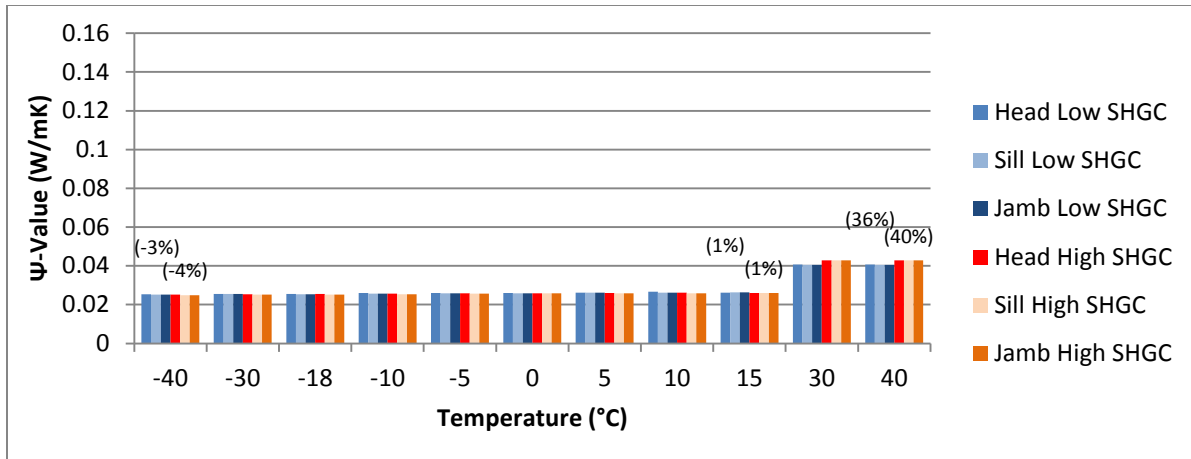


Figure 55 U-PVC Frame with Triple IGU and Spacer C: High vs Low SHGC (Percentage Change)

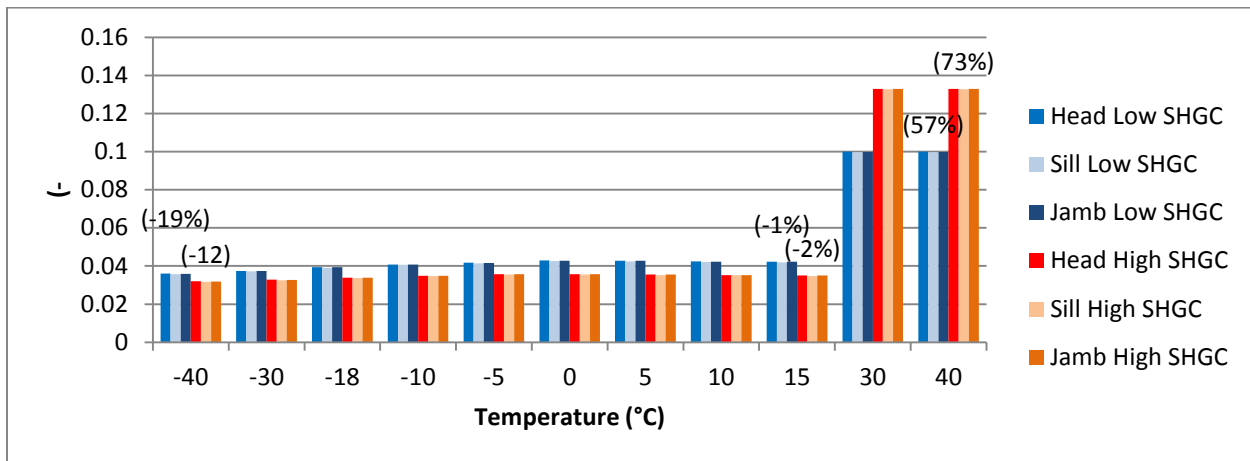


Figure 56 Ψ -Values of Fiberglass Frame with Double IGUs (Percentage Change)

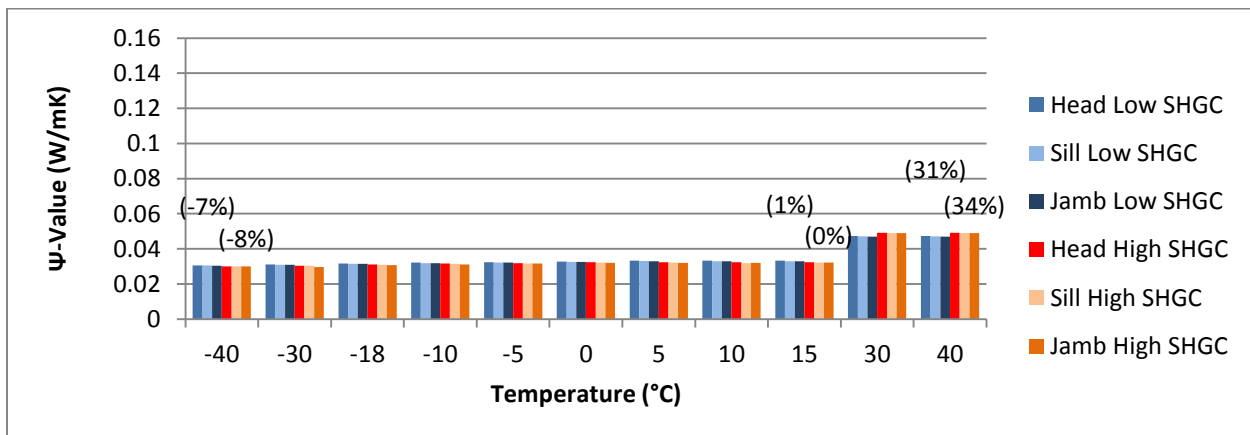


Figure 57 Ψ -Values of Fiberglass Frame with Triple IGUs (Percentage Change)

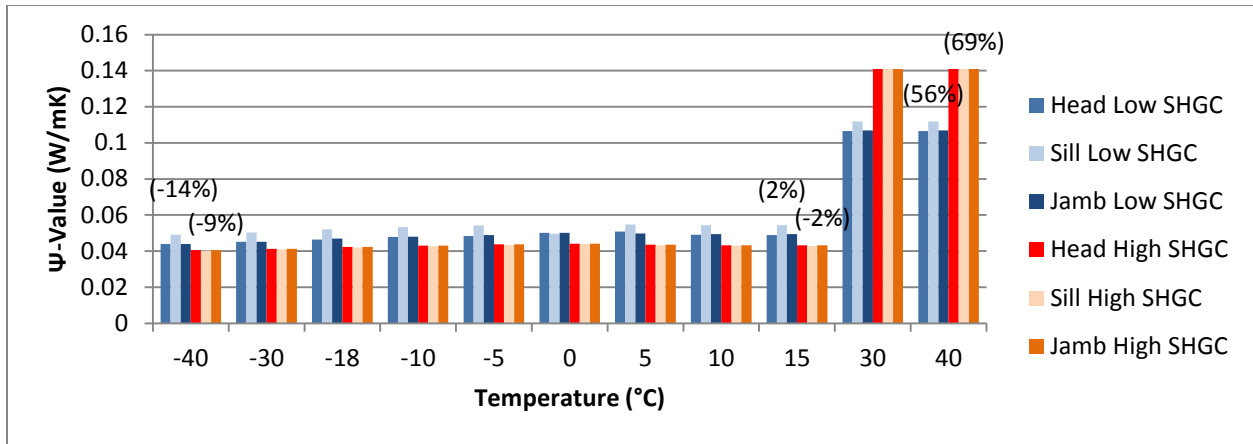


Figure 58 Ψ -Values of TBSW Frame with Double IGUs (Percentage Change)

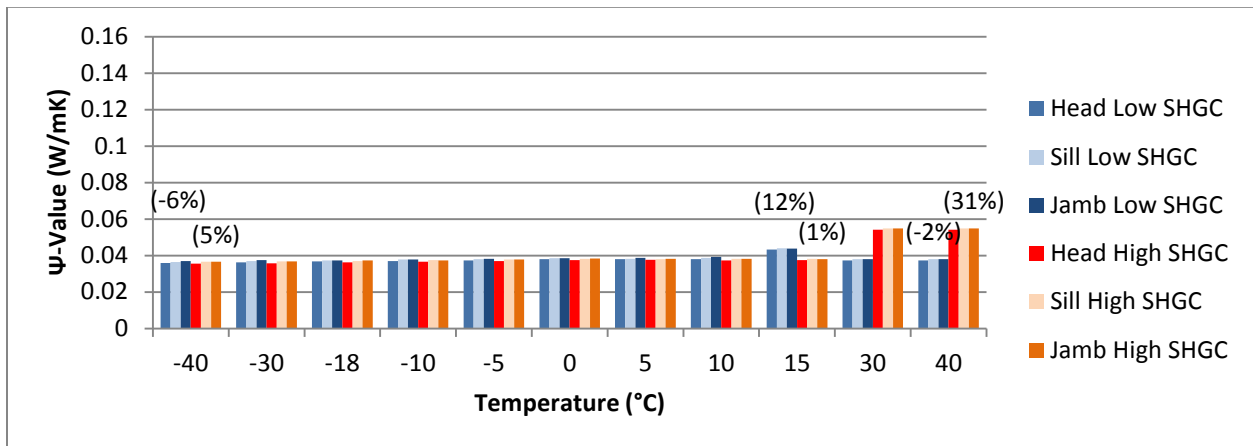


Figure 59 Ψ -Values of TBSW Frame with Triple IGUs (Percentage Change)

For all frame and glazing combinations, the Ψ -values fell in the range of 0.02-0.045 W/mK. The IGUs with a low SHGC had slightly higher Ψ -values than the IGUs with a high SHGC. The double IGUs showed a slightly greater difference between the two SHGCs than the triple IGUs due to the larger gap spacing size and thus greater thermal transmittance through convection. The IGUs with a low SHGC had a larger Ψ -value than the low SHGC IGUs (below 15°C) due to increased conduction through the low-E coatings on the low SHGC IGUs (see Section 5.2.1). At 30°C, the Ψ -values of the high SHGC IGUs are larger than the low SHGC IGUs due to the higher exterior temperature and thus higher difference in interior and exterior temperatures.

In comparing the different frame types, the U-PVC frame had the lowest Ψ -values across the exterior temperature range, and in ascending order; the fiberglass, solid wood and TBSW. The TBSW frame with

the quad IGU had the lowest Ψ -values out of all of the window combinations. There is negligible difference between the high and low SHGC IGUs. Out of all of the frame types, the U-PVC had the lowest Ψ -values (see Figure 55).

The discrepancies in Ψ -values, primarily the double IGUs, occurred at the exterior temperatures of 30 and 40°C due to the lower surface film coefficients used in the summer design conditions of the CEN method and the effect of the lower surface film coefficients in producing higher U_{cog} values. The larger gap size in the double IGU also contributed to the higher U_{cog} values and thus the trend of higher thermal transmittance. The effects of the increased thermal transmittance of the glazing upon the spacer and frame materials is reflected and measured in the larger Ψ -values found at 30 and 40°C. The Ψ -value highlights the intricate thermal interactions between the glazing, spacer and frame materials and thus gives more detailed information as to the thermal efficiency of various glazing, spacer and frame type combinations. In addition, the thermal interactions highlighted by the Ψ -value aids in the explanation of how these interactions are affected by individual window components and the differences of the NFRC and CEN method in determining the overall and individual component thermal transmittance.

The triple and quad IGU combinations with all of the frame types showed the least variation in U-values across the exterior temperature range as well as between the high and low SHGC IGUs (see Section 5.6.1). Thus, the higher thermally performing IGUs and frames had zero to little variation in linear thermal transmittance across the temperature range.

The U-PVC frame simulations had the lowest Ψ -values across the exterior temperature range. This is expected seeing that the $U_{window-CEN}$ results showed that the U-PVC frame had a higher U_{frame} value than the other frame types; the higher rate of heat loss through the U-PVC frame (see Section 5.3.4), area results in a lower linear thermal transmittance. The lower Ψ -values are plausible considering that the distance from the sightline to the bottom of the IGU is the longest for the U-PVC frame, this demonstrates that the deeper inset position of the IGU in the frame minimizes the linear thermal transmittance. Furthermore, the distance from the sightline to the edge of the interior side of the U-PVC frame is longer than the other frames; this in conjunction with air cavities that have a very low conductivity aids in the minimization of the thermal interactions of the glazing and spacer throughout the frame (see Table 39).

Although solid wood has a slightly lower conductivity (NFRC 0.11 W/mK, CEN 0.13 W/mK) than U-PVC (0.17 W/mK), the solid wood frame Ψ -values were higher than the other frames. There are several reasons that explicate why there is more thermal transmittance in the solid wood frame. The solid wood frame has the longest distance from the sightline to the edge of the frame nearer to the exterior side which subjects more surface area of the frame to external conditions; this in conjunction with the solid wood composition of the frame with minimal air cavities leads to potentially more thermal transmittance through conduction, given the higher conductivity of softwood than air cavities. The IGU for the solid wood frame also has the shortest inset into the frame (sightline to bottom of IGU is 12 mm); this shallow inset subjects more of the IGU to the external environmental which leads to increased thermal interactions occurring through the spacer and frame.

Table 39 Frame Measurements from the Sightline

Frame Type	Sightline to Edge of Frame (mm)	Sightline to Bottom of IGU (mm)
Fiberglass	73	14
TBSW	114	15
U-PVC	122	23
Solid Wood	145 (sill: exterior)/76 (interior) 115 (head and jamb: exterior)	12

The Ψ -value results are in line with the spacer comparative results for the U_{window} value. Simulations that used Spacer C resulted in the lowest Ψ -value due to the low thermal conductivity of the constituent materials. Spacer B performed higher than Spacer A due to the smaller height of the spacer which allowed more 90% krypton and 10% air gas infill for the IGU. The greater volume of extremely low thermal conductivity of the gas infill gave the windows with Spacer B a lower Ψ -value.

5.6 U_{window} Simulations in the 8 Climate Zones

5.6.1 $U_{\text{window-NFRC}}$ and $U_{\text{window-CEN}}$ Comparison in the 8 Climate Zones

NFRC and CEN U_{window} values of several IGU and frame types were compared across the temperature range of -40 to 40°C for the eight climate zones (see Figures 60-67). The results from the SHGC, U_{cog} , U_{frame} , U_{window} and Ψ -value simulations in Sections 5.1-5.6 were used to elucidate the results found in the

U_{window} values in the eight climate zones in Section 5.6. Spacer C was used in all simulations unless otherwise noted. The annual average temperature ranges of the eight climate zones were highlighted (see Section 3.11). [Note: the 20°C is omitted because 20°C for NFRC and 15°C for CEN since THERM does not calculate the U-value for a 0°C temperature difference.]

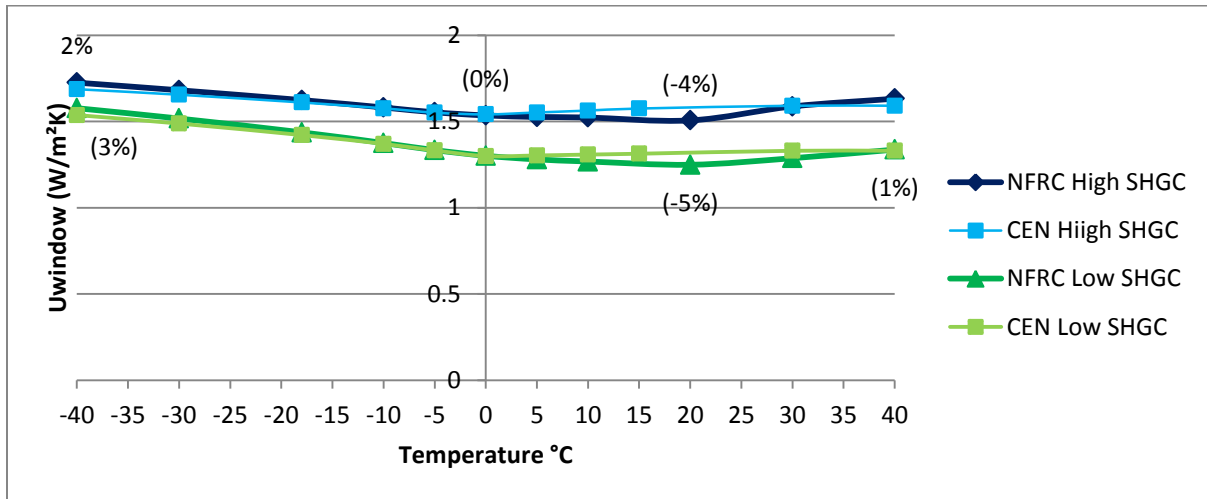


Figure 60 Double IGU Fiberglass Frame: U_{window} Values in 8 Climate Zones (Percentage Change)

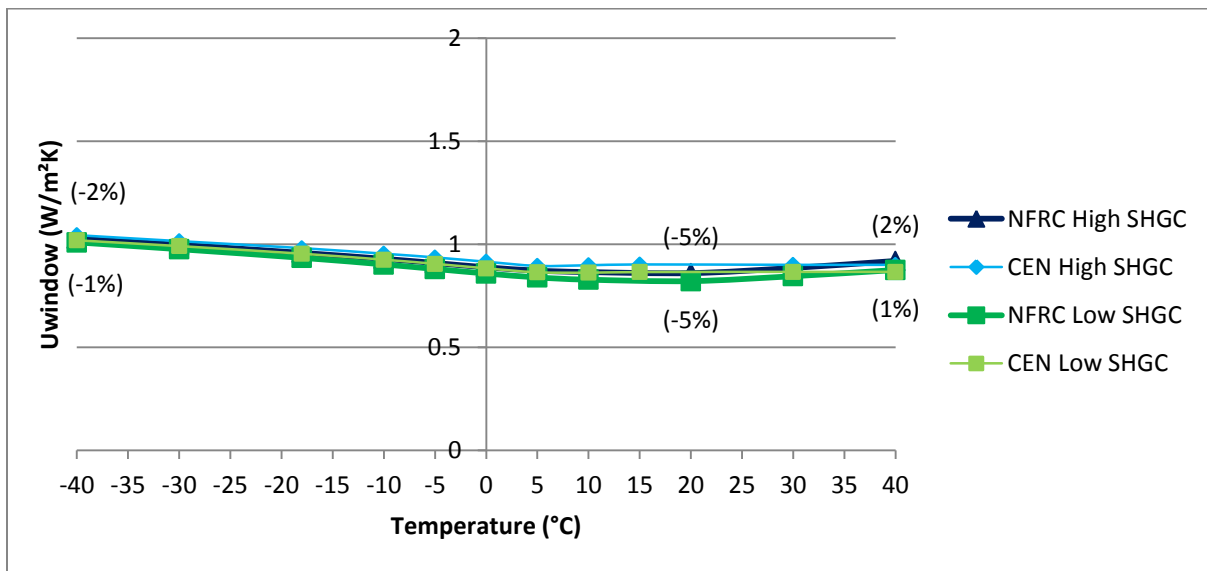


Figure 61 Triple IGU Fiberglass Frame: U_{window} Values in 8 Climate Zones (Percentage Change)

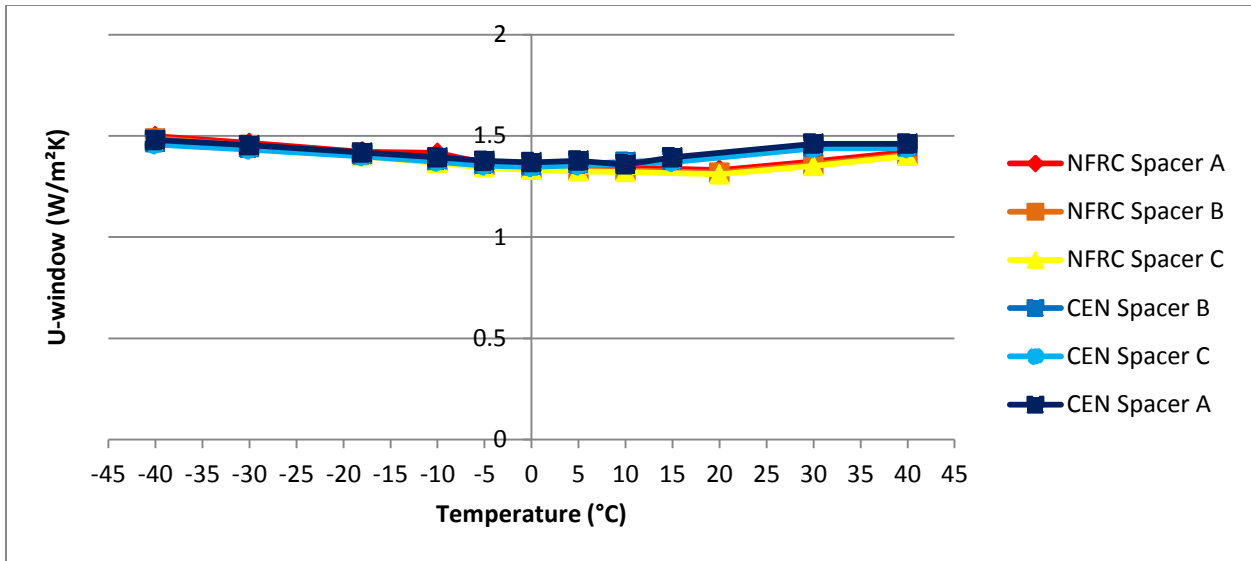


Figure 62 TBSW Frame with a Double IGU: Spacer Comparison

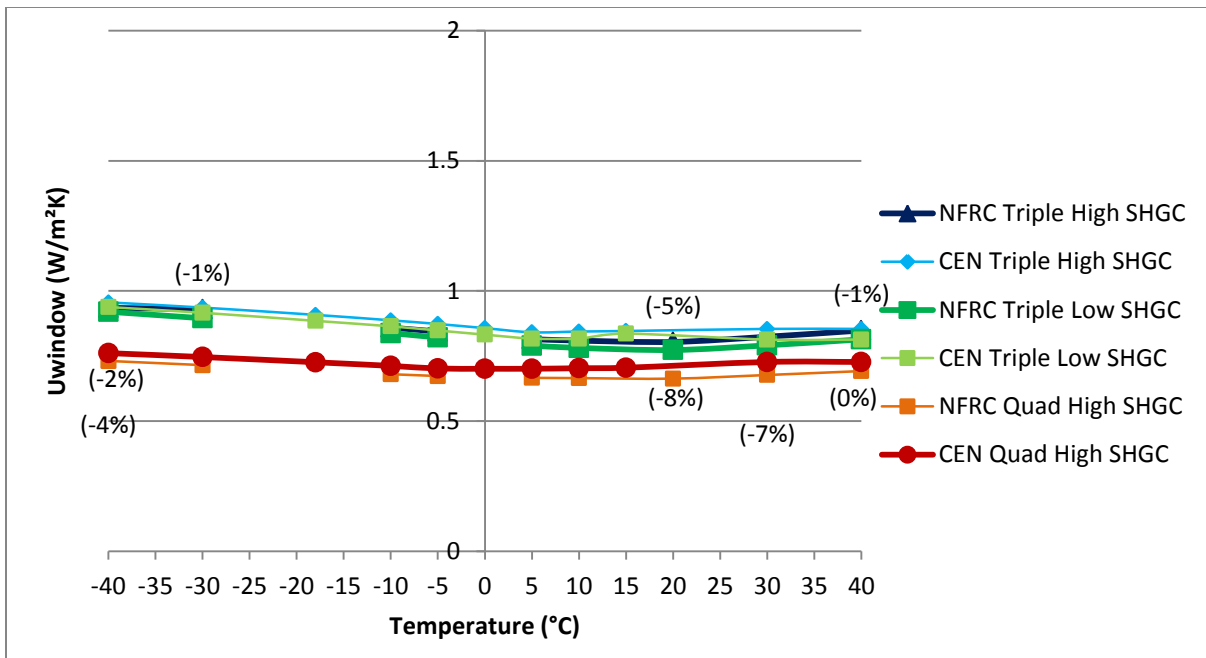


Figure 63 Triple and Quad IGU TBSW Frame: U_{window} Values in 8 Climate Zones (Percentage Change)

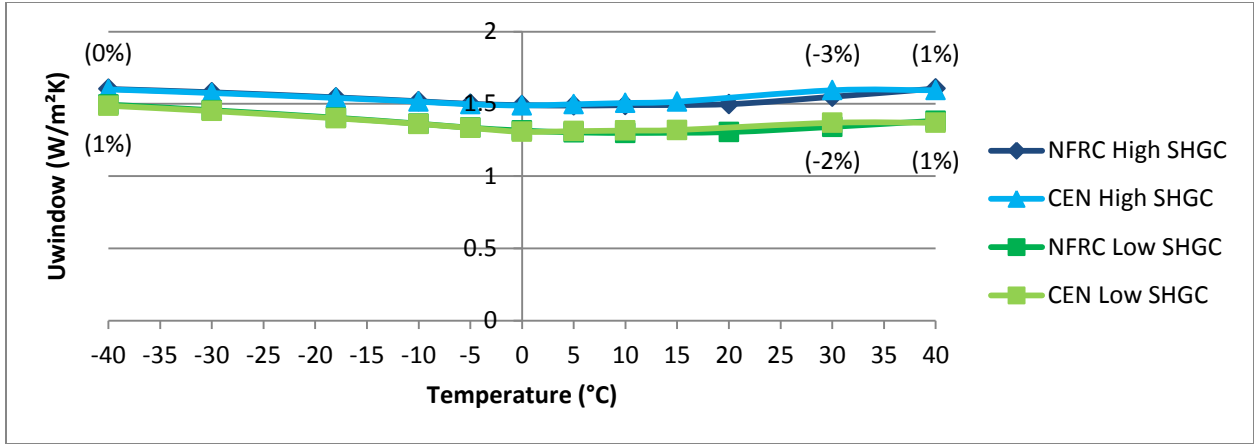


Figure 64 U-PVC Frame with a Double IGU: Climate Zones (Percentage Change)

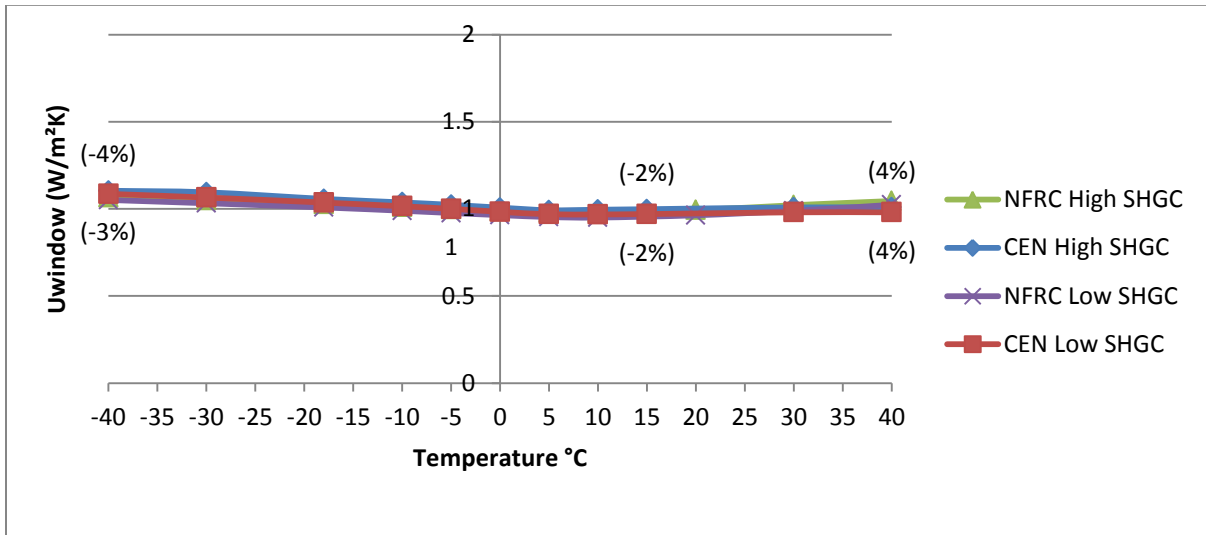


Figure 65 Triple IGU U-PVC Frame: U_{window} Values in 8 Climate Zones (Percentage Change)

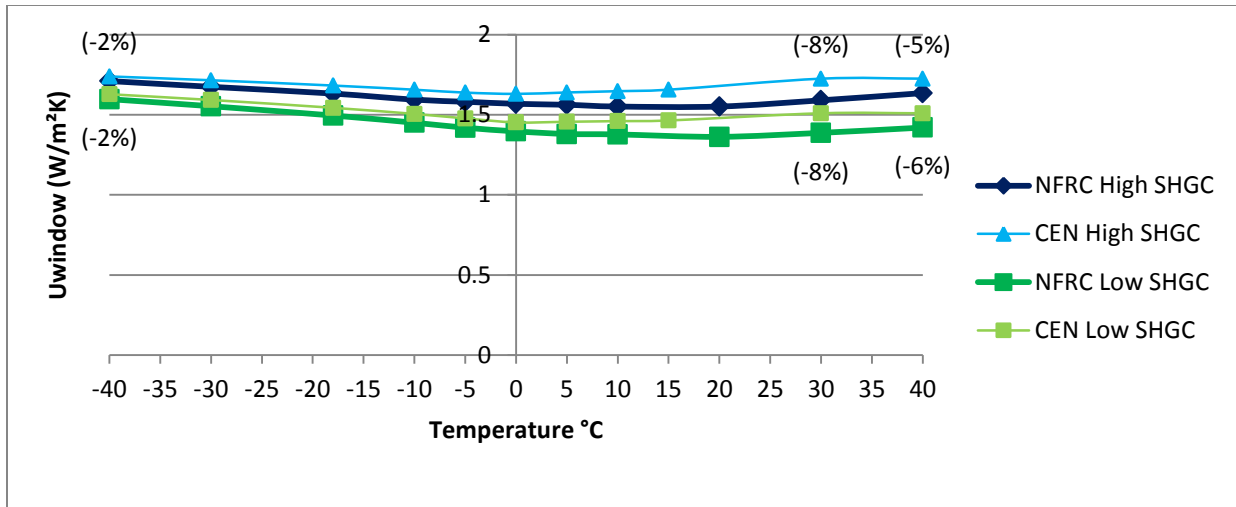


Figure 66 Solid Wood Frame with a Double IGU: Climate Zones (Percentage Change)

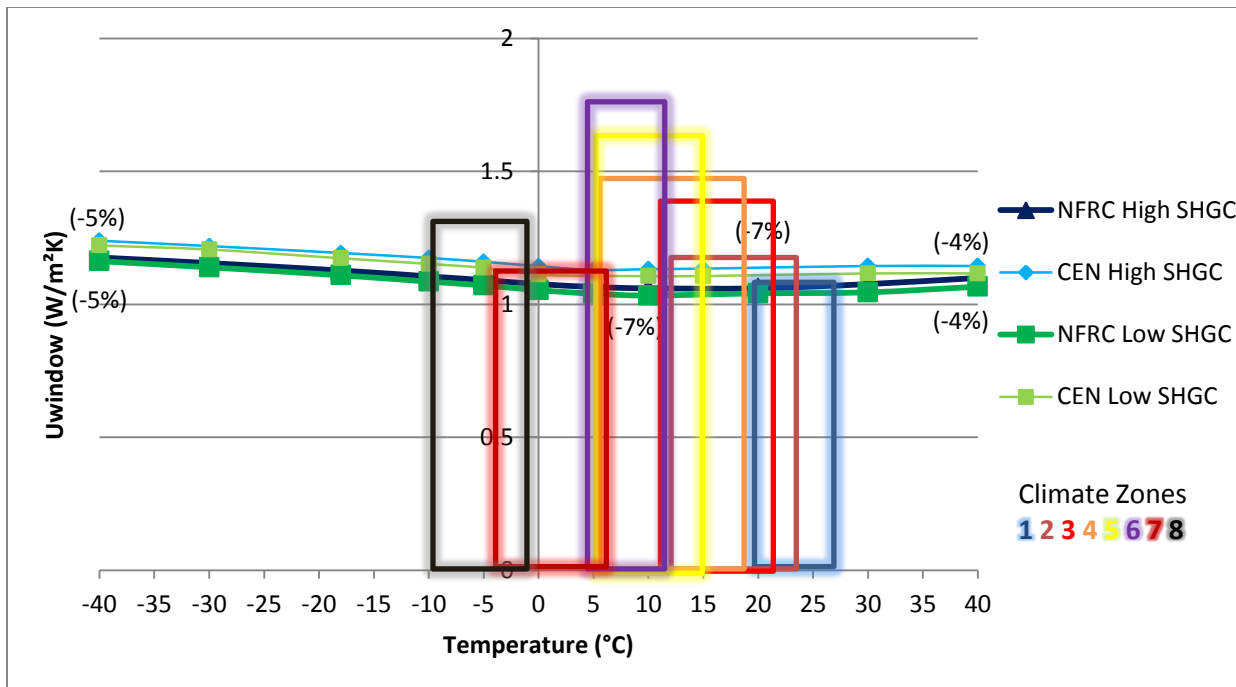


Figure 67 Triple IGU Solid Wood Frame: U_{window} Values in 8 Climate Zones (Percentage Change)

Overall, the $U_{window-NFRC}$ values were 8% lower to 4% higher than $U_{window-CEN}$ values for all of the exterior temperatures. The trend of percentage changes is higher for frames with a longer length (i.e. sightline to edge of frame); the solid wood frame has higher percentage changes than the TBSW, fiberglass and U-PVC (lowest) frames.

As discussed in Section 5.3.2, the length and area of the frame (i.e. sightline to edge of frame) influence the magnitude of the differences between both methods whereby frames with larger lengths have

greater exposure exterior environment and are thus more sensitive to exterior temperature changes within the climate zones. The solid wood frame has the largest exterior length and combined with conductive heat transfer through the solid wood and the absence of insulative frame cavities, larger differences in U_{window} values between methods occur.

All of the U_{window} values for the exterior temperatures of 30 and 40°C were the same for the CEN simulations; whereas the values were different for the NFRC simulations due to the effect of the summer boundary conditions on the different U_{cog} values.

For the fiberglass and U-PVC frames with triple IGUs, the 4% higher CEN than NFRC U_{window} value may be attributed to the temperature differential between the interior and exterior for the CEN method. The largest temperature difference between the interior and exterior temperature (i.e. 20 and 0°C) occurs at 10°C. Since the $U_{\text{values-CEN}}$ measure the thermal transmittance at those temperatures, the fluctuations in U_{window} values are in reference to that temperature and thus differentiate from the NFRC values accordingly.

The TBSW frame U_{window} values were the lowest out of all the frames. The larger differences between both methods occur for the TBSW frame with the higher performing IGUs; this is logical as the thermal performance of the frame plays a more extensive role as the efficiency of the IGU's thermal performance increases. The lower $U_{\text{window-NFRC}}$ value is also attributed to the lower thermal conductivity value of softwood that is used in the NFRC method. The lower thermal conductivity of the softwood is ameliorated by the foam insulation, which is placed between the aluminum siding and the softwood. Heat transfer from the softwood to the exterior and heat transfer from the exterior environment towards the interior through the highly conductive aluminum is abated by the foam insulation. This explicates the lower thermal transmittance of the TBSW frame.

For all of the CEN simulations, the U_{window} and U_{cog} values (with a high and low SHGC) for 30 and 40°C were the same whereas the NFRC had different values for each temperature. The lack of change in the $U_{\text{cog-CEN}}$ at these temperatures accounts for the variations between the U-values of both methods. The reason as to why there is a lack of change at these temperatures is presently unknown at the time of this study; however, some problem areas that may contribute to this finding are identified in Section 11.

The largest differences between both methods across the -40 to 40°C temperature range were found in the solid wood frame double and triple IGU simulations. The NFRC values were all lower than the CEN values. Considering that the frame is composed of softwood, any change in thermal conductivity values

would affect the thermal transmittance of the whole frame. Since the NFRC thermal conductivity of softwood is lower than the CEN value, this lower value accounts for the lower $U_{\text{window-NFRC}}$ results. The thickness and width of the frame also accounts for the lower $U_{\text{window-NFRC}}$ results since the NFRC calculation method is area-weighted, the larger frame area has a heavier weighting in the final U_{window} result.

Foremost, given that the material conductivity does not change with a change in exterior temperature, the change in exterior temperature in both calculation methods directly influences the thermal conductivity of the gas infill in the IGU. In addition, the thickness of the layers of the low-E coatings also influences the convective and conductive heat transfer effects of the gas infill. The heat transfer effects within the IGU are filtered through the spacer and frame materials and frame cavities. Since the U_{cog} and U_{frame} are the main components of the U-value calculations, the interior and exterior temperature difference influences the whole U_{window} value and thus explains some of the differences in U_{window} values for both methods.

In conjunction with the results in Section 5.6.4, the average annual high and low temperature range for each location is not necessary for high performance windows seeing that there were insignificant differences in U_{window} across each range. Therefore, the average annual temperature would suffice to obtain the climate specific U_{window} value for each location.

5.6.2 $U_{\text{window-NFRC}}$ Comparison in Reference to -18°C

$U_{\text{window-NFRC}}$ values were compared in reference to the standard boundary condition of -18°C, in the -40 to 40°C exterior temperature range. These values give an indication as to the degree of change in $U_{\text{window-NFRC}}$ across the aforementioned temperature range.

Table 40 $U_{\text{window-NFRC}}$ Comparison in Reference to -18°C

Frame Type and IGU	Exterior Temps in reference to -18°C
Fiberglass Double	9% lower - 15% higher
Triple	7% lower - 14% higher

TBSW Double	5% lower - 14% higher
Triple	6% lower - 12% higher
Quad	5% lower - 5% higher
Solid Wood Double	6% lower - 10% higher
Triple	5% lower to 7% higher
U-PVC Double	6% lower to 8% higher
Triple	4% lower to 6% higher

The trend is that the higher the IGU thermal performance, the less difference in U_{window} values of both methods. The largest difference in $U_{\text{window-NFRC}}$ values, in relation to the NFRC exterior temperature boundary condition of -18°C , occurs at 20°C , then -40°C in descending order, due to the influence of the 21°C interior temperature boundary condition. The temperature difference is analogous to the difference in U_{window} values as the temperature increases or decreases from -18°C . Above 21°C , the difference in U-values decreases due to the proximity of the exterior temperature to the summer interior design temperature. These observations take place for all of the frame types and IGU combinations.

5.6.3 $U_{\text{window-CEN}}$ Values Comparison in Reference to 0°C

$U_{\text{window-CEN}}$ values were compared in reference to the standard boundary condition of 0°C , in the -40 to 40°C exterior temperature range. These values give an indication as to the degree of change in $U_{\text{window-CEN}}$ across the aforementioned temperature range.

Table 41 $U_{\text{window-CEN}}$ Values Comparison in Reference to 0°C

Frame Type and IGU	Exterior Temps in reference to 0°C
Fiberglass Double	0-15% lower
Triple	13% lower - 2% higher

TBSW Double	0-14% lower
Triple	11% lower - 2% higher
Quad	0-8% lower
Solid Wood Double	0-11% lower
Triple	9% lower - 1% higher
U-PVC Double	0-12% lower
Triple	9% lower - 2% higher

For both methods across the -40 to 40°C temperature range, the $U_{\text{window-NFRC}}$ values were 2-15% higher than the NFRC standard values; and the $U_{\text{window-CEN}}$ values were 15% lower to 2% higher than the CEN standard values. Higher value differences than standard values for both methods occurred for several IGUs with a low SHGC for all frame types; the double IGUs showed the greater differences compared to the triple IGUs (see Section 5.2.1 for further discussion).

These results show how the interior and exterior temperature differential affects the U_{window} value, as well as the shift in percentage change in relation to the difference in standard exterior (-18 vs 0°C) and interior temperatures (21 vs 20°C) for each method.

Examining the effect of exterior temperature changes upon the U_{window} value for both methods shows primarily the impact of the thermal transmittance of the glazing and its effect on the thermal transmittance of the whole window. Seeing that the glazing variable is a large component of the U_{window} calculation for both methods; the glazing area magnifies the influence of the glazing upon the U_{window} value (see Section 5.4.3 for further discussion).

The difference in U_{window} values is highly significant, especially in cases where the winter design temperatures of each climate zone location are considered: in climate zones 1-5 the winter design temperatures do not reach below -18°C and in zones 7 and 8, the winter design temperatures are between -30 and -40°C in some locations. Foremost, the greater difference between interior and exterior temperatures leads to larger discrepancies in U_{window} values.

Since the average U_{window} values give a better indication as to the thermal transmittance that is actually being achieved in each climate zone, the climate specific U_{window} values (between -10 and 30°C) for the high performance windows (i.e. frames with triple and quad IGUs) are approximately 0-14% higher than the standard NFRC value and 7% lower to 2% higher than the CEN standard values. This suggests that a window in Albuquerque, Yellowknife or Toronto, may potentially have a U-value of up to 14% higher than the standard rated $U_{\text{window-NFRC}}$ for the majority of the year. A window with a $U_{\text{window-CEN}}$ value would have a lower variation in U-values than the $U_{\text{window-NFRC}}$ values across the annual average temperatures of the eight climate zones. The lower variation could be interpreted as a more efficient window, however, that is not the case seeing that the only differences between the aforementioned U_{window} values are the calculation methods and the proximity of the climate zone annual average temperatures to the standard exterior temperature; i.e. 0°C (CEN) is closer than -18°C (NFRC) to the climate zone annual average temperature range between -10 and 30°C .

In addition, the U_{cog} standard NFRC values at the exterior temperature of -18°C do not reflect the $U_{\text{cog-NFRC}}$ values when considering the annual average temperatures of the eight climate zones. As seen in the results, $U_{\text{cog-NFRC}}$ values are up to 28% higher than the standard value. Given that $U_{\text{cog-NFRC}}$ values are sensitive to exterior temperature changes, there is a need for climate specific ratings for individual glazing products; this information would be beneficial for window design manufacturers.

This variation of U_{window} and U_{cog} values purports the need for an international standardized method, as well as climate specific U-values when calculating a building's annual energy use intensity.

5.6.4 $U_{\text{window-NFRC}}$ and $U_{\text{window-CEN}}$ Comparison with 3 Spacer Types

Spacers A, B and C were simulated in the double, triple and quad IGUs with a high SHGC for all of the frame types in the NFRC and CEN U_{window} calculation methods (see Figures 68-71, D81-D83).

The annual average high and low temperature ranges for the eight climate zones range from -9°C in Yellowknife to 29°C in Miami. The winter design temperatures, of the eight climate zones, range from -40°C in Yellowknife to 11°C in Miami. The winter design temperatures of locations in climate zones 1-5 all lie above the winter design temperature of -18°C as designated by the NFRC as the standard exterior temperature for North America. The winter design temperatures of locations in climate zones 7-8 range from -30 to -40°C and thus lie well below the NFRC winter design temperature. Thus, the winter design temperature is not representative of all the locations within each climate zone. The variations in climate

and topographical conditions in different locations within each climate zone are unique and should be considered in design strategies. It is important to note that the locations identified within each climate zone only give an impression of a region in that climate zone and they do not represent every location within the same climate zone; it is recognized that there are variations, slight to moderate between locations within each climate zone.

The fiberglass frame with a double IGU where the three spacers were compared had results where the differences between each spacer were minimal across the exterior temperatures of -40 to 40°C. Across the annual average high and low temperatures of the eight climate zone locations (i.e. -10 to 30°C), the NFRC simulations with:

- a) Spacer C ranges from 1.51 to 1.59 W/m²K
- b) Spacer A ranges from 1.53 to 1.6 W/m²K
- c) Spacer B ranges from 1.52 to 1.59 W/m²K

The lowest $U_{\text{window-NFRC}}$ values occurred near 20°C and the highest $U_{\text{window-NFRC}}$ value occurred near -10°C due to their proximity to the NFRC standard interior temperature of 21°C. Generally, the trend shows that the larger the difference in temperature between the interior and exterior, the higher the resulting $U_{\text{window-NFRC}}$ value. The Spacer A simulation at 30°C gave a higher $U_{\text{window-NFRC}}$ value due to the higher interior temperature used for the summer boundary conditions.

For the fiberglass frame with a double IGU and a high SHGC the range of $U_{\text{window-NFRC}}$ values are as follows:

	Spacer C	Spacer A	Spacer B
1. Miami, 21-29°C	1.51-1.59	1.53-1.58	1.52-1.57
2. Austin, 14-16°C	1.51-1.52	1.53-1.55	1.52-1.53
3. Atlanta, 11-22°C	1.51-1.52	1.53-1.55	1.52-1.53
4. Albuquerque, 7-20°C	1.51-1.53	1.53-1.55	1.52-1.53
5. Indianapolis, 6-17°C	1.51-1.53	1.53-1.55	1.52-1.54
6. Toronto, 5-13°C	1.52-1.53	1.55	1.53-1.54
7. Winnipeg, -3-8°C	1.52-1.55	1.55-1.57	1.53-1.56
8. Yellowknife, -9-0°C	1.54-1.58	1.56-1.6	1.55-1.59

Triple IGU with a Solid Wood Frame

	Spacer C	Spacer A	Spacer B
1. Miami, 21-29°C	1.06-1.08	1.09-1.1	1.07-1.08
2. Austin, 14-16°C	1.06	1.01-1.09	1.07
3. Atlanta 11-22°C	1.06	1.01-1.09	1.07
4. Albuquerque, 7-20°C	1.07-1.08	1.03-1.09	1.07-1.08
5. Indianapolis, 6-17°C	1.07-1.08	1.03-1.09	1.07-1.08
6. Toronto, 5-13°C	1.06-1.07	1.01-1.03	1.07-1.08
7. Winnipeg, -3-8°C	1.06-1.09	1.01-1.08	1.07-1.12
8. Yellowknife, -9-0°C	1.14-1.17	1.05-1.11	1.09-1.12

Triple IGU with a Fiberglass Frame

	Spacer C	Spacer A	Spacer B
1. Miami, 21-29°C	.86-.89	.89-.91	.87-.9
2. Austin, 14-16°C	.86-.87	.89	.87
3. Atlanta, 11-22°C	.86-.87	.89	.87
4. Albuquerque, 7-20°C	.87	.89-.9	.87-.88
5. Indianapolis, 6-17°C	.87	.89-.9	.87-.88
6. Toronto, 5-13°C	.87	.89-.9	.87-.88
7. Winnipeg, -3-8°C	.87-.91	.89-.93	.87-.92
8. Yellowknife, -9-0°C	.89-.93	.91-.95	.9-.94

Triple IGU with a TBSW Frame

	Spacer C	Spacer A	Spacer B
1. Miami, 21-29°C	.8-.82	.83-.85	.81-.83
2. Austin, 14-16°C	.8-.81	.83	.81
3. Atlanta, 11-22°C	.8-.81	.83	.81
4. Albuquerque, 7-20°C	.8-.82	.83-.84	.81-.82
5. Indianapolis, 6-17°C	.8-.82	.83-.84	.81-.82
6. Toronto, 5-13°C	.81-.82	.83-.84	.81-.82
7. Winnipeg, -3-8°C	.81-.84	.83-.87	.81-.85
8. Yellowknife, -9-0°C	.83-.86	.85-.88	.83-.87

As stated in Section 5.6.1, there were no significant differences (0-5%) in $U_{\text{window-NFRC}}$ across the annual average high and low temperature ranges for each location. Therefore, the average annual temperature for each location is sufficient to account for the climate specific U-value.

The differences in U_{window} values between each spacer are minute. Out of the three spacers, Spacer C gave the lowest U_{window} value and Spacer A gave the highest U_{window} values in these simulations. Spacer C had a slightly higher thermal performance than Spacer A given that their height is identical, 12 mm. In Spacer C, the material adjacent to the gas infill contributed to its higher performance due to its lower thermal conductivity (i.e. 0.2 W/mK) than Spacer A and B (i.e. 0.19 and 4.6 W/mK respectively). Spacer B has a slightly higher thermal performance than Spacer C despite the metal component (4.6 W/mK). This is due to its smaller height of 7.874 mm which allows for a slightly larger volume of the krypton/air gas infill which has an extremely low conductivity; lower than the spacer. The CEN values increase from 0 and 20°C because those are the interior and exterior temperature boundary conditions. The NFRC values increase from 21°C because that is the interior temperature boundary condition and the exterior temperature boundary condition allows for a greater range and does not influence the incremental change in $U_{\text{window-CEN}}$ values at 0°C.

In comparing the three spacer products, there were no significant differences (up to 5%) between the NFRC and CEN U_{window} values for the fiberglass and U-PVC frame types. The $U_{\text{window-NFRC}}$ values were generally slightly lower than CEN values. For the majority of the frame types and IGUs, Spacer C had the lowest conductivity out of all of the spacers and this information was used to justify the use of Spacer C in the simulations that required one spacer type (i.e. Sections 5.2.1-5.2.5). The lower conductivity of Spacer C minimized the influence of the spacer on the frame and IGU components upon U_{window} values; this aided the focused examination of the frame and IGU components.

There were only slightly higher $U_{\text{window-NFRC}}$ values in the double IGU combination with the fiberglass frame. This slight increase in $U_{\text{window-NFRC}}$ value is due to the additional thermal transmittance that occurs with the double IGU in comparison to the triple and quad IGUs. The double IGU has a higher thermal transmittance as the difference in exterior temperature from -18°C increases to -40°C; thus the larger increase in $U_{\text{window-NFRC}}$ occurs at -40°C. Overall, this increase is minor compared to the CEN values.

The TBSW frames with double, triple and quad IGUs showed relatively lower $U_{\text{window-NFRC}}$ values than CEN values; up to 7% higher than CEN values. The higher difference in percentage changes were found at 30°C due to the same $U_{\text{cog-CEN}}$ value given and the summer boundary conditions used in the CEN method for 30 and 40°C.

For the quad IGU simulations the two spacers showed no change in the percentage difference between the CEN and NFRC methods between the -40 and 10°C temperature range. The results for 30 and 40°C

showed a greater difference for simulations with Spacer C. Overall, the $U_{\text{window-NFRC}}$ values were lower than the CEN values. Spacer C simulations showed a $U_{\text{window-NFRC}}$ value range of .663-.731 and Spacer A showed a range of .685-.749 W/m²K. The results show that the higher the thermal performance of the glazing, the more significant the role of the thermal characteristics of the frame and spacers. In addition, the higher the thermal performance of the spacer also accentuates the thermal performance characteristics of the frame, allowing for the clearer identification of these characteristics. For example, the U_{window} values with Spacer C were the lowest and showed the greatest differences between both methods out of all the spacers for the quad IGU. The lower NFRC thermal conductivity of the softwood, as well as the lower surface film coefficients used for the summer design conditions at 30 and 40°C, account for the lower $U_{\text{window-NFRC}}$ values.

The solid wood U_{window} values with double and triple IGUs had the largest discrepancies between both methods. The $U_{\text{window-NFRC}}$ values were up to 13% lower than $U_{\text{window-CEN}}$ values. Seeing that the frame is composed of softwood with only minute frame cavities (in size and number), the factor that most likely contributes to the lower $U_{\text{window-NFRC}}$ value is the NFRC lower thermal conductivity of softwood. As stated previously, the NFRC's lower thermal conductivity value does give lower U_{window} values, therefore this applies to these simulations. The double IGU results show a larger difference between both methods in the temperatures between 15 and 35°C. The surface film coefficients at 30°C and above are according to the NFRC and CEN exterior temperature summer design values of 2.75 and 8 W/m²K respectively (the interior surface film coefficients are similar; 2.44 and 2.5 respectively). The CEN value has a higher exterior surface film coefficient which results in higher $U_{\text{window-CEN}}$ values which also contributes to the higher $U_{\text{window-CEN}}$ values found in the double IGU results.

The Spacer A simulations with the solid wood frame showed higher U_{window} values and greater differences between both methods due to its slightly lower thermal performance. Spacer B contains materials that have a higher thermal conductance than Spacer A's materials, however, the height of Spacer B is only 7.874 mm and is set deeper within the frame which allows more space for the krypton/air gas mixture as well as being less subject to the effects of the exterior conditions upon the IGU, by being protected from the frame.

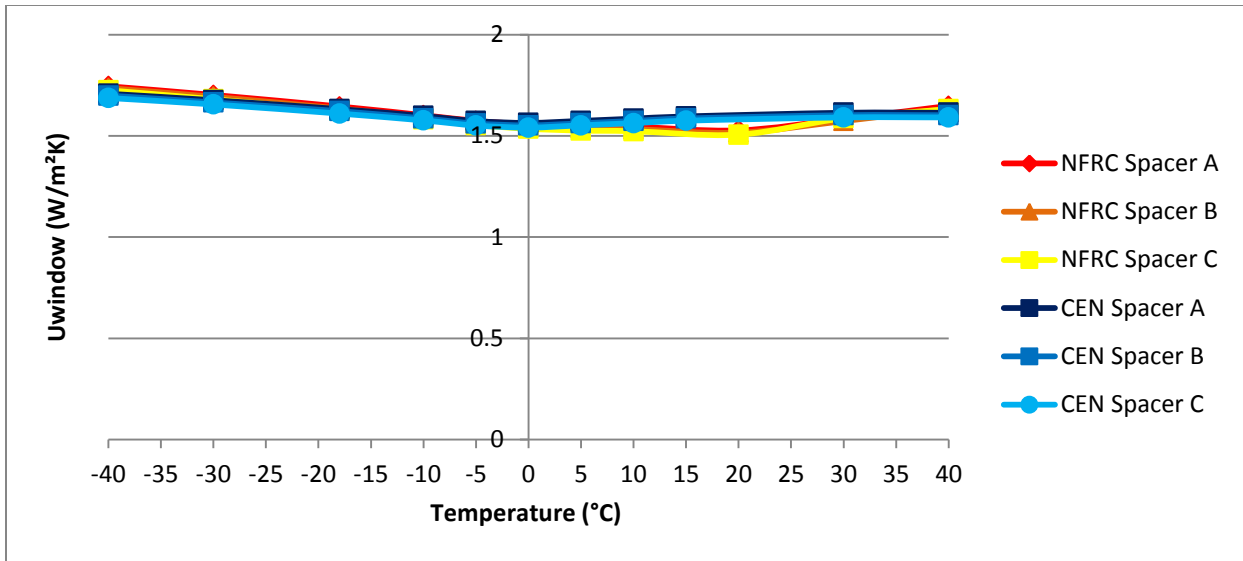


Figure 68 Double IGU Fiberglass Frame: Different Spacers in 8 Climate Zones

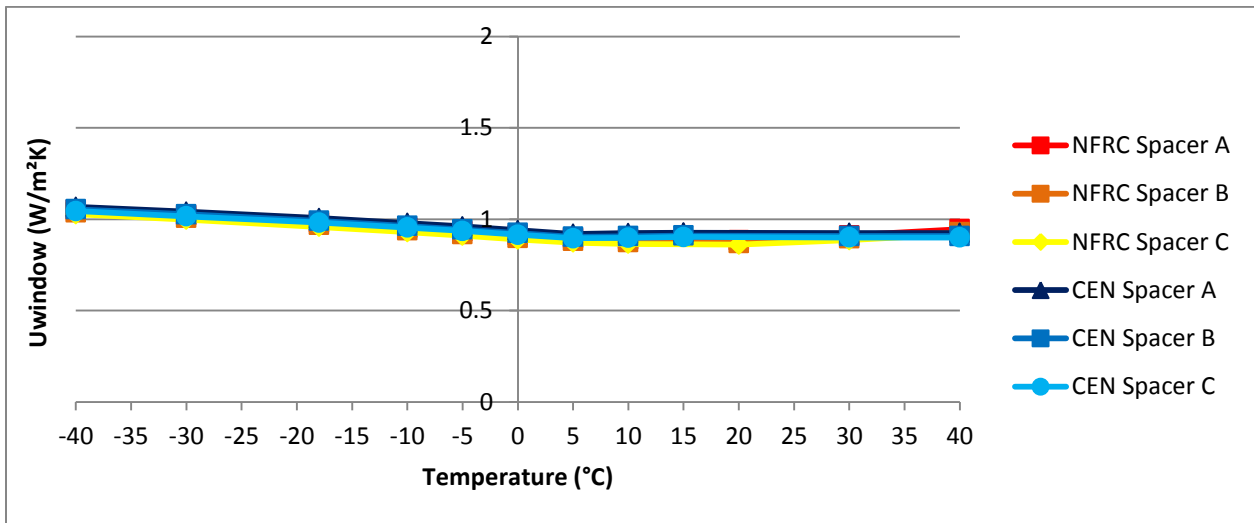


Figure 69 Triple IGU Fiberglass Frame: Different Spacers in 8 Climate Zones

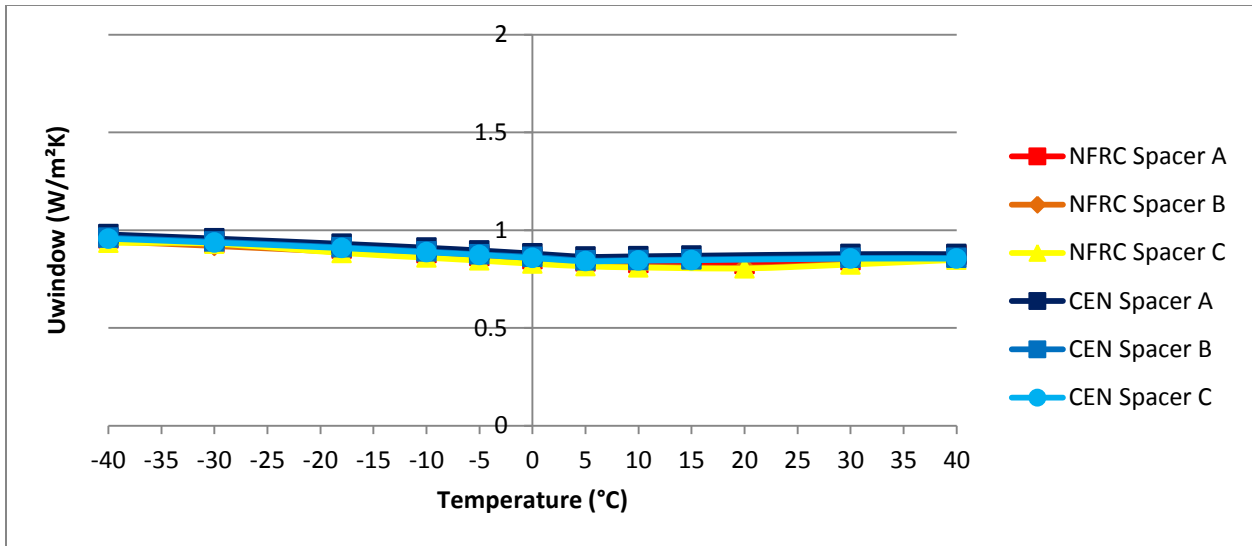


Figure 70 Triple IGU TBSW Frame: Different Spacers in 8 Climate Zones

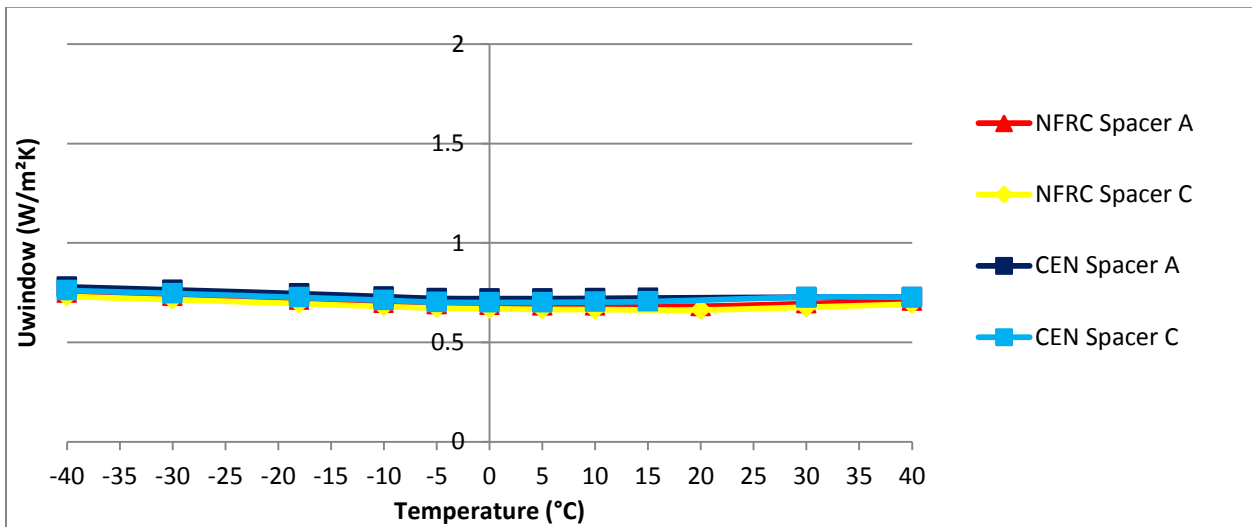


Figure 71 Quad IGU TBSW Frame: Different Spacers in 8 Climate Zones

5.6.5 $U_{\text{window-NFRC}}$ and $U_{\text{window-CEN}}$ Comparison of Inland and Coastal Locations

Double, triple and quad IGUs were simulated with the different wind velocities and exterior temperatures specific to inland and coastal locations within the eight climate zones. All IGUs simulated had a high SHGC and Spacer C.

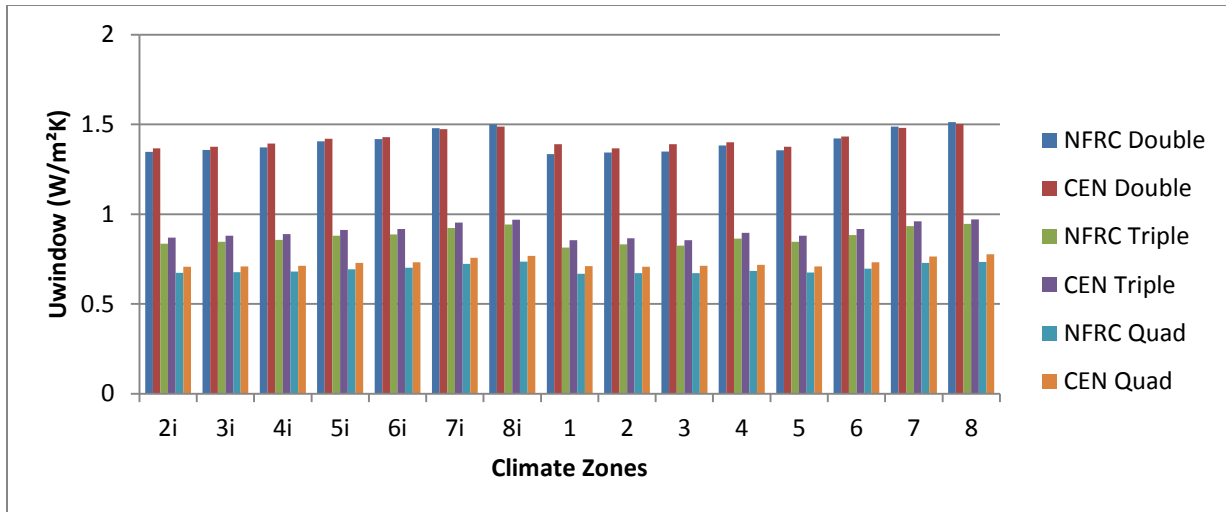


Figure 72 TBSW Frame: U_{window} NFRC and CEN Values of Inland and Coastal Location in 8 Climate Zones

$U_{\text{window-NFRC}}$ values for the TBSW frame were 6% lower to 1% higher than CEN values for the inland and coastal locations in the 8 climate zones. The quad IGU showed higher differences between both methods (see Figure 72). The original $U_{\text{window-NFRC}}$ values for the TBSW frame with double, triple and quad IGUs were 8% lower to 7% higher than the NFRC values for the inland and coastal locations.

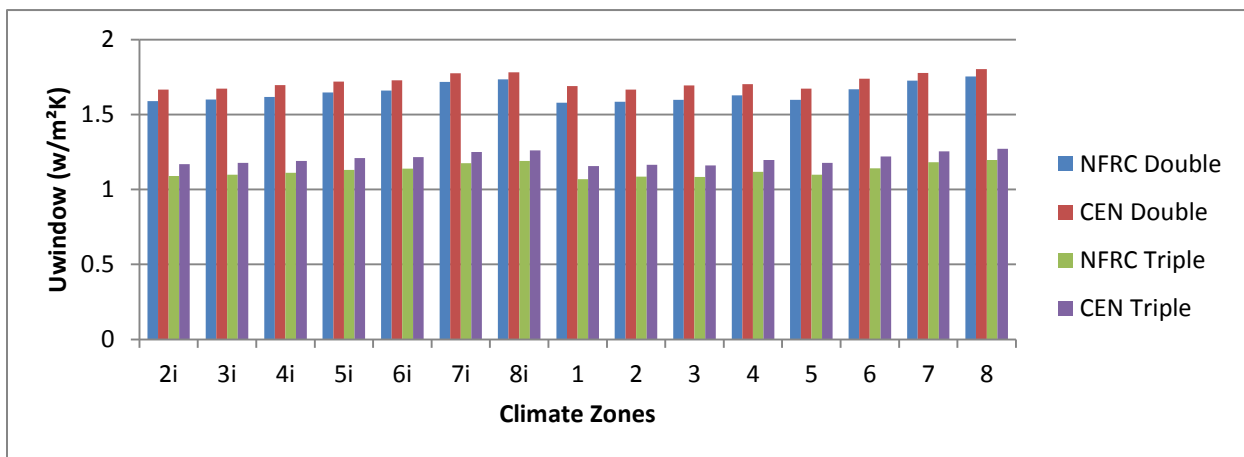


Figure 73 Solid Wood Frame: U_{window} NFRC and CEN Values of Inland and Coastal Location in 8 Climate Zones

Overall, the $U_{\text{window-NFRC}}$ values for the solid wood frame were 7% lower to 3% lower than CEN values for the inland and coastal locations in the 8 climate zones (see Figure 73). The original $U_{\text{window-NFRC}}$ values for the solid wood frame with double, triple and quad IGUs were 10% lower to 5% higher than inland and coastal NFRC values.

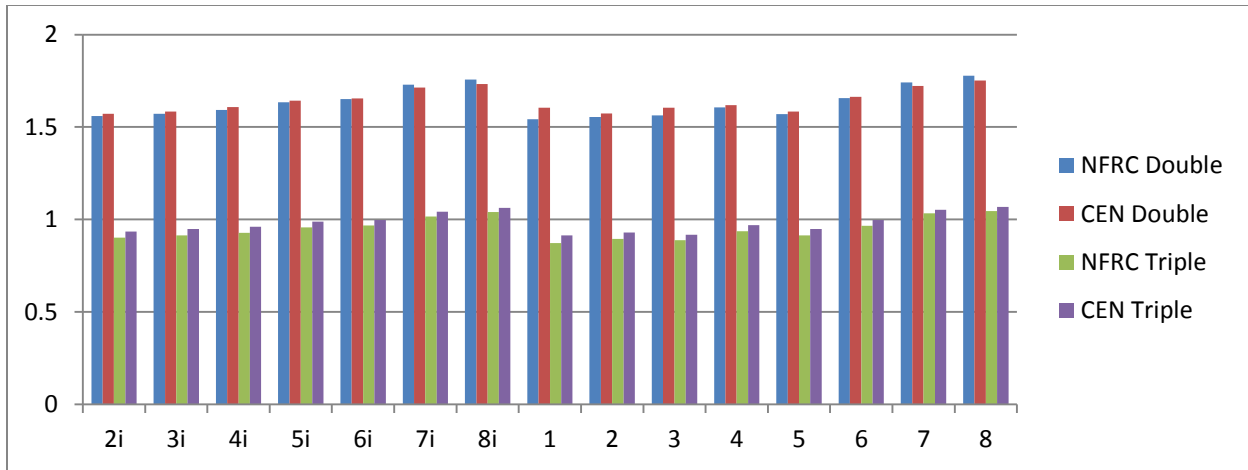


Figure 74 Fiberglass Frame: U_{window} NFRC and CEN Values of Inland and Coastal Location in 8 Climate Zones

The $U_{\text{window-NFRC}}$ values for the fiberglass frame were 5% lower to 1% higher than CEN values for the inland and coastal locations in the 8 climate zones (see Figure 74). The original $U_{\text{window-NFRC}}$ values for the solid wood frame with double, triple and quad IGUs were 9% lower to 10% higher than inland and coastal values.

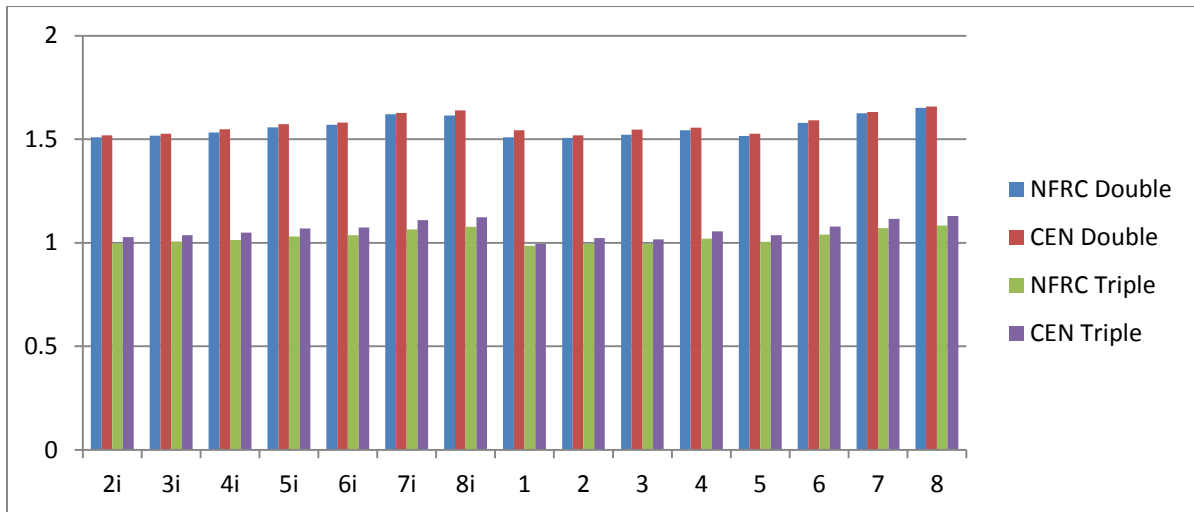


Figure 75 U-PVC Frame: U_{window} NFRC and CEN Values of Inland and Coastal Location in 8 Climate Zones

$U_{\text{window-NFRC}}$ values for the U-PVC frame were 0- 4% lower than CEN values for the inland and coastal locations in the 8 climate zones (see Figure 75). The original $U_{\text{window-NFRC}}$ values for the solid wood frame with double, triple and quad IGUs were 6% lower to 4% higher than inland and coastal values.

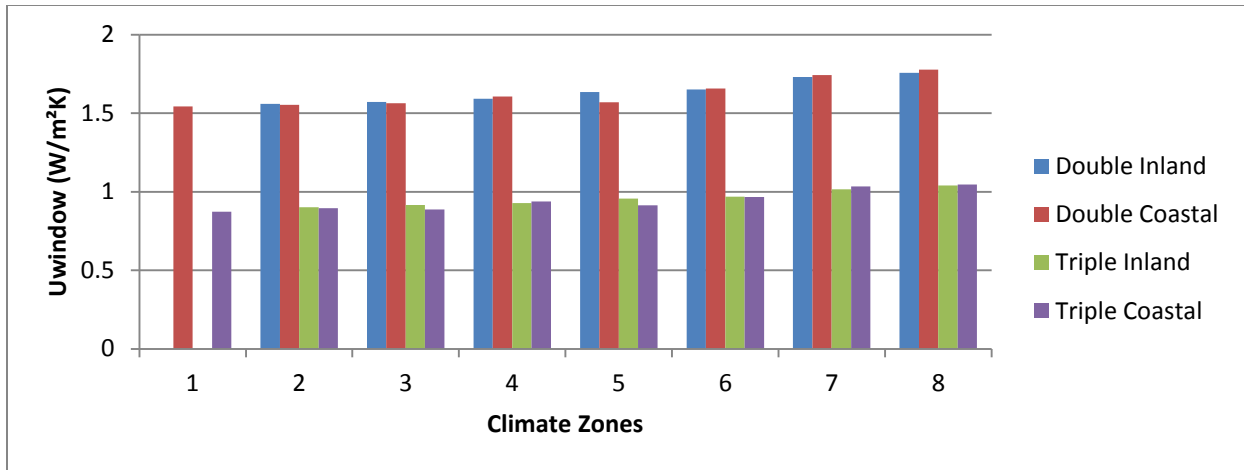


Figure 76 Fiberglass Frame: $U_{\text{window-NFRC}}$ Values of Inland and Coastal Locations in 8 Climate Zones

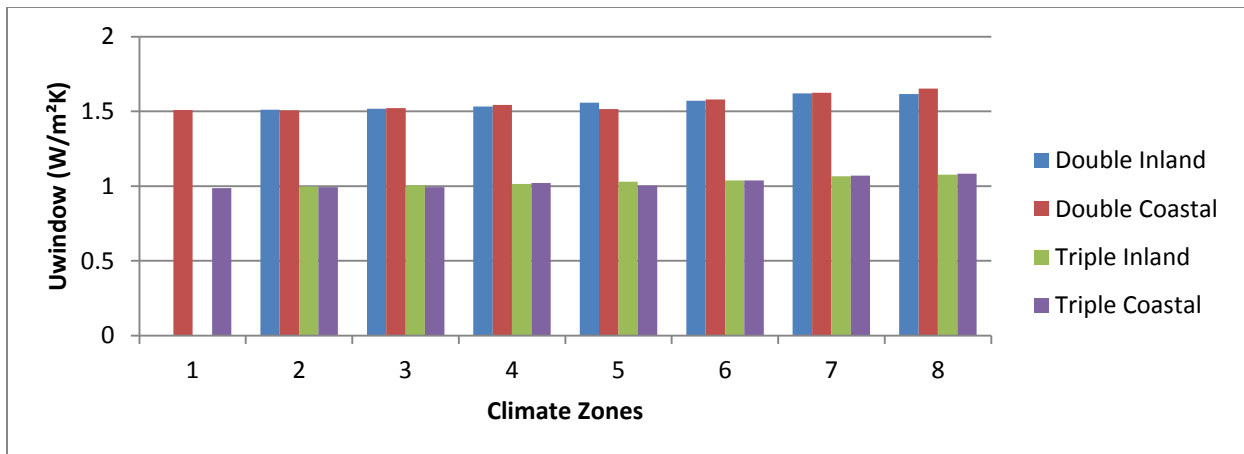


Figure 77 U-PVC Frame: $U_{\text{window-NFRC}}$ Values of Inland and Coastal Locations in 8 Climate Zones

Since extreme annual wind velocities were used in the simulations, they produced surface film coefficients and U_{window} results that represent more extreme conditions (see Section 3.14). The trend showed that the frames with the higher performing IGUs had larger differences between both methods; in addition, there were not any significant differences between the inland and coastal U_{window} values (see Figures 76 & 77). Overall, $U_{\text{window-NFRC}}$ values were again primarily lower than $U_{\text{window-CEN}}$ values in the 8 climate zones due to the lower NFRC surface film coefficient values. The U-PVC and fiberglass frames had the least differences in U_{window} values between both methods due to their smaller widths (from the sightline to the edge of the frame). A smaller frame width leads to less heat transfer through conduction as influenced by the various exterior temperatures and surface film coefficients of the inland and coastal locations. Again, the different approaches to configuring U_{cog} ; NFRC's higher solar irradiance

used for the detailed radiation model on the interior side (ISO, 2003); and the different radiation procedures of both methods, all contribute to higher $U_{\text{window-NFRC}}$ values.

It is interesting to note that for the inland location of Climate Zone 5, Indianapolis, IN, there was a considerable increase in thermal transmittance compared to Vancouver, BC. Indianapolis has a slightly higher annual average temperature and extreme annual wind velocity than Vancouver. These values account for the higher U_{window} values for Indianapolis. The slight variation between inland and coastal locations in all of the other climate zones is attributed to the higher and lower wind velocities and annual average temperature. For example, an inland and coastal location within the same climate zone will have similar U_{window} values (i.e. Toronto, ON and St. John's, NFLD), if the annual average temperature of the inland location is higher (9.2 vs 4.7°C) and the wind velocity is lower than the coastal location (9.1 vs 12.3 m/s). Similarly, an inland location with a lower annual average temperature will have a similar U_{window} value if the wind velocity is higher than the coastal location; they balance each other. However, if both the annual average temperature and wind velocity is higher for one location than the other, the U_{window} values were found to be higher as well.

5.7 Harmonization of the CEN and NFRC U_{window} Calculation Methods

Taking into account the percentage changes of all of the frame types and glazing combinations, the overall weighting of the magnitude of the percentage changes for each frame type was determined. Figure 78 and Table B-43 compare the NFRC and CEN methods using the NFRC exterior temperature of -18°C and the CEN exterior temperature of 0°C. Out of 34 window simulations, the majority of simulations showed only a 0-4% difference in NFRC and CEN values for the same window. Only 5 outliers were between a 5 and 6% difference in NFRC and CEN U_{window} values for the same window (i.e. triple IGUs solid wood frame in both methods and the quad TBSW in the CEN method). This finding may support a possible amalgamation between the two methods whereby using the same exterior temperature boundary conditions yields analogous results that primarily lie in a percentage error margin of 0-4%. A 4% lower $U_{\text{window-NFRC}}$ value translates to a 0.05 W/m²K lower value than the CEN value. A 4% higher $U_{\text{window-CEN}}$ value translates to a 0.05 W/m²K higher value than the NFRC value. The results that lie in the higher 5-6% percentage error margin also support the possibility of amalgamating both methods for it translates to 0.06 W/m²K higher $U_{\text{window-CEN}}$ values in this study. When comparing the percentage errors found in the RDH Building Engineering Ltd. (2014) study, where $U_{\text{window-NFRC}}$ values were found to be 14% lower to 18% higher than CEN values, and this study where $U_{\text{window-NFRC}}$ values were 1% lower to 11% higher than CEN values, the proposed amalgamation results (see Sections 5.6.2 & 5.6.3), have a

minimal percentage error margin of 0-6%. Two of the outliers were found with the triple IGUs with the solid wood frame; this may be attributed to the larger width of the frame that is exposed to the exterior and thus the change in exterior temperature is more pronounced with these frames.

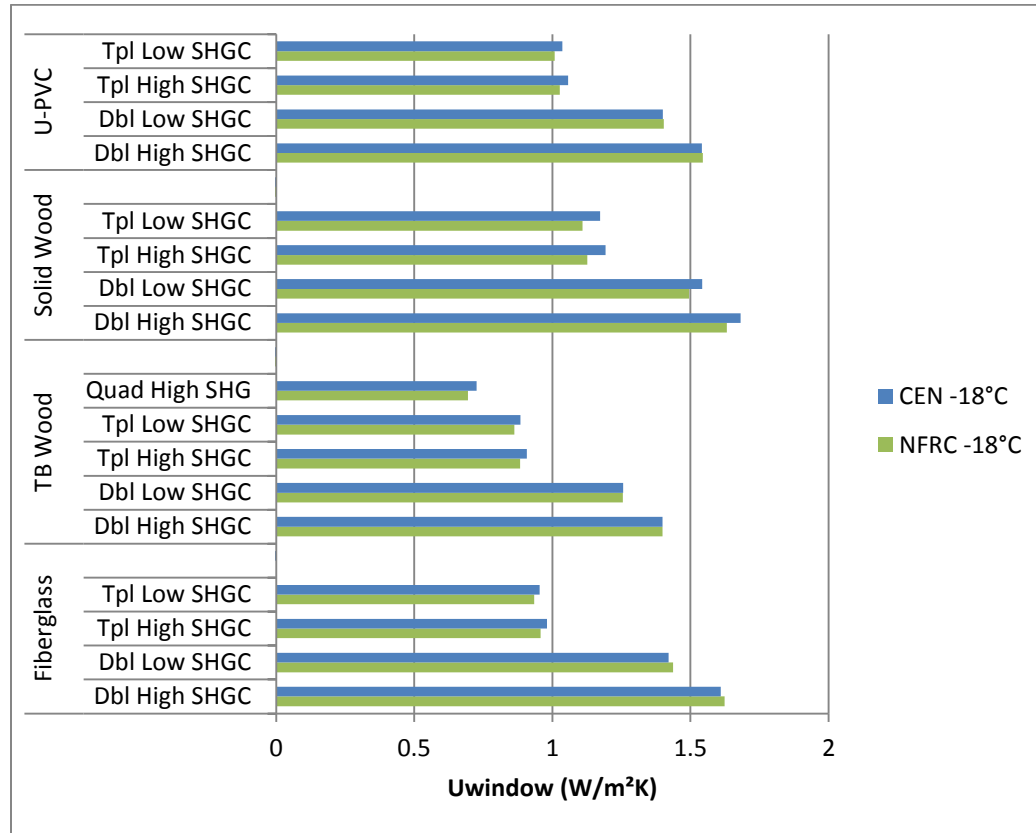


Figure 78 NFRC and CEN U-window Values with NFRC Exterior Temperature Boundary Condition

In addition, this study’s findings in comparing NFRC and CEN U_{window} values for the same window unit, have less of a variation than the generalized notion in the building community that NFRC values were approximately 10% higher or lower than CEN values. Generally, considering the triple and quad high performance window combinations with Spacer C, there is a minimal, 0 to 6% difference between the standard NFRC and CEN methods and boundary conditions. For several triple IGU combinations where the $U_{window-NFRC}$ values are 6% lower than CEN values, this difference translates to a minimal increase in U-window value by 0.067 W/m²K. The impact of this increase upon a building’s annual energy intensity use would need further research considering the size and quantity and cardinal direction of the aforementioned triple glazed window units; this is presently outside the scope of this study.

However, the lower $U_{window-NFRC}$ values are slightly beneficial for North American window manufacturer as it gives a slightly higher thermal performance value in the NFRC and CEN calculation methods and

thus in both North American and European markets. On the other hand, other factors need to be deliberated upon along with thermal performance. Depending on one's location, a North American window with a $0.05 \text{ W/m}^2\text{K}$ lower U-value may be chosen for a building located in North America which results in financial and environmental savings for the builder as shopping locally (within North America) does not incur overseas transportation costs and thus reduces carbon emissions and fossil fuel consumption. Likewise, for a building located in Europe, the same North American window may be competitive within that market when this amalgamation method is used. For example, for a standard NFRC rated window with a $0.96 \text{ W/m}^2\text{K}$ U-value and a CEN rating of $0.91 \text{ W/m}^2\text{K}$, the CEN value would be favoured when selecting for higher thermal performance and achieving specified metrics for primary energy such as that for the Passive House standard. However, the little gain in thermal performance (in a whole building energy simulation) may not justify the transportation costs of importing the European window product into North America. On the other hand, this window may be competitive in the European market for its thermal performance when using the amalgamation method which gives a $U_{\text{window-NFRC}}$ of $0.88 \text{ W/m}^2\text{K}$. Similarly, overseas transportation costs to Europe need to be considered as well.

Using the proposed amalgamation method by synchronizing the exterior temperatures according to the standard exterior temperatures, the North American windows used in this study would have a lower U_{window} value using both the NFRC and CEN calculation methods. In terms of thermal performance, simply using the same exterior temperature boundary conditions in computer simulations could potentially support and enable the effort in creating a fairer method in comparing window products.

To evaluate the proposed amalgamation method, a comparison of U_{window} values, according to the NFRC and CEN method, was conducted at an exterior temperature range from -40 to 40°C . The NFRC and CEN U_{window} values were compared at nine temperature points in this range for all frame types with double, triple and quad IGUs with a high and low SHGC. Overall, the $U_{\text{window-NFRC}}$ values were 8% lower to 4% higher than $U_{\text{window-CEN}}$ values for all of the exterior temperatures (see Figures 79 & 80). The majority of NFRC values were lower than CEN values. 88% of the values each had between a 0-5% difference between both methods. However, 12% of the values were between a 6 and 8% percentage change. By using the same thermal conductivities and tweaking the variations between the center-of-glazing simulations, the percentage change margin could be altered. Foremost, further research is needed to test the proposed amalgamation method to measure its suitability for windows that varying levels of thermal performance.

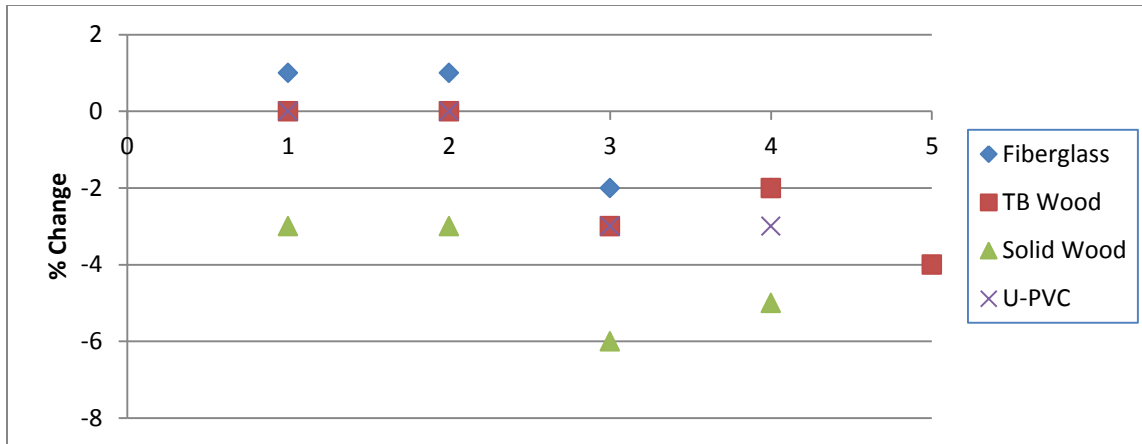


Figure 79 NFRC and CEN U-window Values Percentage Changes at NFRC Exterior Temperature Boundary Condition

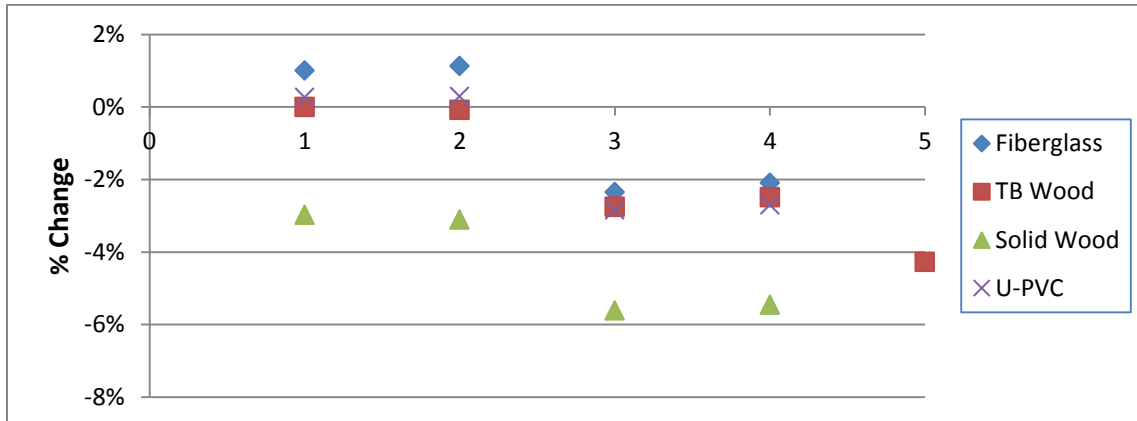


Figure 80 NFRC and CEN U-window Values Percentage Changes at CEN Exterior Temperature Boundary Condition

Note: 1- Double High SHGC, 2- Double Low SHGC, 3- Triple High SHGC, 4- Triple Low SHGC, 5- Quad High SHGC

Frame Cavity Method

For the high performance frames in this study, the difference in the frame cavity methods of both methods is negligible. However, caution needs to be taken for lower performing frames where there is a plethora of cavity regions within the frame. Out of all the frames, the U-PVC frame had the most frame cavities without any insulation materials and the results showed a larger difference of 4% in U-frame values between both methods. The number, size and configuration of the frame cavities impact the frame cavity surface temperatures where the larger the frame cavity and the more thermally conductive the frame materials are, the greater the likelihood of heat transfer to occur through

conduction, radiation and convection. Computational Fluid Dynamics (CFD) analysis can specify the impact of heat transferred through increased convection flows within frame cavities; this has been identified by Curcija (2005) and other studies. This study also supports the need for further research into the CFD analysis of high performance frames in order to measure and standardize the impact of CFD of convection flows in frame cavities. Therefore, the difference in frame cavity methods has more of an impact in frames with more frame cavities, and materials that are more thermally conductive seeing that they impact the frame cavity surface temperatures.

Radiation Model

The radiation models of both methods could potentially be synchronized seeing that the NFRC detailed radiation model and the CEN simplified radiation model are the same. The harmonization of several aspects both methods could be achieved where both methods could use the same radiation model and use the same thermal conductivities for all the materials and gases.

U_{frame} Method

When comparing aspects of a whole window unit, the CEN method's procedure in determining U_{frame} is considered to be the most accurate in giving the thermal transmittance of the frame by itself, without the influence of the IGU. Since U_{frame-NFRC} does not give the thermal transmittance of the frame by itself, the CEN U_{frame} method would be beneficial as an international standard for determining U_{frame} in order for different frames to be fairly compared in the international market. Keeping in mind that the different boundary conditions and calculation methods produce different results, the NFRC boundary conditions could be used. Further research and collaboration between NFRC and CEN experts would be needed to determine an NFRC method of determining U_{frame} with a calibration panel. Foremost, simulation results would need to be compared with physical lab testing to determine the accuracy of this. The NFRC method may potentially adopt the proposed amalgamation method of using the same exterior temperature for the calibration panel where the calibration panel is drawn in THERM and simulated according to the NFRC method; however boundary conditions would need to be altered.

Other Harmonizing Strategies and Areas that need Improvement

A clearer labeling system of glazing products is needed where the SHGC is specified for an individual glazing product (glazing only) and window product (with the frame) separately. Although each method for determining the SHGC of the glazing by itself are similar to each other, using the same boundary

conditions and thermal conductivities would aid in synchronizing SHGC values. Similarly, adopting the same thermal conductivities of gas infill mixtures and the same U_{cog} procedure would be beneficial for comparing individual glazing products. Due to the trends found in this study, where U_{cog} values largely influenced the differences in U-values of both methods, the harmonization of the U_{cog} procedure of both methods needs further research. Likewise, harmonized surface film coefficient sets and summer and winter boundary conditions for an international standard needs further research.

The NFRC and CEN methods each have inherent strengths, however, elements of both could be viable in the international market. This study supports the findings identified by RDH Building Science Engineering Ltd. (2014), where the CEN method is found to be more accurate in comparing individual window components. The NFRC method is considered to be more accurate in determining thermal transmittance, SHGC and center-of-glass values of the actual window product at specified product dimensions as identified by the NFRC standard (see Table 7).

In consideration of the results of this study, the CEN method is considered to be the preferred method of calculating the whole window U-value (i.e. $U_{\text{W-ITN'L}}$). However, a whole window U-value, for each climate zone in North America and Europe, would be ideal for each window product using the annual average exterior temperatures. A unified material and gas thermal conductivity list is necessary for a fairer comparison of products. The NFRC interior surface film coefficients are considered to be more accurate as they are specified according to the type of frame material; the interior reduced radiation sections may be omitted seeing that using one interior surface film coefficient simplifies the simulation process. Physical lab testing is needed to test the applicability and accuracy of this method.

Foremost, physical lab testing of an array of current high performance window products would also help identify which method is more accurate in calculating thermal transmittance. In addition, further testing using computer simulations could be performed to narrow the scope of physical lab testing that would be necessary, thereby reducing costs. Using 3D software may highlight the heat transfer characteristics in a more detailed manner, particularly in the IGU; this is beyond the scope of this study, however, physical lab testing would need to be rigorous (see Section 7).

6 Further Research and Conclusions

6.1 Conclusion

This study has shown the critical importance and intricacies of the calculation methods and procedures used in determining the thermal transmittance of window products. A comparative evaluation of the NFRC and CEN U-value calculation methods was conducted for several North American residential high performance window products. An evaluation of the several parameters that are most influential in determining the whole window U-value for high performance windows in North America's eight climate zones was also performed. Given that certified Passive House windows are among the most high performance windows in the North American market, four frame types with double, triple and quad glazing combinations selected from several certified PHIUS windows, were simulated and calculated according to the NFRC and CEN standard methods.

The differences that were found between both calculation methods showed that each window product configuration and material property react distinctively to the assumptions and boundary conditions of each method. The results of this study aid in identifying and explaining the percentage change between both methods, as well as, determining how each method defines and utilizes various parameters. The trend showed that the higher the performance of the IGU, the lesser the differences in U_{window} between the NFRC and CEN methods. The variances are accrued to the effect of the different exterior and interior temperature differences, surface film coefficients, frame cavity methods, U_{frame} methods, U_{cog} methods, material thermal conductivities and different U_{window} calculations. Lower performing windows would exhibit larger differences between both methods due to the greater influence of the exterior temperature on the gas infill in the lower insulative IGU. This is due to the heat transfer effects of the IGU transferring to the lower performing frame. The significant weighting of the U_{cog} in the U_{window} calculation results in a lower U_{window} value. Different calculations, assumptions and boundary conditions highlight the uniqueness of the NFRC and CEN standard thermal transmittance methods and therefore each method should be treated as such.

Seeing that the average U-values give a better indication as to the thermal transmittance being achieved in each climate zone, the climate specific $U_{\text{window-NFRC}}$ values for the high performance windows (i.e. frames with triple and quad IGUs) were found to be approximately 0-14% higher than the standard NFRC value and 7% lower to 2% higher than the CEN standard values. This study has shown that the overall U-value for each window combination can potentially vary significantly across specific North

American cities in the eight climate zones. Although the material conductivity does not change with different exterior temperatures, the change in exterior temperature in both calculation methods directly influences the convective and conductive heat transfer effects upon the gas infill in the IGU. The heat transfer effects within the IGU are filtered through the spacer and frame materials and frame cavities. Since the U_{cog} and U_{frame} are the main components of the U-value calculations, the interior and exterior temperature difference influences the whole U_{window} value. Furthermore, the thermal transmittance of the IGU is critical in the thermal performance of a building, considering that the primary insulative barrier to changes in exterior temperature in the IGU is the gas infill.

Climate specific U_{window} values can aid energy modellers, designers and builders in configuring a clearer impression of the annual energy use intensity of a building. The average annual temperature is considered suitable to obtain climate specific U_{window} values seeing that there are not any significant differences in U_{window} for the average annual high and low temperature ranges.

Considering the differences in the U-values of each method were generally smaller for high performance windows, the varying values of boundary conditions had less influence than on lower performing windows, as seen in previous studies. Altogether, this leads to the harmonization of both methods. Some of the parameters that could be harmonized include the exterior and interior temperatures, surface film coefficients, frame cavity methods, SHGC of the IGU without the frame and the U_{frame} method. Ideally, a single ISO international window calculation procedure for determining thermal transmittance would allow for an equitable and fair comparison of window products in the international market. In working towards this, using the same exterior temperature, as shown in this study, could aid in harmonizing the NFRC and CEN methods, until an international standardized method is conceived. A harmonized international thermal transmittance calculation method would be highly beneficial for the window and high performance building industry in creating a fair market and more accurate performance metrics for energy models.

6.2 Areas of Further Research

- 1) Physical lab testing of the proposed amalgamation in the goal of attaining a single harmonized international calculation method for determining a window product's thermal transmittance.
- 2) Physical lab testing of each method and comparing their accuracy to current high performance window products. The following details need to be considered:

- a) Accurate U-values are difficult to achieve seeing that it is challenging to reflect the environmental conditions of actual use in physical laboratories (Klems & Reilly, 1990). Physical lab testing does not allow for a stringent test of the frame calculations, however, frame effects are somewhat detectable, yet do not mar with calculation results; experiments are also not sensitive to edge corrections (Klems & Reilly, 1990).
 - b) In comparison with the European EN ISO 8990 and the American ASTM C1363-05 hot box tests, the Russian GOST 26602.1-99 test is more precise in obtaining “the individual measurements of the thermal characteristics of sample components” (Asdrubali & Baldinelli, 2011). This Russian test combined with the European or American test for comparative purposes would be an ideal approach to testing the thermal characteristics of specific components (Asdrubali & Baldinelli, 2011).
 - c) Further research could involve the measurement of the frame junctions with thermocouples since present measurement methods of the NFRC and CSA do not measure those areas; measuring the frame junctions could in effect give a clearer picture as to the amount of heat transfer that is happening in those specific areas. This may change the overall U_{frame} value.
 - d) Further research utilizing 3D simulations to measure the thermal transmittance of various high performance windows and comparing those results with physical lab tests could determine the accuracy 3D simulations.
 - e) There is also the need for further research into the CFD analysis of high performance frames in order to measure and standardize the impact of CFD of convection flows in frame cavities.
 - f) Comparing the U_{window} values of differently-sized windows and window types.
- 3) There were some issues that was found through the breadth of the research that was largely absent from the literature. There is thus a need for research to estimate, reconcile and rectify the historical environmental and social impact of the building industry: namely, education and honouring of First Nation Treaties where respectful relationships and negotiations are needed in regards to accessing natural resources. Environmental and social impacts of other local communities also need to be researched and respected.

7 Appendix A

Computer Simulations vs Physical Lab Tests

Chen and Wittkopf (2012) showed that in their calorimetric hot box measurements and THERM and WINDOWS simulations, both test measurements were in congruence and both methods were capable of accounting for the thermal effects of specific parts of a window component using summer conditions, specifically the positive effects caused by warm edge spacers (Chen & Wittkopf, 2012). Lawrence Berkeley National Laboratory found that there was an agreement between observed and calculated results which supported the suitability of using computer simulations to measure thermal performance (Arasteh, Beck, Stone, duPont, Mathis, & Koenig, 1994). In addition, Klems and Reilly (1989) and Wright and Sullivan (1988) found that numerical calculations could be based on computer simulations and could “accurately predict the thermal performance of edge-seals” (Wright & H.F., Glazing system U-value measurements using a guarded heater plate apparatus, 1988).

The Passive House certification in Europe and the U.S., and other European rating councils such as the British Fenestration Rating Council solely require computer simulation to verify and rate the thermal performance of window products. Canada, the U.S. and Australia are also increasingly relying on computer simulations for verifying thermal performance (Curcija C. , 2005). The NFRC presently uses physical lab tests and computer simulations, however, due to the time consuming process and the high cost of physical lab tests, the NFRC is leaning toward a reliance on computer simulations to rate window products (Curcija C. , 2005). Computer simulations not only cost less than physical lab tests; they allow manufacturers to simulate numerous ideas to thousands of products in an iterative design process, thereby expanding design possibilities (Arasteh, Mathis, & DuPont, The NFRC Window U-Value Rating Procedure, 1992) (Arasteh, Finlayson, Huang, Huizenga, Mitchell, & Rubin, 1998). Computer simulations also help to distinguish differences in products that have similar thermal performance that may not be noticeable or clearly identified in physical lab tests (Arasteh, Mathis, & DuPont, The NFRC Window U-Value Rating Procedure, 1992) (Arasteh, Finlayson, Huang, Huizenga, Mitchell, & Rubin, 1998).

Lab testing procedures have several difficulties in measuring thermal performance, these include:

1. “Repeatability and accuracy: a lab test can produce a reasonably accurate U-value, however, it will not always produce the same number and may fail to properly distinguish between 2 or more products with performance levels that are very close to each other (i.e. High performance products)” (Arasteh, Mathis, & DuPont, The NFRC Window U-Value Rating Procedure, 1992) (Arasteh, Finlayson, Huang, Huizenga, Mitchell, & Rubin, 1998)

2. Waste of Resources: since there are similar products by different manufacturers, it is not efficient to replicate tests when the information already exists (Arasteh, Mathis, & DuPont, The NFRC Window U-Value Rating Procedure, 1992)

In light of these limitations for physical lab tests, it is acknowledged that other physical lab testing methods may give accurate results for identifying specific thermal loss regions, such as those that use thermographic cameras. This is included in the further areas of research and is beyond the scope of this research.

8 Appendix B

U_{window}: NFRC vs CEN Methods and Exterior Temperature Symmetry

Table B-42 Uwindow: Percentage Change between NFRC and CEN Methods

		NFRC	CEN	% Change
Fiberglass	DbI High SHGC	1.624	1.542	5%
	DbI Low SHGC	1.437	1.299	11%
	TpI High SHGC	0.958	0.915	5%
	TpI Low SHGC	0.934	0.883	6%
TB Wood	DbI High SHGC	1.399	1.346	4%
	DbI Low SHGC	1.255	1.161	8%
	TpI High SHGC	0.883	0.857	3%
	TpI Low SHGC	0.863	0.832	4%
	Quad High SHG	0.695	0.701	-1%
Solid Wood	DbI High SHGC	1.632	1.63	0%
	DbI Low SHGC	1.495	1.452	3%
	TpI High SHGC	1.127	1.143	-1%
	TpI Low SHGC	1.109	1.12	-1%
U-PVC	DbI High SHGC	1.545	1.489	4%
	DbI Low SHGC	1.404	1.307	7%
	TpI High SHGC	1.027	1.007	2%
	TpI Low SHGC	1.008	0.983	3%

Table B-43 Exterior Temperature Symmetry of the NFRC and CEN Methods: Uwindow

		NFRC - 18°C	CEN - 18°C	% Change	CEN 0°C	NFRC 0°C	% Change
Fiberglass	Dbl High SHGC	1.624	1.61	1%	1.542	1.535	0%
	Dbl Low SHGC	1.437	1.421	1%	1.299	1.301	0%
	Tpl High SHGC	0.958	0.981	-2%	0.915	0.888	3%
	Tpl Low SHGC	0.934	0.954	-2%	0.883	0.858	3%
TB Wood	Dbl High SHGC	1.399	1.399	0%	1.346	1.331	1%
	Dbl Low SHGC	1.255	1.256	0%	1.161	1.15	1%
	Tpl High SHGC	0.883	0.908	-3%	0.857	0.828	4%
	Tpl Low SHGC	0.863	0.885	-2%	0.832	0.804	3%
	Quad High SHG	0.695	0.726	-4%	0.701	0.669	5%
Solid Wood	Dbl High SHGC	1.632	1.682	-3%	1.63	1.568	4%
	Dbl Low SHGC	1.495	1.543	-3%	1.452	1.396	4%
	Tpl High SHGC	1.127	1.194	-6%	1.143	1.076	6%
	Tpl Low SHGC	1.109	1.173	-5%	1.112	1.053	6%
U-PVC	Dbl High SHGC	1.545	1.541	0%	1.489	1.491	0%
	Dbl Low SHGC	1.404	1.4	0%	1.307	1.315	-1%
	Tpl High SHGC	1.027	1.057	-3%	1.007	0.986	2%
	Tpl Low SHGC	1.008	1.036	-3%	0.983	0.964	2%

9 Appendix C

U_{cog}: Various Gap Spacing Sizes

Table C-44 Double High SHGC: U_{cog} Values with Various Gap Spacing Sizes

NFRC	Climate Zones								CEN	Climate Zones							
	1	2	3	4	5	6	7	8		1	2	3	4	5	6	7	8
6	2.12	2.047	2.082	2.092	2.093	2.093	2.084	2.067	2.131	2.16	2.187	2.176	2.168	2.157	2.136	2.107	
8	1.865	1.804	1.829	1.833	1.833	1.83	1.819	1.801	1.857	1.882	1.913	1.902	1.895	1.884	1.862	1.833	
10	1.69	1.638	1.656	1.658	1.656	1.653	1.643	1.631	1.67	1.692	1.727	1.716	1.709	1.698	1.676	1.647	
12	1.564	1.516	1.53	1.531	1.53	1.527	1.525	1.536	1.535	1.555	1.592	1.581	1.574	1.563	1.541	1.512	
14	1.468	1.424	1.435	1.437	1.437	1.44	1.458	1.519	1.432	1.45	1.49	1.479	1.471	1.46	1.439	1.487	
16	1.393	1.351	1.361	1.366	1.372	1.386	1.443	1.539	1.352	1.368	1.409	1.398	1.391	1.38	1.418	1.499	
18	1.335	1.292	1.304	1.317	1.332	1.367	1.459	1.558	1.287	1.302	1.345	1.334	1.326	1.345	1.428	1.51	
20	1.289	1.243	1.259	1.287	1.318	1.377	1.475	1.575	1.234	1.248	1.291	1.28	1.297	1.353	1.437	1.519	

Table C-45 Double Low SHGC: U_{cog} Values with Various Gap Spacing Sizes

NFRC	Climate Zones								CEN	Climate Zones							
	1	2	3	4	5	6	7	8		1	2	3	4	5	6	7	8
6	1.83	1.778	1.806	1.814	1.816	1.817	1.813	1.803	1.854	1.888	1.892	1.885	1.881	1.874	1.86	1.841	
8	1.523	1.485	1.502	1.506	1.506	1.506	1.501	1.493	1.532	1.562	1.567	1.561	1.556	1.55	1.537	1.52	
10	1.31	1.28	1.291	1.294	1.294	1.293	1.292	1.295	1.31	1.336	1.343	1.337	1.333	1.327	1.316	1.3	
12	1.153	1.129	1.137	1.139	1.14	1.143	1.154	1.19	1.148	1.562	1.179	1.173	1.17	1.164	1.154	1.139	
14	1.034	1.013	1.02	1.024	1.029	1.04	1.081	1.186	1.025	1.046	1.053	1.048	1.045	1.04	1.03	1.133	
16	0.942	0.921	0.929	0.94	0.952	0.981	1.078	1.208	0.927	0.947	0.955	0.95	0.947	0.942	1.03	1.148	
18	0.869	0.846	0.858	0.882	0.909	0.969	1.097	1.231	0.849	0.867	0.875	0.87	0.867	0.923	1.042	1.161	
20	0.813	0.785	0.804	0.851	0.903	0.985	1.116	1.252	0.784	0.801	0.809	0.805	0.854	0.933	1.052	1.172	

Table D-46 Triple High SHGC: Ucoq Values with Various Gap Spacing Sizes

NFRC		Climate Zones							
(mm)	1	2	3	4	5	6	7	8	
6	0.879	0.862	0.864	0.862	0.86	0.857	0.849	0.838	
8	0.726	0.712	0.712	0.71	0.708	0.705	0.699	0.692	
10	0.628	0.617	0.616	0.614	0.613	0.611	0.61	0.617	
12	0.561	0.551	0.55	0.549	0.549	0.551	0.563	0.602	
14	0.513	0.502	0.502	0.504	0.508	0.519	0.558	0.616	
16	0.477	0.465	0.467	0.476	0.487	0.514	0.569	0.629	
18	0.451	0.436	0.442	0.463	0.487	0.522	0.579	0.641	
20	0.433	0.412	0.425	0.465	0.493	0.53	0.589	0.652	

CEN		Climate Zones							
(mm)	1	2	3	4	5	6	7	8	
6	0.896	0.906	0.917	0.913	0.91	0.905	0.896	0.885	
8	0.733	0.741	0.753	0.749	0.747	0.743	0.735	0.725	
10	0.629	0.636	0.649	0.646	0.643	0.64	0.633	0.624	
12	0.558	0.564	0.577	0.574	0.572	0.569	0.564	0.611	
14	0.506	0.511	0.524	0.521	0.52	0.517	0.563	0.62	
16	0.466	0.47	0.484	0.481	0.481	0.515	0.57	0.627	
18	0.434	0.438	0.453	0.455	0.484	0.52	0.576	0.634	
20	0.409	0.412	0.427	0.459	0.488	0.525	0.581	0.64	

Table C-47 Triple Low SHGC: Ucoq Values with Various Gap Spacing Sizes

NFRC		Climate Zones							
(mm)	1	2	3	4	5	6	7	8	
6	0.83	0.815	0.818	0.816	0.815	0.812	0.806	0.797	
8	0.672	0.661	0.662	0.66	0.659	0.656	0.652	0.649	
10	0.571	0.562	0.562	0.561	0.56	0.56	0.562	0.574	
12	0.502	0.494	0.494	0.494	0.495	0.499	0.516	0.56	
14	0.451	0.443	0.444	0.448	0.454	0.467	0.512	0.574	
16	0.414	0.404	0.408	0.42	0.434	0.463	0.523	0.587	
18	0.387	0.373	0.382	0.408	0.434	0.471	0.533	0.599	
20	0.37	0.349	0.366	0.411	0.441	0.48	0.543	0.612	

CEN		Climate Zones							
(mm)	1	2	3	4	5	6	7	8	
6	0.853	0.853	0.869	0.865	0.862	0.858	0.85	0.839	
8	0.686	0.686	0.701	0.697	0.695	0.691	0.685	0.676	
10	0.58	0.579	0.593	0.59	0.588	0.585	0.58	0.575	
12	0.506	0.506	0.519	0.516	0.515	0.512	0.516	0.563	
14	0.452	0.452	0.465	0.462	0.461	0.465	0.512	0.572	
16	0.41	0.41	0.423	0.42	0.429	0.46	0.519	0.579	
18	0.377	0.377	0.39	0.4	0.428	0.466	0.525	0.586	
20	0.351	0.351	0.363	0.401	0.432	0.47	0.53	0.592	

10 Appendix D

U_{window} : Spacer Comparison

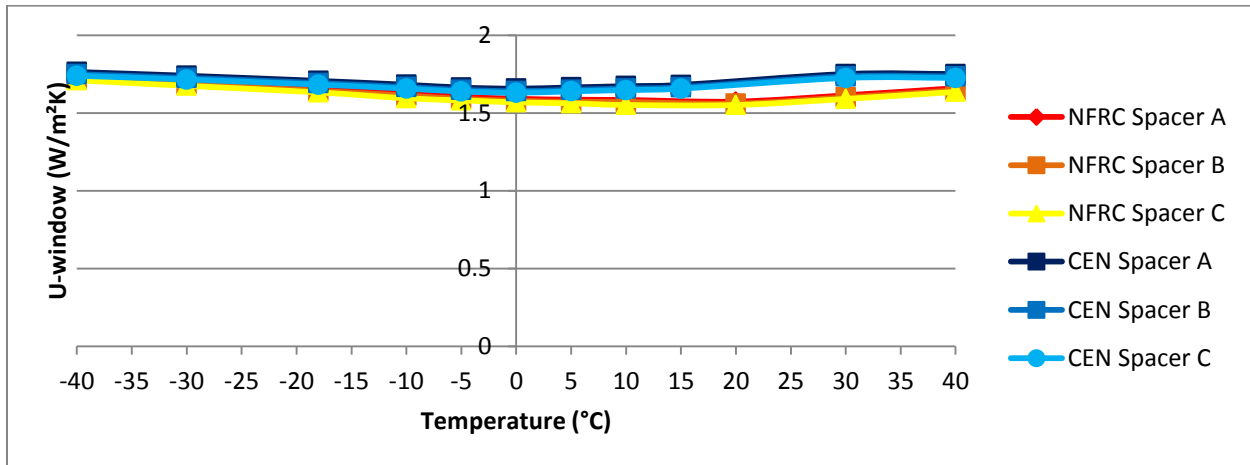


Figure D-81 Solid Wood Frame with a Double IGU: Spacer Comparison

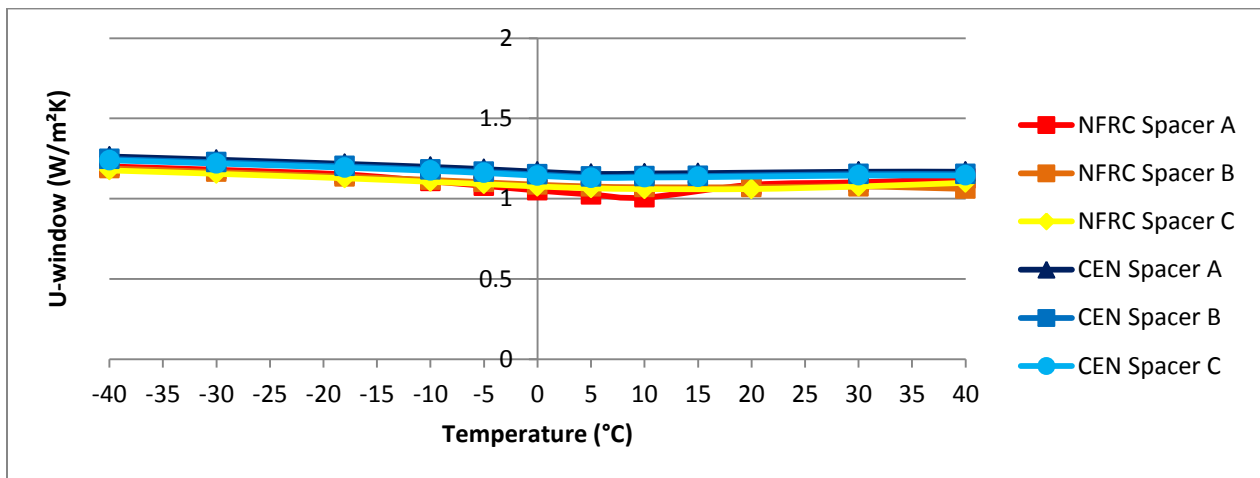


Figure D-82 Solid Wood Frame with a Triple IGU: Spacer Comparison

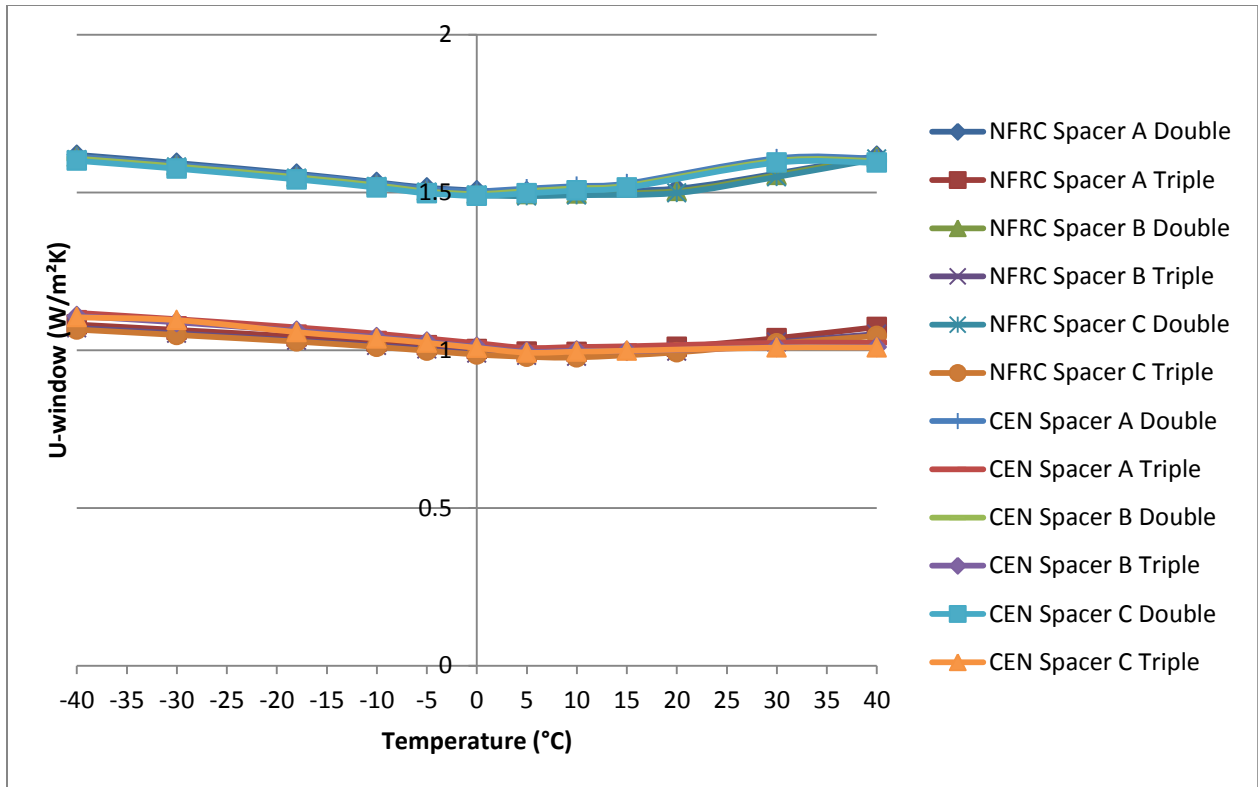


Figure D-83 U-PVC Frames with Double and Triple IGUs: Spacer Comparison

11 Appendix E

Problems with Computer Simulations and Error Possibilities

1. In WINDOW, when “-1 Glz system table cannot be found” pop-up window appears when simulating a whole window U-values, simply copy the file and calculate again. Clicking “New File” results in the error pop-up window again.
2. For the NFRC method, you need to calculate and save the results in the THERM file in order for WINDOW to upload the results for the whole window calculations.
3. THERM does not calculate U-values across a 0° temperature differential. Using the CEN method in WINDOW at 20, 30 and 40°C gives different Ug values every time “calculate” is pressed. WINDOW gives different center-of-glass U-values for each method sometimes, even when no variables are changed. Clicking calculate in the standard NFRC and CEN method then going back to the simulation sometimes corrects this.
4. Working with new boundary conditions in the NFRC and CEN methods need to be redefined in WINDOW before importing in THERM. For example, for each minute change in temperature and other boundary conditions, the WINDOW file needs to be changed accordingly. Simply changing the boundary conditions in THERM *after* an IGU is imported does not change the U-value of the IGU according to the *new* boundary conditions for that THERM session. There needs to be a method to change the U-cog in THERM without having to insert the glazing each time a boundary condition is changed.
5. When doing total window calculations in WINDOW, sometimes an error pop-up states that the U-cog cannot be calculated. Here, the glazing IGU has to be recalculated at the specified boundary conditions and then the total window calculations can be performed.
6. Sometimes when files are opened in THERM, the boundary conditions changed and sometimes the U-values changed. The reason is unknown. For this thesis, the THERM files were calculated, saved and imported into WINDOW in the same session; the U-values of the files from THERM were checked with the imported WINDOW files to ensure they were the same.
7. For the CEN method, when drawing boundary conditions, the THERM file draws them according to the CEN Interior boundary conditions used when importing the IGU. There is not an option for specified interior reduced radiation segments for the CEN interior when importing an IGU. Therefore, the reduced radiation segments need to be redrawn *then* “calculate” can be pressed; otherwise the original interior boundary conditions will be assigned to the entire interior surface.
8. When importing IGUs from WINDOW, import should not be pressed too quickly; make sure that the pop-up window appears that asks for the library to be reloaded, otherwise the previous IGU is inserted.
9. Some minor errors were found in the original THERM files that were changed for the simulations. For example, a U-surface factor tag in one boundary segment can change the U-value results quite significantly, especially if the wrong U-surface factor tag and surface

film coefficient is assigned in the edge-of-glazing area; even a millimeter can make a difference of $0.05 \text{ W/m}^2\text{K}$.

10. When using different exterior temperatures in the NFRC method, the temperatures used in both the convection and black body radiation model needs to be the same temperature. If they are not the same temperature, this will alter the U-value results significantly.

12 References

- AIS Glass Solutions. (2005). *Insulated Glass Units*. Retrieved 07 16, 2013, from AIS Glassolutions: http://www.aisglass.com/insulated_glass_units.asp
- Allen, G. (2013, 03 18). Senior Associate, Sustainable EDGE Ltd. (P.-G. Ebanks, Interviewer)
- Apte, J., & Arasteh, D. (2006). *Window-Related Energy Consumption in the US Residential and Commercial Building Stock*. Berkeley, CA: Lawrence Berkeley National Laboratory.
- Arasteh, D., Beck, F., Stone, N., duPont, W., Mathis, C., & Koenig, M. (1994). PHASE 1 Results of the NFRC U-Value Procedure Validation Project. *ASHRAE Transactions, Vol. 100, Pt. 1*.
- Arasteh, D., Finlayson, E., Huang, Y., Huizenga, C., Mitchell, R., & Rubin, M. (1998). State-of-the-Art Software for Window Energy-Efficiency Rating and Labeling. *ACEEE 1998 Summer Study on Energy Efficiency in Buildings*. Pacific Grove, CA: LBNL.
- Arasteh, D., Mathis, R. C., & DuPont, W. (1992). The NFRC Window U-Value Rating Procedure. *Thermal performance of the exterior envelopes of buildings V* (pp. 349-356). Atlanta, GA: ASHRAE; United States; Department of Energy; Building Thermal Envelope Coordinating Council.
- Arasteh, D., Mitchell, R., Kohler, C., Huizenga, C., & Curcija, D. (2001, 06 06). *Improving information technology to maximize fenestration energy efficiency*. Retrieved 10 02, 2013, from Lawrence Berkeley National Laboratory: <http://escholarship.org/uc/item/25x3w856>
- Asdrubali, F., & Baldinelli, G. (2011). Thermal transmittance measurements with the hot box method: Calibration, experimental procedures, and uncertainty analyses of three different approaches. *Energy and Buildings Vol. 43, Iss. 7*, 1618-1626.
- ASHRAE. (1998). Standard Method for Determining and Expressing the Heat Transfer and Total Optical Properties of Fenestration Products. *Public Review Draft of Standard 142P*. Atlanta, Georgia: American Society of Heating, Refrigerating and Air Conditioning Engineers.
- ASHRAE. (2009). *ASHRAE Handbook - Fundamentals (SI Edition)*. Atlanta, Georgia: American Society of Heating, Refrigerating and Air-Conditioning Engineers, Inc.
- ASHRAE. (2014). *Withdrawn Standards and Guidelines*. Retrieved 02 12, 2014, from ASHRAE: <https://www.ashrae.org/standards-research--technology/standards--guidelines/withdrawn-standards>
- ASHRAE Standards Project Committee SPC 142. (2000). *ASHRAE Standard 142 (Draft)*. Atlanta, GA: ASHRAE.
- Avasoo, D. (2007). The European window energy labelling challenge. *Proceedings of the European council for an energy efficient economy (ECEEE) summer study* (pp. 4-9). Göteborg, Sweden: WSP Environmental.

- Aydin, O. (2000). Determination of optimum air-layer thickness in double-pane windows. *Energy and Buildings*, Vol. 32, Issue 3, 303-308.
- Aydin, O. (2006). Conjugate heat transfer analysis of double pane windows. *Building and Environment*, vol. 41 , issue 2, 109-116.
- Barry, B. (2011, 11 22). *A Tale of Two Rating Systems: NFRC and PHI window testing protocols*. Retrieved 09 05, 2013, from slideshare: <http://www.slideshare.net/Bronwynb/a-taleof-two-rating-systems-20111122-final>
- BBC. (2013, 08 29). *Evidence for new periodic table element boosted*. Retrieved 09 13, 2013, from newsfirst: <http://www.newsfirst.lk/english/sites/default/files/PeriodicTable.png>
- Ben-Nakhi, A. (2002). Minimizing thermal bridging through window systems in buildings of hot regions. *Applied Thermal Engineering* 22 , 989–998.
- Blanusa, P. (2001). *A comparison of different heat transfer calculation methods for fenestration systems*, Master of Science Thesis. Amherst, Massachusetts: University of Massachusetts.
- Blanusa, P., Goss, W., Roth, H., Weitzmann, P., Jensen, C., Svendsen, S., et al. (2007). Comparison between ASHRAE and ISO thermal transmittance calculation methods. *Energy and Buildings* 39, 374–384.
- Brown, W., & Ruberg, K. (1988). *Window Performance Factors*. Retrieved 07 18, 2013, from National Research Council Canada: <http://archive.nrc-cnrc.gc.ca/eng/ibp/irc/bsi/88-window-performance.html>
- Canadian Standards Association. (2009). *User guide to CSA A440.2-09/ Fenestration energy performance*. Mississauga, Ontario: Canadian Standards Association.
- Canty and Associates LLC. (2014). *Various U.S. Cities*. Retrieved 02 20, 2014, from weatherbase: <http://www.weatherbase.com/>
- Carmody, J., & Haglund, K. (2012, 11). *Measure Guideline: Energy-Efficient Window Performance and Selection* . Retrieved 10 11, 2013, from U.S. Department of Energy: http://apps1.eere.energy.gov/buildings/publications/pdfs/building_america/measure_guide_windows.pdf
- Carpenter, S., & Elmahdy, A. (1994). Thermal performance of complex fenestration. *ASHRAE Transactions* 100.
- EN 673. (1997). *Glass in building - Determination of thermal transmittance (Uvalue) - Calculation method*. Brussels, Netherlands: European Committee for Standardization.
- Chen, F., & Wittkopf, S. (2012). Summer condition thermal transmittance measurement of fenestration systems using calorimetric hot box . *Energy and Buildings*, Vol. 53, 47-56.

- Curcija, C. (2005). *Discrepancies Between ISO Window Simulations Standards*. Amherst, Massachusetts: Center for Energy Efficiency and Renewable Energy.
- Curcija, C. (2013, 09 24). Windows and Envelope Materials Group, Lawrence Berkeley National Laboratory. (P.-G. Ebanks, Interviewer)
- Curcija, C. (2014, 01 17). Windows and Envelope Materials Group, LBNL. (P.-G. Ebanks, Interviewer)
- Curcija, D., & Goss, W. (1994). Two-dimensional finite element model of heat transfer in complete fenestration systems. *ASHRAE Transactions 100 (Pt 2)*, 1207–1221.
- DiPinto, M. (2013, 10 15). Zola European Windows. (P.-G. Ebanks, Interviewer)
- Ducker Research Company, I. (2012). *Study of the U.S. Market*. Troy, MI: American Architectural Manufacturers Association (AAMA) and Window and Door Manufactures Association (WDMA) .
- EEL. (1995). *The FRAMEplus Toolkit for Heat Transfer Assessment of Building Components, Version 3.0*. Kitchener, Ontario: Enermodal Engineering.
- Efficient Windows Collaborative. (2012). *Efficient Windows Collaborative*. Retrieved 10 11, 2013, from Efficient Windows Collaborative: http://www.efficientwindows.org/gtypes_3lowe.php
- Elliot, R. (2012, 11 11). Certified Passive House Consultant. (P.-G. Ebanks, Interviewer)
- Elmahdy, A. (2004). Effects of Improved Spacer Bar Design on Window Performance. *Construction Technology Update No. 58*.
- Elmahdy, A., & Comick, S. (1988). *New Technology in the Window Industry*. Retrieved 07 18, 2013, from National Research Council Canada: <http://archive.nrc-cnrc.gc.ca/eng/ibp/irc/bsi/88-window-industry.html>
- Environment Canada. (2007, 08 23). *Climate Normals 1971-2000*. Retrieved 02 05, 2014, from Environment Canada: <http://www.statcan.gc.ca/tables-tableaux/sum-som/I01/cst01/phys08b-eng.htm>
- Environment Canada. (2013, 11 12). *Canadian Climate Normals*. Retrieved 02 05, 2014, from Canada.gc.ca: <http://climate.weather.gc.ca/> and <http://www.eldoradocountyweather.com/canada>
- Energy, U.S. Department of. (2011, 12 14). *Window and Envelope Solutions for Today and Tomorrow*. Retrieved 23 11, 2013, from Office of Energy Efficiency and Renewable Energy: http://www1.eere.energy.gov/buildings/windows/volume/purchase/pdfs/nahb_webinar.pdf
- Fanger, P. (1972). *Thermal comfort: analysis and applications in environmental engineering*. New York: McGraw-Hill.

- Feist, D. W. (2006, 05 01). *Window - Heat Transfer Coefficient Uw and Glazing - Heat Transfer Coefficient Ug*. Retrieved 03 18, 2013, from Passive House Institute: http://www.passivhaustagung.de/Passive_House_E/window_U.htm
- Fenestration Canada. (2013). *A Brief History*. Retrieved 07 17, 2013, from Fenestration Canada: http://www.fenestrationcanada.ca/video/english/windows/1w_what/1w_what_2.html
- Fenestration Canada. (2013, 01 13). *Ontario puts window energy requirement into law*. Retrieved 03 16, 2013, from Glass Canada: <http://www.glasscanadamag.com/content/view/2497/>
- Fourier, J. (1955). *The Analytical Theory of Heat*. New York: Dover Publications.
- German Institute for Standardization. (1999). *Excerpt from the tables and formulas of the DIN EN ISO 6946*. Retrieved 02 27, 2014, from University of Duisburg-Essen: https://www.uni-due.de/ibpm/Aufgabensammlung/NeuNorm_A4.pdf
- Gibson, S. (2012). *Do Europeans Make Better Windows Than We Do? - comments*. Retrieved 10 07, 2013, from GreenBuildingAdvisor.com: <http://www.greenbuildingadvisor.com/blogs/dept/qa-spotlight/do-europeans-make-better-windows-we-do>
- Goudey, H. (n.d.). *Selected Thermographs*. Retrieved 02 03, 2014, from Windows & Daylighting: <http://windows.lbl.gov/facilities/irlab/therms.html>
- Griffith, B., Türler, D., & Arasteh, D. (1996). Surface Temperatures of Insulated Glazing Units: Infrared. *ASHRAE Transactions 1996, V. 102 PT. 2.*, 1-24.
- Gustavsen, A., Arasteh, D., Petter Jelle, B., & Curcija, C. (2008). Developing Low-Conductance Window Frames: Capabilities and Limitations of Current Window Heat Transfer Design Tools. *Journal of Building Physics 32*, 131-153.
- Gustavsen, A., Grynning, S., Arasteh, D., Petter Jelle, B., & Goudey, H. (2011). Key elements of and material performance targets for highly insulating window frames. *Energy and Buildings 43*, 2583-2594.
- Gustavsen, A., Kohler, C., Arasteh, D., & Dalehaug, A. (2007). Two-dimensional computational fluid dynamics and conduction simulations of heat transfer in horizontal window frames with internal cavities. *ASHRAE Transactions, 113(1)*, 165-175.
- Gustavsen, A., Petter Jelle, B., Arasteh, D., & Kohler, C. (2007). *State-of-the-Art Highly Insulating Window Frames – Research and Market Review*. Oslo, Norway: SINTEF Building and Infrastructure.
- Hanam, B. (2013, 04 10). Building Science Engineer, RDH Building Engineering Limited. (P.-G. Ebanks, Interviewer)
- Hawthorne, W., Reilly, S., Anderson, R., & Hancock, E. (1998). Minimized Duct Design: Initial Comfort Guidelines. *Excellence in Building Conference*.

- Herron, T. (2013, 02 04). Senior Manager, Communications and Marketing. (P.-G. Ebanks, Interviewer)
- Hopwood, S. (2013, 01 16). Account Manager, Natural Resources Canada. (P.-G. Ebanks, Interviewer)
- Hutcheon, N., & Handegord, G. (1995). *Building Science for a Cold Climate*. Ottawa, ON: National Research Council of Canada.
- IESO. (2012). *Supply Overview*. Retrieved 09 13, 2013, from Independent Electricity System Operator (IESO): http://www.ieso.ca/imoweb/media/md_supply.asp
- ISO 10077-1. (2000). *Thermal Performance of Windows, Doors and Shutters-Calculation of Thermal Transmittance—Part 1: Simplified Method*. Geneva, Switzerland: International Organization for Standardization.
- ISO 15099. (2003). *Thermal performance of windows, doors and shading devices -- Detailed calculations*. Geneva, Switzerland: International Organization for Standardization.
- ISO 10077-2. (2012). *Thermal performance of windows, doors and shutters -- Calculation of thermal transmittance -- Part 2: Numerical method for frames*. Geneva, Switzerland: International Organization for Standardization.
- Janssens, A., Van Londersele, E., Vandermarcke, B., Roels, S., Standaert, P., & Wouters, P. (2007). Development of Limits for the Linear Thermal Transmittance of Thermal Bridges in Buildings. *Thermal performance of the exterior envelopes of whole buildings X, International conference*. Clearwater, Florida: ASHRAE.
- Jaugelis, A. (2012, 11 23). *NAFS and The 2012 Building Code*. Retrieved 07 24, 2013, from British Columbia Building Envelope Council: <http://www.bcbec.com/docs/RDH%20NAFS%20presentation%20BCBEC%202013-04-18.pdf>
- Jefferson Lab. (n.d.). *The Element Hydrogen*. Retrieved 09 25, 2013, from Jefferson Lab, US Department of Energy: <http://education.jlab.org/itselemental/ele001.html>
- Jenkins, A. (2012, 11 29). Senior Policy Specialist of the Ministry of Energy and Infrastructure. (P.-G. Ebanks, Interviewer)
- King, T. (1987). *Glass in Canada*. Erin, Ontario: The Boston Mill Press.
- Klems, J. (2003). *Measured Summer Performance of Storm Windows*. Berkeley, California: Lawrence Berkeley National Laboratory.
- Klems, J., & Reilly, S. (1989). Window Nighttime U-values: A Comparison between Computer Calculations and MoWiTT Measurements. *ASHRAE 1990 Winter meeting*. Atlanta, GA: ASHRAE.
- Klems, J., & Reilly, S. (1990). Window Nighttime U-values: A Comparison between Computer Calculations and MoWiTT Measurements. *ASHRAE Transactions, Vol. 96*.

- Kohler, C. a. (2012). *Optimal gap width for double and triple glazing systems*. Retrieved 07 16, 2014, from Windows and Daylighting: http://windows.lbl.gov/adv_Sys/hi_R_insert/GapWidths.html
- LBL. (1994). *WINDOW 4.1: PC Program for Analyzing Window Thermal Performance, LBL-35298*. Berkeley, California: Lawrence Berkeley National Laboratory.
- LBL. (1998). *THERM 2: PC Program for Analyzing Two-Dimensional Heat Transfer Through Building Products, LBL-37371*. Berkeley, California: Lawrence Berkeley National Laboratory.
- LBL. (2006, 06 20). *Conrad 5 & Viewer 5 Technical and Programming* . Retrieved 01 25, 2014, from Windows and Daylighting: http://windows.lbl.gov/software/window/6/Conrad%20and%20Viewer%20Documentation_06-20-06.pdf
- LBL. (2009, 01 08). *Calculating Fenestration Product Performance In Window 6 And Therm 6 According to EN 673 and EN 10077*. Retrieved 02 03, 2014, from Windows and Daylighting: http://windows.lbl.gov/software/window/6/EN673+ISO%2010077_Using%20THERM+WINDOW-LBNL_rev4.pdf
- LBL. (2013). *THERM 6.3 / WINDOW 6.3 NFRC Simulation Manual*. Berkeley, CA: Lawrence Berkeley National Laboratory.
- Lingnell, A. W. (2011, 06). *An Introduction to Insulating Glass* . Retrieved 07 16, 2013, from Insulating Glass Manufacturers Alliance: <http://www.igmaonline.org/technical/Lingnell%20-%20An%20Introduction%20to%20Insulating%20Glass.ppt.pdf>
- Lovins, A. (1991). If it's not efficient, it's not beautiful. *Fine Homebuilding*, 66, 4.
- Lstiburek, J. (2006). *Water Management Guide* . Westford, MA: Building Science Press Inc. .
- McGowan, R. (2013, 08 21). Senior Program Manager, National Fenestration Rating Council. (P.-G. Ebanks, Interviewer)
- Ministry of Municipal Affairs and Housing. (2006). *Ministry of Municipal Affairs and Housing*. Retrieved 08 28, 2014, from Ministry of Municipal Affairs and Housing: <http://www.mah.gov.on.ca/Asset10095.aspx?method=1>
- National Fenestration Rating Council. (1997). *NFRC Test Procedure for Measuring the Steady-State Thermal Transmittance of Fenestration Systems*. Silver Spring, MD: NFRC.
- Natural Resources Canada. (2012, 07 09). *Office of Energy Efficiency; Energy Efficiency Trends in Canada, 1990 to 2009*. Retrieved 02 04, 2013, from Natural Resources Canada: <http://oee.rncan.gc.ca/publications/statistics/trends11/chapter3.cfm?attr=0#graph11>
- NECB. (2011). *Updated National Energy Code Calls For 25% Higher Efficiency*. Retrieved 07 16, 2014, from RENX.ca: <http://renx.ca/updated-national-energy-code-calls-for-25-higher-efficiency/>

- NFRC. (2010). *NFRC 102-2010: Procedure for Measuring the Steady-State Thermal Transmittance of Fenestration Systems*. Greenbelt, MD: National Fenestration Rating Council, Inc.
- NFRC. (2012). *Energy Ratings*. Retrieved 10 11, 2013, from Window Ratings: <http://www.nfrc.org/windowratings/Energy-ratings.html>
- NFRC. (2012). *NFRC Approved Software List*. Retrieved 03 24, 2013, from National Fenestration Rating Council: <http://www.nfrc.org/software.aspx>
- Novakovic, V., & Endre Lexow, T. (n.d.). *ISO/TC 163 Thermal Performance and Energy Use in the Built Environment, SC 2: Calculation Methods*. Oslo, Norway: Norwegian University of Science and Technology, Standards Norway.
- NRC. (2012, 05 18). *Energy performance*. Retrieved 10 11, 2013, from Natural Resources Canada: <http://oee.nrcan.gc.ca/equipment/windows-doors/18021>
- NRC. (2013). *Photovoltaic potential and solar resource maps of Canada*. Retrieved 02 28, 2014, from Natural Resources Canada: <http://pv.nrcan.gc.ca/>
- NREL. (1994). *Solar Radiation Data Manual for Flat Plate and Concentrating Collectors*. Golden, Colorado: NREL.
- Pacey, A. (1981). A History of Window Glass Manufacture in Canada. *Architectural Glass: History and Conservation, Vol. 13, No.3, 33-47*.
- Pacific Northwest National Laboratory and Oak Ridge National Laboratory. (2010, 08). *Guide to Determining Climate Regions by County*. Retrieved 09 20, 2013, from U.S. Department of Energy: Energy Efficiency and Renewable Energy: http://apps1.eere.energy.gov/buildings/publications/pdfs/building_america/ba_climateguide_7_1.pdf
- Parekh, A. (2010, April 21). *Low-Solar and High-Solar Gain Glazings –which one to choose/specify in our climate?* Retrieved 02 01, 2013, from Building Envelope Council Ottawa Region: http://www.becor.org/content/downloads/20100421_presentation3.pdf
- Passivhaus Institut. (2012). *Certification Criteria for Certified Passive House Glazings and Transparent Components*. Darmstadt, Germany: Passivhaus Institut.
- Passivhaus Institut. (2012). *Zertifikat: Certified Passive House component*. Retrieved 09 13, 2013, from Passivhaus Institut: http://passiv.de/komponentendatenbank/files/pdf/zertifikate/z_a-hus_a-hus-passive-house-system_en.pdf
- Pittsburgh Plate Glass Company. (1899). *Pittsburgh Plate Glass Company*. Retrieved 09 23, 2013, from Internet Archive: <http://archive.org/stream/PittsburghPlateGlassCompany/Cca46248PittsburghPlateGlassCo.#page/n0/mode/2up>

- Prowler, D. (2010, 06 15). *Mold and Moisture Dynamics*. Retrieved 03 18, 2013, from Whole Building Design Guide (WBDG): <http://www.wbdg.org/resources/moisturedynamics.php>
- RDH Building Engineering Ltd. (2014). *International Window Standards*. Vancouver, BC: RDH Building Engineering Ltd. Retrieved 06 08, 2014, from Homeowner Protection Office: <http://www.hpo.bc.ca/files/download/Report/International-Window-Standards.pdf>
- Rogers, T. (2014). *Quanex building products*. Retrieved 08 28, 2014, from Quanex building products: http://www.quanex.com/QuanexDotCom/media/DocumentFiles/governance/Quanex-Fenestration-Canada-Update_TRogers_FINAL_111813.pdf
- Rosenbaum, M., & White, D. (2009, 10 14). *In Defense of the Passive House Standard*. Retrieved 09 05, 2012, from right environments: <http://www.greenbuildingadvisor.com/blogs/dept/green-building-blog/defense-passive-house-standard>
- Roth. (1998). *Comparison of Thermal Transmittance Calculation Methods Based on ASHRAE and CEN/IOS Standards, Masters of Science Thesis*. Amherst, Massachusetts: Department of Mechanical Engineering, University of Massachusetts.
- Sack, N. (2013, 08 12). Convenor CEN TC89/WG7. (P.-G. Ebanks, Interviewer)
- Selkowitz, S. (1979). Thermal Performance of Insulating Window Systems LBL-8835. *ASHRAE Symposium on Window Management as it Affects Energy Conservation in Buildings* (pp. Sec. De-79-5). Detroit, MI: ASHRAE.
- Solvason, K., & Wilson, A. (1963). Factory-sealed Double-Glazing Units. *Canadian Building Digest* 46, 4.
- Speier, F. (2012). High Performance Window Installation - Challenges for Durability and Opportunities for Thermal Performance - Part I. *Energy Design Update* 32. 11, 12-16.
- Stetson, T. (1865, 08 01). *Improvement in Window-Glass*. Retrieved 07 16, 2013, from Google Patents: <http://www.google.com/patents?id=4zYAAAAAEBAJ&printsec=abstract&zoom=4#v=onepage&q&f=false>
- Stevens, G. (1967). *Canadian Glass ca. 1825-1925*. Toronto: Ryerson Press.
- Straube, J. (2003). *Heat Flow Basics*. Retrieved 02 14, 2014, from University of Waterloo: <http://www.civil.uwaterloo.ca/beg/arch264/arch264%20heat%20flow%20basics.pdf>
- Straube, J. (2009, 09 07). *BSI-025: The Passive House (Passivhaus) Standard—A comparison to other cold climate low-energy houses*. Retrieved 09 05, 2013, from buildingscience.com: <http://www.buildingscience.com/documents/insights/bsi-025-the-passivhaus-passive-house-standard/?topic=/doctypes/building-science-insights>
- The World Bank. (2013). *Energy use (kg of oil equivalent per capita)*. Retrieved 02 04, 2013, from The World Bank: <http://data.worldbank.org/indicator/EG.USE.PCAP.KG.OE>

- Tian, J., Wang, Y., & Dong, X. (2010, 10). *Methanoculleus hydrogenitrophicus sp. nov., a methanogenic archaeon isolated from wetland soil*. Retrieved 03 25, 2013, from International Journal of Systemic and Evolutionary Microbiology: <http://ijs.sgmjournals.org/content/60/9/2165.full>
- Tutton, M., Hirst, E., & Pearce, J. (2007). *Windows: History, Repair and Conservation*. Dorset, U.K.: Donhead Publishing Ltd.
- U.S. Department of Energy. (2011). *Impact on US Energy Consumption: Why worry about windows?* Retrieved 02 04, 2013, from U.S Department of Energy: Building Technologies Program: http://www1.eere.energy.gov/buildings/windowsvolumepurchase/pdfs/2011_ohio_wvp_workshop.pdf DOE
- U.S. Dept. of Energy. (2009). *The Carbon Neutral Design Project*. Retrieved 07 16, 2014, from The American Institute of Architects: <http://tboake.com/carbon-aia/strategies.html>
- UCSB. (2012). *If water is made up of hydrogen and oxygen, two gasses, then how is it a liquid?* Retrieved 03 13, 2013, from UCSB ScienceLine: <http://scienceline.ucsb.edu/getkey.php?key=2894>
- van Dijk, D. (2013, 03 2). Senior Scientist, TNO Energy and Comfort Systems. (P.-G. Ebanks, Interviewer)
- Varshneya, K., Rosaa, J., & Shapiroa, I. (2012). Method to Diagnose Window Failures and Measure U-Factors on Site. *International Journal of Green Energy, Vol. 9, Issue 3*, 280-296.
- Weitzmann, P., Jensen, C. F., & Svendsen, S. (2000). Comparison of calculations of thermal transmittance of windows using two-and three-dimensional models. *EuroSun Conference*. Copenhagen, Denmark.
- Wilson, A. (1960). *Condensation on Inside Window Surfaces*. Retrieved 07 18, 2013, from Canadian Building Digests: http://web.mit.edu/parmstr/Public/NRCan/CanBldgDigests/cbd004_e.html
- Wilson, A. (2009, 12 08). *Making the Case for Triple-Glazed Windows*. Retrieved 07 17, 2013, from GreenBuildingAdvisor.com: <http://www.greenbuildingadvisor.com/blogs/dept/energy-solutions/making-case-triple-glazed-windows>
- Wright, G. (2012, 02 24). Calculating Window Performance Parameters for Passive House Energy Modeling. *PHIUS Tech Corner, Vol. 1, No. 4*, pp. 1-19.
- Wright, J. (1995). *VISION4, Glazing System Thermal Analysis: User and Reference Manuals*. Waterloo, Ontario: University of Waterloo.
- Wright, J., & H.F., S. (1988). Glazing system U-value measurements using a guarded heater plate apparatus. *ASHRAE Transactions, vol. 94, 2*, 1325-1337.
- Wright, J., & Sullivan, H. (1989). Natural Convection in Sealed Glazing Units: A Review. *ASHRAE Transactions, V.95, Pt.1*, 592-603.

Young, S. (2012). *European windows vs. North American windows: comments*. Retrieved 10 07, 2013, from GreenBuildingAdvisor.com:
<http://www.greenbuildingadvisor.com/community/forum/energy-efficiency-and-durability/25365/european-windows-vs-north-american-windows>

Zola European Windows. (n.d.). *Thermowood*. Retrieved 07 18, 2014, from Zola European Windows:
http://www.zolawindows.com/wp-content/uploads/2012/04/zola_thermo_wood.pdf